Title

Disulfide HMGB1-Induced Immune Activation During and Following Ischemia-Reperfusion Injury in Human Orthotopic Liver Transplantation

Author

Terry, Allyson Queenth

Publication Date

2023

Peer reviewed|Thesis/dissertation

UNIVERSITY OF CALIFORNIA

Los Angeles

Disulfide HMGB1-Induced Immune Activation During and Following Ischemia-Reperfusion Injury in Human Orthotopic Liver Transplantation

A dissertation submitted in partial satisfaction of the

requirements for the degree Doctor of Philosophy

in Molecular and Medical Pharmacology

by

Allyson Queenth Terry

2023

ABSTRACT OF THE DISSERTATION

Disulfide HMGB1-Induced Immune Activation During and Following Ischemia-Reperfusion Injury in Human Orthotopic Liver Transplantation

by

Allyson Queenth Terry

Doctor of Philosophy in Molecular and Medical Pharmacology

University of California, Los Angeles, 2023

Professor Elaine F. Reed, Co-Chair

Professor Robert M. Prins, Co-Chair

Ischemia-reperfusion injury (IRI) is an intrinsic risk of solid organ transplantation due to the cellular damage and subsequent immune activation induced by current allograft procurement protocols. Increased severity of IRI contributes to poor clinical outcomes, including early allograft dysfunction and alloimmune-mediated graft rejection, following orthotopic liver transplantation (OLT). Circulating recipient monocytes are one of the first cell populations to infiltrate the donor liver. Once activated, these monocytes can differentiate into macrophages capable of crosstalk with the adaptive immune cells responsible for the development of alloimmunity. The intracellular protein high mobility group box 1 (HMGB1) is released during IRI in mouse models and correlates with degree of IRI. HMGB1 is unique in that each of its three oxidative forms have different functions and it can bind multiple immune receptors on monocytes and macrophages, including

toll-like receptor 4 (TLR4) and TLR9. Blood from IRI+ human OLT recipients activates TLR4 and TLR9. We therefore investigated whether the pro-inflammatory oxidative form of HMGB1 (disulfide HMGB1, diS-HMGB1) is increased in IRI+ patients and, if so, the mechanisms behind diS-HMGB1-induced innate and adaptive immune activation during and following OLT. First, we determined that diS-HMGB1 was increased in post-reperfusion portal vein blood of IRI+ patients and that this same blood sample induced a pro-inflammatory response in healthy volunteer monocytes *in vitro*. The augmented diS-HMGB1 levels in IRI+ patient blood were mediated by secretion of diS-HMGB1 from pro-inflammatory liver resident macrophages in the donor allograft that became activated during the transplant process. We confirmed the detrimental effect of increased diS-HMGB1 levels in a murine model of IRI. Second, we developed an *in vitro* model of human primary monocyte-to-macrophage differentiation to elucidate the specific effects of diS-HMGB1 on this process. We determined that diS-HMGB1 functions by inducing secreted factors, surface markers, and oxidative functions that allow monocytes and macrophages to create a local pro-inflammatory environment and to induce a pro-inflammatory adaptive immune response through interactions with CD4+ T cells. Finally, we report how both TLR4 and TLR9 contribute to the manifestation of this phenotype. In sum, this work provides insight into the impact of diS-HMGB1 on occurrence and severity of IRI during OLT and how the release of diS-HMGB1 at the time of transplant can have lasting impacts on the immune landscape, and therefore graft and recipient health and survival, following OLT.

The dissertation of Allyson Queenth Terry is approved.

Jerzy W. Kupiec-Weglinski

Kenneth A. Dorshkind

Elaine F. Reed, Committee Co-Chair

Robert M. Prins, Committee Co-Chair

University of California, Los Angeles

2023

DEDICATION

To Una, who, in response to a question I asked her during my first year at UCLA, said:

“You’re in grad school, figure it out!”

TABLE OF CONTENTS

LIST OF FIGURES

LIST OF TABLES

ACKNOWLEDGEMENTS

I would first like to thank my advisor, Dr. Elaine F. Reed. Thank you for your holistic approach to mentoring me as an entire person. Your advice and guidance helped me become a better scientist and cultivate the goal of becoming a successful woman in the field of transplantation, while your genuine kindness, positivity, and *joie de vivre* helped me persevere through challenging times. We often talked about how resilience is a requirement for a career in research. I am grateful for your unwavering support that provided me with the opportunity to develop my own resilience – something that will serve me well as I move through the rest of my career.

I would like to thank my committee members Dr. Jerzy Kupiec-Weglinski, Dr. Kenneth Dorshkind, and co-chair Dr. Robert Prins. Your guidance and feedback throughout the years made this research more impactful than I anticipated it could be at the beginning of my studies. I would especially like to thank Dr. Kupiec-Weglinski for his collaboration on the mouse experiments in Chapter 3.

I would like to thank all the members, past and present, of the research and clinical arms of the Reed lab. Your scientific insights helped me view my research with fresh eyes and your friendships made my daily lab life fun, especially when experiments didn't work out as planned. A special thank you to Dr. Rebecca Sosa who introduced me to this project when I rotated in the lab and provided a wealth of advice throughout the years. Your friendship and our perfect pairing of someone who writes too much with someone who loves cutting words has been one of the highlights of my graduate experience.

I would like to thank all of my friends, near and far, who supported my journey towards receiving my PhD. Grad school taught me how to be a scientist, but you taught me (and continue to teach me) how to live life to the fullest. Thank you for your constant support and for all the laughs, the great meals shared, the birthdays and life milestones celebrated, the much-needed vacations, and the rendezvous that took advantage of conference locations. A special thanks to BFFs for our Saturday zooms during COVID that kept us connected during a very isolating time.

I would like to thank Mom, Dad, Katy, Papa, and the rest of my family. Thank you for all you do for me and for Ben. Your love and support has been a constant in my life since before grad school. It was no different over the past six years. Even though my schedule required school to take priority sometimes, I am thankful for the constants of Sunday dinners, Friday night theater performances, UCLA football games, and Christmas casserole and the impromptu morning coffees, Porto's breakfast sandwiches and donut taste tests that made sure we spent time together. I would also like to thank Ferial, Hossein, Mike, and the rest of Ben's family. You welcomed me with open arms and I grateful to have found such a fun, loving, and supportive extended family to become a part of.

Finally, I would like to thank Ben, my fiancé. Thank you for your support before and during grad school, especially during my 3rd, 4th, and 5th years at UCLA. Your patience helped me persevere, cultivate my inner *shirzan*, and reach a point where I believed in myself when I couldn't see the light at the end of the tunnel. Thank you for also knowing when I need to be pushed out of my comfort zone…even though I really like my comfort zone. Finally, thank you for accepting the

fact that whenever you suggest potentially eating sushi, we will 100% be eating sushi. I am grateful for our life together and I am excited for what our next chapter holds. Love you!

Chapter 2 is a version of Sosa RA, Terry AQ, Kaldas FM, Jin YP, Rossetti M, Ito T, Li F, Ahn RA, Naini BV, Groysberg VM, Zheng Y, Aziz A, Nevarez-Mejia J, Zarrinpar A, Busuttil RW, Gjertson DW, Kupiec-Weglinski JW, Reed EF. Disulfide High-Mobility Group Box 1 Drives Ischemia-Reperfusion Injury in Human Liver Transplantation. *Hepatology*. 19 May 2020. doi: 10.1002/hep.31324. This work was supported by National Institutes of Health (NIH) Ruth L. Kirschstein National Research Service Award T32CA009120 to RAS, NIH L60 MD011903 to RAS, NIH PO1 AI120944 to JWKW and EFR, and NIH UL1TR001881 to UCLA Clinical and Translational Science Institute.

Chapter 3 is a version of unpublished work currently under revision: Terry AQ, Kojima H, Sosa RA, Kaldas FM, Chin JL, Zheng Y, Naini BV, Noguchi D, Nevarez-Mejia J, Jin YP, Busuttil RW, Meyer AS, Gjertson DW, Kupiec-Weglinski JW, Reed EF. Disulfide-HMGB1 signaling through TLR4 and TLR9 induces inflammatory macrophages mediating innate-adaptive crosstalk in liver transplantation. I would like to thank Hidenobu Kojima for performing the mouse surgeries, Yiping Jin for executing the Western blots used to determine diS-HMGB1 levels in mouse and patient samples, and David W. Gjertson and Ying Zheng for their extensive assistance with statistical analysis of patient-focused datasets. This work was supported by the following NIH grants: PO1 AI120944 to JWKW and EFR, Ruth L. Kirschstein National Research Service Award T32CA009120 and L60 MD011903 to RAS, and U01AI148119 to ASM.

VITA

EDUCATION

2008-2012 BS, Molecular Biology, *Cum Laude*
Minor: Urban Studies and Planning
University of California, San Diego

EMPLOYMENT

2017-Present Graduate Student Researcher
Lab of Dr. Elaine Reed
Department of Pathology and Laboratory Medicine
University of California, Los Angeles

Jan-Mar 2022 Teaching Assistant
Department of Microbiology, Immunology, and Molecular Genetics
University of California, Los Angeles

2015-2017 Research Associate II
Agensys, Inc.
Santa Monica, CA

2012-2015 Research Associate I, II
Sorrento Therapeutics, Inc.
San Diego, CA

AWARDS AND HONORS

2021 Travel Award, ASHI 47th Annual Meeting, Orlando, FL

2021 Finalist, Lay Summary Competition, ASHI 47th Annual Meeting, Orlando, FL

2019 Finalist, UCLA Grad Slam Three-Minute Thesis Competition

PUBLICATIONS

Terry AQ, Kojima H, Sosa RA, Kaldas FM, Chin JL, Zheng Y, Naini BV, Noguchi D, Nevarez-Mejia J, Jin YP, Busuttil RW, Meyer AS, Gjertson DW, Kupiec-Weglinski JW, Reed EF. Disulfide-HMGB1 Signals Through TLR4 and TLR9 to Induce Inflammatory Macrophages Capable of Innate-Adaptive Crosstalk in Human Liver Transplantation. 2023, Under revision.

Sosa RA, **Terry AQ**, Ito T, Naini BV, Zheng Y, Pickering H, Nevarez-Mejia J, Busuttil RW, Gjertson DW, Kupiec-Weglinski JW, Reed EF, Kaldas, FM. Underlying Immune Mechanisms of Hispanic Female Disparities in Liver Transplantation for Nonalcoholic Steatohepatitis. 2023, Under revision.

Sosa RA*, Ahn R*, Li F, **Terry AQ**, Qian Z, Bhat A, Sen S, Naini BV, Ito T, Kaldas FM, Hoffmann A, Busuttil RW, Kupiec-Weglinski JW, Gjertson DW, Reed EF. Myeloid Molecular Signature of Ischemia Reperfusion Injury in Human Liver Transplantation. 2023, Under revision.
* denotes co-first authors

Jin YP, Nevarez-Mejia J, **Terry AQ**, Sosa RA, Heidt S, Valenzuela NM, Rozengurt E, Reed EF. Crosstalk between HLA class I and TLR4 Mediates P-selectin Surface Expression and Monocyte Capture to Human Endothelial Cells. The Journal of Immunology. 2022 Oct 1;209(7):1359-1369. doi: 10.4049/jimmunol.2200284. Epub 2022 Sep 2. PMID: 36165200

Sosa, RA, **Terry, AQ**, Kaldas, FM, Jin, YP, Rossetti, M, Ito, T, Li, F, Ahn, R, Naini, BV, Groysberg, V, Zheng, Y, Aziz, A, Nevarez-Mejia, J, Zarrinpar, A, Busuttil, RW, Gjertson, DW, Kupiec-Weglinski, JW, Reed, EF. (2020) Disulfide-HMGB1 Drives Ischemia-Reperfusion Injury in Human Liver Transplantation. Hepatology. 2021 Mar;73(3):1158-1175. doi: 10.1002/hep.31324. Epub 2020 Oct 30. PMID: 32426849.

Chapter 1:

Introduction

1.1 ORTHOTOPIC LIVER TRANSPLANTATION

Orthotopic liver transplantation (OLT) is a last-resort treatment for end stage liver diseases such as acute liver failure, non-alcoholic steatohepatitis, and hepatocellular carcinoma [1-3]. The process of OLT involves identifying a suitable donor liver (allograft), safely procuring the graft, transporting the graft to the transplant center where the recipient is located, placing the graft into the recipient, and finally connecting the donor liver to the recipient blood supply. Almost 10,000 liver transplants were performed in 2022 in the United States, with thousands more occurring around the world every year [2, 4, 5].

The main goal following transplantation is to keep the allograft healthy and functioning properly. Similar to a bacterial or viral infection, the recipient immune system can detect the donor liver as foreign and launch an immune response to clear the "intruding" cells. This anti-donor alloimmune response is detrimental to the graft. The main proteins driving the donor-specific response are human leukocyte antigens (HLA) expressed on the cell surface of donor cells. Eliciting a persistent immune response specific to the donor requires activation of and crosstalk between the innate and adaptive immune systems [6-8]. There are three accepted mechanisms for how this crosstalk occurs: direct recognition, indirect recognition, and semi-direct recognition [6, 9]. The work in this dissertation focuses on indirect recognition. It proceeds as follows:

1. Donor-derived proteins, most often donor HLA molecules, are phagocytosed by macrophages and/or dendritic cells (DCs) of the recipient's innate immune system. The phagocytosed proteins are processed and loaded onto the recipient's own HLA class II molecules on the cell surface. This gives the classification of "antigen-presenting cells (APCs)" to these two cell populations. Other co-stimulatory (CD80, CD86) and/or co-

inhibitory molecules (PD-L1) are also present on the cell surface with HLA molecules. These molecules help determine if the induced adaptive immune response will be pro- or anti-inflammatory.

2. CD4+ T cells of the adaptive immune systems come into contact with the presented donor peptides in the HLA class II molecules of the APCs. This happens through the T cell expressing a T cell receptor that can specifically detect the HLA-peptide complex. The balance of co-stimulatory/co-inhibitory molecules on the APCs determines if CD4+ T cells will become pro- or anti-inflammatory.
3. CD4+ T cells then interact with B cells of the adaptive immune system. B cells and their matured plasma cell counterparts are responsible for antibody production in the recipient. When a B cell produces an immunoglobulin against the same donor peptide that a CD4+ T cell has encountered on an APC, the CD4+ T cell can produce cytokines to induce maturation and class switching in the B cell. This results in production of antibodies against the donor's HLA molecules – donor-specific antibodies (DSA).
4. Soluble DSA bind to donor epitopes and facilitate antibody-mediated rejection of the allograft.

Current avenues aimed at decreasing the alloimmune response consist of long-term, non-specific immunosuppression regimens [10, 11]. However, these treatments come with their own immunological side effects due to the immune system not functioning at its full capacity. Incidence of cancer is increased in liver transplant recipients following OLT compared to the general population [12, 13]. Opportunistic infections are also increased by immunosuppression treatments [14, 15]. Finally, these treatments can also be toxic, again resulting in poor health of the recipient

[16]. Delineating more detailed mechanisms of how alloimmunity develops and creating more targeted approaches to decrease the alloimmune response following OLT can aid in elongating the life of the donor liver and allowing recipients to live healthier lives post-transplant.

1.2 ISCHEMIA-REPERFUSION INJURY

Ischemia-reperfusion injury (IRI) occurs when a blood supply is removed and subsequently re-introduced to tissue [17, 18]. This can occur in settings such as myocardial infarction, ischemia stroke, and solid organ transplantation [19-24]. In the context of solid organ transplantation such as OLT, this pause in blood supply compounds with cold storage to cause necrosis, oxidative stress, immunogenic cell death, and ultimately, the release of pro-inflammatory cytokines and intracellular molecules (damage-associated molecular patterns; DAMPs) into the extracellular environment upon reperfusion of the allograft with recipient blood [17, 18, 25]. The immune response triggered by these molecules immediately after reperfusion, along with parenchymal damage, is characteristic of IRI and involves infiltration by multiple innate and adaptive immune cells – monocytes, neutrophils, natural killer cells, T cells, etc. [1, 17, 26, 27]. In our cohort of human OLT recipients, approximately 50% of patients experience IRI (notated as IRI+) [26, 28, 29]. IRI correlates with early allograft dysfunction (EAD), in which the donor liver fails to achieve optimal metabolic function within the first week post-OLT and a risk factor for poorer post-OLT survival [30]. Finally, IRI severity negatively correlates with 5-year graft and patient survival and positively correlates with the incidence of alloimmune-mediated rejection events in OLT recipients such as rejection facilitated by DSA [26, 31]. This connection with alloimmunity suggests that immune activation at the time of transplant can impact the long-term anti-donor immune response.

The cytokines and DAMPs associated with IRI positivity influence the differentiation of infiltrating recipient monocytes into macrophages which can, in turn, differentially activate $CD4^+$ T cells contribute to the adaptive alloimmune response. IRI causes increased expression of multiple pro-inflammatory factors such as TNFα, IL-1α, IL-6, and IFNγ in mouse models, both at the mRNA and protein levels [32-38]. TNFα and IFNγ differentiate monocytes into pro-inflammatory macrophages with the capacity to further secrete IL-1α, IL-1β, and IL-6 to perpetuate the inflamed environment [39]. Our published data corroborates this trend in humans, as a pro-inflammatory cytokine profiles occurs in IRI+ OLT patient blood across pre-, intra- and post-operative time points [26].

Toll-like receptors (TLRs) are a family of pattern recognition receptors, crucial components of the innate immune system that each detect specific types of pathogenic antigens [40-42]. Along with detecting pathogens, these receptors have also evolved to detect DAMPs in the context of sterile inflammation [18, 43]. TLR4 is expressed on the cell surface and induces a pro-inflammatory response in macrophages when it binds lipopolysaccharides (LPS) from gram-negative bacteria or an assortment of DAMPs [18, 44]. TLR4 is widely accepted as important in the manifestation of IRI in both murine models [1, 37, 41, 45-48] and in our human cohort [28]. TLR9 is located in intracellular vesicles and detects unmethylated CpG DNA fragments [18, 44]. TLR9 can also detect extracellular DAMPs through a mechanism reliant on binding of DNA to the receptor for advanced glycation end products (RAGE) on the cell surface that then translocates the DNA to TLR9-containing vesicles [20]. Activation of TLR9 is also associated with IRI in murine models of liver transplant and myocardial infarction [20-22, 49]. Like TLR4, TLR9 is also activated by

DAMP-containing portal vein blood collected from the hepatic vein immediately following reperfusion of the donor liver (liver flush, LF) from IRI+ patients [28].

Both TLR4 and TLR9 are implicated in development of alloimmunity [40]. Concurrent deletion of TLR adaptor molecules MyD88 and Trif in donor skin diminished migration of donor cells to draining lymph nodes and delayed graft infiltration by host T cells, prolonging allograft survival [50]. MyD88-silenced DCs also increase the production of Th2-type cytokines from stimulated CD4+ T cells, resulting in decreased donor-specific alloreactivity [51]. Separately, treatment with a variety of different TLR ligands in a mouse model of allogeneic skin transplant prevents graft acceptance and leads to rejection [52]. In contrast to pro-inflammatory macrophages induced by TLR4 and TLR9 signaling, anti-inflammatory macrophages are associated with less injury immediately following the ischemic event [53, 54] while CD4+ T regulatory and exhausted cells are associated with improved allograft function and survival post-transplant in multiple solid organ transplant settings [6, 55-58]. Therefore, it is imperative to understand the mechanisms of immune activation and/or suppression during and following IRI in order to limit the immune response and decrease the potential for development of alloimmunity post-transplant.

1.3 HIGH MOBILITY GROUP BOX 1 (HMGB1)

High mobility group box 1 (HMGB1) is a ubiquitously-expressed DNA binding protein that functions as a DAMP when found in the extracellular environment. The oxidation state of three cysteine residues at positions 23, 45, and 106 determines the capacity of HMGB1 to stimulate an immune response. Fully-reduced HMGB1 (all-thiol HMGB1, aT-HMGB1) is passively released from necrotic cells and acts as a chemoattractant. Partially-oxidized HMGB1 contains a disulfide

bond between C23-C45 (disulfide HMGB1, diS-HMGB1), induces pro-inflammatory cytokine secretion and can be actively secreted by activated monocytes and macrophages. Fully-oxidized HMGB1 (all-sulfonyl HMGB1, aS-HMGB1) is thought to have no immune function [44, 59, 60].

Multiple studies implicate HMGB1 in the differentiation of murine and human pro-inflammatory macrophages [44, 61-66], although only a few explicitly use diS-HMGB1 [59, 67, 68]. These studies mainly profile cells through cytokine production, a response that is acute and transient in nature. Along with cytokines, it is imperative to assess surface markers and other functions such as reactive oxygen species (ROS) production and T cell activation to gain a fuller picture of how these macrophages function in the context of an *in vivo* immune response [39, 69-71]. Mouse studies implicate HMGB1 in the pro-inflammatory response present during IRI [38, 72, 73]. In other transplant models, murine DCs treated with HMGB1 promote T cell proliferation and differentiation while HMGB1 blockade ameliorates chronic cardiac transplant vasculopathy and decreases T cell infiltration/pro-inflammatory cytokine production [38, 73-75]. None of these murine studies comment on HMGB1 oxidation states. Further, none of these *in vitro* or *in vivo* studies address the impact of diS-HMGB1 on the differentiation of recipient monocytes into macrophages (monocyte-derived macrophages, MDMs) or the capability of these MDMs to augment the development of the longer-term, post-transplant immune response.

HMGB1 binds multiple receptors to facilitate its multiple functions [76]. diS-HMGB1 is reported to bind and activate TLR4 [44]. HMGB1 can also bind unmethylated DNA fragments and be endocytosed by RAGE to trigger activation of intracellular TLR9, although the oxidative state of HMGB1 activating TLR9 has not been elucidated [21]. In early murine studies exploring the

connection between HMGB1 and hepatic IRI, both TLR4 and TLR9 were determined to serve as HMGB1 sensors and exacerbate the innate immune response [38, 49]. Post-reperfusion portal LF from IRI+ OLT patients induces higher activation of both TLR4- and TLR9-transfected reporter cells, suggesting a dual role for these PRRs in pro-inflammatory signaling, potentially activated by diS-HMGB1 [28]. Given the connection between TLRs and development of alloimmunity, it is also tempting to postulate that pro-inflammatory diS-HMGB1 can also influence the post-OLT alloimmune response. However, the definitive mechanism(s) underpinning if and how diS-HMGB1 differentiates monocytes into pro-inflammatory macrophages that promote graft inflammation and prime alloreactive CD4+ T cells in human OLT are unknown.

1.4 SUMMARY

IRI occurring during OLT has the potential to influence the long-term post-transplant alloimmune response in liver recipients. The following work aims to address the hypothesis that diS-HMGB1 1) is released and increases inflammation during IRI, 2) induces a pro-inflammatory macrophage capable of pro-inflammatory crosstalk with CD4+ T cells to activate an alloimmune response, and 3) TLR4 and TLR9 are responsible for facilitating these functions of diS-HMGB1.

1.5 REFERENCES

[1] Zhai Y, Petrowsky H, Hong JC, Busuttil RW, Kupiec-Weglinski JW. Ischaemia-reperfusion injury in liver transplantation--from bench to bedside. Nat Rev Gastroenterol Hepatol 2013;10:79-89.

[2] Kim WR, Lake JR, Smith JM, Schladt DP, Skeans MA, Noreen SM, et al. OPTN/SRTR 2017 Annual Data Report: Liver. 2019;19:184-283.

[3] Kim B, Kahn J, Terrault NA. Liver transplantation as therapy for hepatocellular carcinoma. Liver Int 2020;40 Suppl 1:116-121.

[4] Health Resources and Services Administration UG. 2022 Transplant and Waiting List Numbers. 2023.

[5] Younossi Z, Stepanova M, Ong JP, Jacobson IM, Bugianesi E, Duseja A, et al. Nonalcoholic Steatohepatitis Is the Fastest Growing Cause of Hepatocellular Carcinoma in Liver Transplant Candidates. Clin Gastroenterol Hepatol 2019;17:748-755 e743.

[6] Siu JHY, Surendrakumar V, Richards JA, Pettigrew GJ. T cell Allorecognition Pathways in Solid Organ Transplantation. Front Immunol 2018;9:2548.

[7] Louis K, Macedo C, Lefaucheur C, Metes D. Adaptive immune cell responses as therapeutic targets in antibody-mediated organ rejection. Trends Mol Med 2022;28:237-250.

[8] Valenzuela NM, Hickey MJ, Reed EF. Antibody Subclass Repertoire and Graft Outcome Following Solid Organ Transplantation. Front Immunol 2016;7:433.

[9] DeWolf S, Sykes M. Alloimmune T cells in transplantation. J Clin Invest 2017;127:2473-2481.

[10] Moini M, Schilsky ML, Tichy EM. Review on immunosuppression in liver transplantation. World J Hepatol 2015;7:1355-1368.

[11] Tasdogan BE, Ma M, Simsek C, Saberi B, Gurakar A. Update on Immunosuppression in Liver Transplantation. Euroasian J Hepatogastroenterol 2019;9:96-101.

[12] Aberg F, Gissler M, Karlsen TH, Ericzon BG, Foss A, Rasmussen A, et al. Differences in long-term survival among liver transplant recipients and the general population: a population-based Nordic study. Hepatology 2015;61:668-677.

[13] Jiang Y, Villeneuve PJ, Fenton SS, Schaubel DE, Lilly L, Mao Y. Liver transplantation and subsequent risk of cancer: findings from a Canadian cohort study. Liver Transpl 2008;14:1588-1597.

[14] Levitsky J, Thudi K, Ison MG, Wang E, Abecassis M. Alemtuzumab induction in non-hepatitis C positive liver transplant recipients. Liver Transpl 2011;17:32-37.

[15] Bamoulid J, Staeck O, Crepin T, Halleck F, Saas P, Brakemeier S, et al. Anti-thymocyte globulins in kidney transplantation: focus on current indications and long-term immunological side effects. Nephrol Dial Transplant 2017;32:1601-1608.

[16] Christians U, Klawitter J, Klawitter J, Brunner N, Schmitz V. Biomarkers of immunosuppressant organ toxicity after transplantation: status, concepts and misconceptions. Expert Opin Drug Metab Toxicol 2011;7:175-200.

[17] Kalogeris T, Baines CP, Krenz M, Korthuis RJ. Cell biology of ischemia/reperfusion injury. Int Rev Cell Mol Biol 2012;298:229-317.

[18] Chen GY, Nunez G. Sterile inflammation: sensing and reacting to damage. Nat Rev Immunol 2010;10:826-837.

[19] Kaczorowski DJ, Tsung A, Billiar TR. Innate Immune Mechanisms in Ischemia/Reperfusion. Frontiers in Bioscience 2009:91-98.

[20] Tian J, Avalos AM, Mao SY, Chen B, Senthil K, Wu H, et al. Toll-like receptor 9-dependent activation by DNA-containing immune complexes is mediated by HMGB1 and RAGE. Nat Immunol 2007;8:487-496.

[21] Tian Y, Charles EJ, Yan Z, Wu D, French BA, Kron IL, et al. The myocardial infarct-exacerbating effect of cell-free DNA is mediated by the high-mobility group box 1-receptor for advanced glycation end products-Toll-like receptor 9 pathway. J Thorac Cardiovasc Surg 2019;157:2256-2269 e2253.

[22] Tian Y, Pan D, Chordia MD, French BA, Kron IL, Yang Z. The spleen contributes importantly to myocardial infarct exacerbation during post-ischemic reperfusion in mice via signaling between cardiac HMGB1 and splenic RAGE. Basic Res Cardiol 2016;111:62.

[23] Muhammad S, Barakat W, Stoyanov S, Murikinati S, Yang H, Tracey KJ, et al. The HMGB1 receptor RAGE mediates ischemic brain damage. J Neurosci 2008;28:12023-12031.

[24] Wu H, Ma J, Wang P, Corpuz TM, Panchapakesan U, Wyburn KR, et al. HMGB1 contributes to kidney ischemia reperfusion injury. J Am Soc Nephrol 2010;21:1878-1890.

[25] Giwa S, Lewis JK, Alvarez L, Langer R, Roth AE, Church GM, et al. The promise of organ and tissue preservation to transform medicine. Nat Biotechnol 2017;35:530-542.

[26] Sosa RA, Zarrinpar A, Rossetti M, Lassman CR, Naini BV, Datta N, et al. Early cytokine signatures of ischemia/reperfusion injury in human orthotopic liver transplantation. JCI Insight 2016;1:e89679.

[27] Rao J, Lu L, Zhai Y. T cells in organ ischemia reperfusion injury. Curr Opin Organ Transplant 2014;19:115-120.

[28] Sosa RA, Rossetti M, Naini BV, Groysberg VM, Kaldas FM, Busuttil RW, et al. Pattern Recognition Receptor-reactivity Screening of Liver Transplant Patients: Potential for Personalized and Precise Organ Matching to Reduce Risks of Ischemia-reperfusion Injury. Ann Surg 2018.

[29] Kaldas FMI, T.; Younan, S.; Aziz, J.; Lu, M.; Agopian, V. G.; III JDiNorcia; Yersiz, H.; Farmer, D. G.; Busuttil, R. W. Histologic Ischemia Reperfusion Injury in Liver Transplantation: A Large Single Center Experience [abstract]. American Journal of Transplantation 2019;19.

[30] Ito T, Naini BV, Markovic D, Aziz A, Younan S, Lu M, et al. Ischemia-reperfusion injury and its relationship with early allograft dysfunction in liver transplant patients. American Journal of Transplantation 2020;21:614-625.

[31] Ali JM, Davies SE, Brais RJ, Randle LV, Klinck JR, Allison ME, et al. Analysis of ischemia/reperfusion injury in time-zero biopsies predicts liver allograft outcomes. Liver Transpl 2015;21:487-499.

[32] Liu Y, Ji H, Zhang Y, Shen X, Gao F, He X, et al. Recipient T cell TIM-3 and hepatocyte galectin-9 signalling protects mouse liver transplants against ischemia-reperfusion injury. J Hepatol 2015;62:563-572.

[33] Hirao H, Uchida Y, Kadono K, Tanaka H, Niki T, Yamauchi A, et al. The protective function of galectin-9 in liver ischemia and reperfusion injury in mice. Liver Transpl 2015;21:969-981.

[34] Tang B, Wang Z, Qi G, Yuan S, Yu S, Li B, et al. MicroRNA-155 deficiency attenuates ischemia-reperfusion injury after liver transplantation in mice. Transpl Int 2015;28:751-760.

[35] Guo H, Wang Y, Zhao Z, Shao X. Platelet factor 4 limits Th17 differentiation and ischaemia-reperfusion injury after liver transplantation in mice. Scand J Immunol 2015;81:129-134.

[36] Liu Y, Ji H, Zhang Y, Shen XD, Gao F, Nguyen TT, et al. Negative CD4 + TIM-3 signaling confers resistance against cold preservation damage in mouse liver transplantation. Am J Transplant 2015;15:954-964.

[37] Tsung A, Hoffman RA, Izuishi K, Critchlow ND, Nakao A, Chan MH, et al. Hepatic ischemia/reperfusion injury involves functional TLR4 signaling in nonparenchymal cells. J Immunol 2005;175:7661-7668.

[38] Tsung A, Sahai R, Tanaka H, Nakao A, Fink MP, Lotze MT, et al. The nuclear factor HMGB1 mediates hepatic injury after murine liver ischemia-reperfusion. J Exp Med 2005;201:1135-1143.

[39] Murray PJ. Macrophage Polarization. Annu Rev Physiol 2017;79:541-566.

[40] Alegre ML, Chong A. Toll-like receptors (TLRs) in transplantation. Front Biosci (Elite Ed) 2009;1:36-43.

[41] Evankovich J, Billiar T, Tsung A. Toll-like receptors in hepatic ischemia/reperfusion and transplantation. Gastroenterol Res Pract 2010;2010.

[42] El-Zayat SR, Sibaii H, Mannaa FA. Toll-like receptors activation, signaling, and targeting: an overview. Bulletin of the National Research Centre 2019;43.

[43] Gong T, Liu L, Jiang W, Zhou R. DAMP-sensing receptors in sterile inflammation and inflammatory diseases. Nat Rev Immunol 2020;20:95-112.

[44] Yang H, Hreggvidsdottir HS, Palmblad K, Wang H, Ochani M, Li J, et al. A critical cysteine is required for HMGB1 binding to Toll-like receptor 4 and activation of macrophage cytokine release. Proc Natl Acad Sci U S A 2010;107:11942-11947.

[45] Shen XD, Ke B, Zhai Y, Gao F, Tsuchihashi S, Lassman CR, et al. Absence of toll-like receptor 4 (TLR4) signaling in the donor organ reduces ischemia and reperfusion injury in a murine liver transplantation model. Liver Transpl 2007;13:1435-1443.

[46] Zhai Y, Qiao B, Shen XD, Gao F, Busuttil RW, Cheng G, et al. Evidence for the pivotal role of endogenous toll-like receptor 4 ligands in liver ischemia and reperfusion injury. Transplantation 2008;85:1016-1022.

[47] Zhai Y, Shen XD, O'Connell R, Gao F, Lassman C, Busuttil RW, et al. Cutting edge: TLR4 activation mediates liver ischemia/reperfusion inflammatory response via IFN regulatory factor 3-dependent MyD88-independent pathway. J Immunol 2004;173:7115-7119.

[48] Wu HS, Zhang JX, Wang L, Tian Y, Wang H, Rotstein O. Toll-like receptor 4 involvement in hepatic ischemia/reperfusion injury in mice. Hepatobilliary and Pancreatic Diseases International 2004.

[49] Bamboat ZM, Balachandran VP, Ocuin LM, Obaid H, Plitas G, DeMatteo RP. Toll-like receptor 9 inhibition confers protection from liver ischemia-reperfusion injury. Hepatology 2010;51:621-632.

[50] McKay D, Shigeoka A, Rubinstein M, Surh C, Sprent J. Simultaneous deletion of MyD88 and Trif delays major histocompatibility and minor antigen mismatch allograft rejection. Eur J Immunol 2006;36:1994-2002.

[51] Bao W, Qin X, Guan N, Wang S, Zhu J, Sun X, et al. MyD88-silenced dendritic cells induce T-cell hyporesponsiveness and promote Th2 polarization in vivo. Cytotherapy 2015;17:1240-1250.

[52] Thornley TB, Brehm MA, Markees TG, Shultz LD, Mordes JP, Welsh RM, et al. TLR agonists abrogate costimulation blockade-induced prolongation of skin allografts. J Immunol 2006;176:1561-1570.

[53] Zhang M, Nakamura K, Kageyama S, Lawal AO, Gong KW, Bhetraratana M, et al. Myeloid HO-1 modulates macrophage polarization and protects against ischemia-reperfusion injury. JCI Insight 2018;3.

[54] Yue S, Rao J, Zhu J, Busuttil RW, Kupiec-Weglinski JW, Lu L, et al. Myeloid PTEN deficiency protects livers from ischemia reperfusion injury by facilitating M2 macrophage differentiation. J Immunol 2014;192:5343-5353.

[55] Wherry EJ, Kurachi M. Molecular and cellular insights into T cell exhaustion. Nat Rev Immunol 2015;15:486-499.

[56] Sarraj B, Ye J, Akl AI, Chen G, Wang JJ, Zhang Z, et al. Impaired selectin-dependent leukocyte recruitment induces T-cell exhaustion and prevents chronic allograft vasculopathy and rejection. Proc Natl Acad Sci U S A 2014;111:12145-12150.

[57] Trzonkowski P, Debska-Slizien A, Jankowska M, Wardowska A, Carvalho-Gaspar M, Hak L, et al. Immunosenescence increases the rate of acceptance of kidney allotransplants in elderly recipients through exhaustion of CD4+ T-cells. Mech Ageing Dev 2010;131:96-104.

[58] Yoshida O, Dou L, Kimura S, Yokota S, Isse K, Robson SC, et al. CD39 deficiency in murine liver allografts promotes inflammatory injury and immune-mediated rejection. Transpl Immunol 2015;32:76-83.

[59] Venereau E, Casalgrandi M, Schiraldi M, Antoine DJ, Cattaneo A, De Marchis F, et al. Mutually exclusive redox forms of HMGB1 promote cell recruitment or proinflammatory cytokine release. J Exp Med 2012;209:1519-1528.

[60] Yang H, Lundback P, Ottosson L, Erlandsson-Harris H, Venereau E, Bianchi ME, et al. Redox modification of cysteine residues regulates the cytokine activity of high mobility group box-1 (HMGB1). Mol Med 2012;18:250-259.

[61] Son M, Porat A, He M, Suurmond J, Santiago-Schwarz F, Andersson U, et al. C1q and HMGB1 reciprocally regulate human macrophage polarization. Blood 2016;128:2218-2228.

[62] Andersson U, Wang H, Palmblad K, Aveberger AC, Bloom O, Erlandsson-Harris H, et al. High mobility group 1 protein (HMG-1) stimulates proinflammatory cytokine synthesis in human monocytes. J Exp Med 2000;192:565-570.

[63] Guerriero JL, Ditsworth D, Catanzaro JM, Sabino G, Furie MB, Kew RR, et al. DNA alkylating therapy induces tumor regression through an HMGB1-mediated activation of innate immunity. J Immunol 2011;186:3517-3526.

[64] Karuppagounder V, Giridharan VV, Arumugam S, Sreedhar R, Palaniyandi SS, Krishnamurthy P, et al. Modulation of Macrophage Polarization and HMGB1-TLR2/TLR4 Cascade Plays a Crucial Role for Cardiac Remodeling in Senescence-Accelerated Prone Mice. PLoS One 2016;11:e0152922.

[65] Schaper F, de Leeuw K, Horst G, Bootsma H, Limburg PC, Heeringa P, et al. High mobility group box 1 skews macrophage polarization and negatively influences phagocytosis of apoptotic cells. Rheumatology (Oxford) 2016;55:2260-2270.

[66] Su Z, Zhang P, Yu Y, Lu H, Liu Y, Ni P, et al. HMGB1 Facilitated Macrophage Reprogramming towards a Proinflammatory M1-like Phenotype in Experimental Autoimmune Myocarditis Development. Sci Rep 2016;6:21884.

[67] Tirone M, Tran NL, Ceriotti C, Gorzanelli A, Canepari M, Bottinelli R, et al. High mobility group box 1 orchestrates tissue regeneration via CXCR4. J Exp Med 2018;215:303-318.

[68] Zhou S, Lu H, Chen R, Tian Y, Jiang Y, Zhang S, et al. Angiotensin II enhances the acetylation and release of HMGB1 in RAW264.7 macrophage. Cell Biol Int 2018;42:1160-1169.

[69] Martinez FO, Gordon S. The M1 and M2 paradigm of macrophage activation: time for reassessment. F1000Prime Rep 2014;6:13.

[70] Edwards JP, Zhang X, Frauwirth KA, Mosser DM. Biochemical and functional characterization of three activated macrophage populations. J Leukoc Biol 2006;80:1298-1307.

[71] Mosser DM, Edwards JP. Exploring the full spectrum of macrophage activation. Nat Rev Immunol 2008;8:958-969.

[72] Evankovich J, Cho SW, Zhang R, Cardinal J, Dhupar R, Zhang L, et al. High mobility group box 1 release from hepatocytes during ischemia and reperfusion injury is mediated by decreased histone deacetylase activity. J Biol Chem 2010;285:39888-39897.

[73] Tsung A, Klune JR, Zhang X, Jeyabalan G, Cao Z, Peng X, et al. HMGB1 release induced by liver ischemia involves Toll-like receptor 4 dependent reactive oxygen species production and calcium-mediated signaling. J Exp Med 2007;204:2913-2923.

[74] Chen Y, Zhang W, Bao H, He W, Chen L. High Mobility Group Box 1 Contributes to the Acute Rejection of Liver Allografts by Activating Dendritic Cells. Front Immunol 2021;12:679398.

[75] Zou H, Yang Y, Gao M, Zhang B, Ming B, Sun Y, et al. HMGB1 is involved in chronic rejection of cardiac allograft via promoting inflammatory-like mDCs. Am J Transplant 2014;14:1765-1777.

[76] Bertheloot D, Latz E. HMGB1, IL-1alpha, IL-33 and S100 proteins: dual-function alarmins. Cell Mol Immunol 2017;14:43-64.

Chapter 2:

Disulfide High-Mobility Group Box 1 Drives Ischemia-Reperfusion Injury in Human Liver Transplantation

2.1 ABSTRACT

Background & Aims: Sterile inflammation is a major clinical concern during ischemia-reperfusion injury (IRI) triggered by traumatic events, including stroke, myocardial infarction, and solid organ transplantation. Despite high-mobility group box 1 (HMGB1) clearly being involved in sterile inflammation, its role is controversial because of a paucity of patient-focused research.

Approach and Results: Here, we examined the role of HMGB1 oxidation states in human IRI following liver transplantation. Portal blood immediately following allograft reperfusion (liver flush; LF) had increased total HMGB1, but only LF from patients with histopathological IRI had increased disulfide-HMGB1 and induced Toll-like receptor 4–dependent tumor necrosis factor alpha production by macrophages. Disulfide HMGB1 levels increased concomitantly with IRI severity. IRI+ pre-reperfusion biopsies contained macrophages with hyperacetylated, lysosomal disulfide-HMGB1 that increased post-reperfusion at sites of injury, paralleling increased histone acetyltransferase general transcription factor IIIC subunit 4 and decreased histone deacetylase 5 expression. Purified disulfide-HMGB1 or IRI+ blood stimulated further production of disulfide-HMGB1 and increased pro-inflammatory molecule and cytokine expression in macrophages through a positive feedback loop.

Conclusions: These data identify disulfide-HMGB1 as a mechanistic biomarker of, and therapeutic target for, minimizing sterile inflammation during human liver IRI.

2.2 INTRODUCTION

Sterile inflammation involves a complex interplay between the innate and adaptive immune systems, thereby playing a key role in the overall outcome of mechanical trauma, chemical and environmental insults, and ischemia-reperfusion injury (IRI). IRI is a common clinical condition

triggered by sepsis, cardiogenic shock, vascular surgery, or organ retrieval for transplantation. Despite this significant clinical concern, there are currently no therapeutics or patient-specific diagnostics available because of the continuing lack of knowledge of the underlying IRI immune mechanisms.

Damage-associated molecular patterns (DAMPs) were proposed as endogenous danger signals generated in response to cellular stress that could be recognized by germline-encoded pattern recognition receptors (PRRs) typically expressed by innate immune cells [1]. With the potential for any intracellular component that is detected in the extracellular space by a PRR-bearing cell to act as a DAMP, the search for one specific to IRI has proven difficult. We previously showed, by longitudinal evaluation of cytokine signatures in the human blood of orthotopic liver transplantation (OLT) recipients, that the innate-adaptive immune switch occurs during transplantation, once the recipient portal vein blood (PV) is reperfused through the donor organ (liver flush; LF) [2]. Screening for activation of a panel of 10 PRRs by these two blood samples, we then showed that Toll-like receptor (TLR) 4 and TLR9 were preferentially activated by OLT patient portal blood with biopsy-proven IRI pathology [3], considerably narrowing the search for IRI-mediating DAMPs.

High-mobility group box 1 (HMGB1) is a well-characterized DAMP that can bind to TLR4, TLR9, or other receptors, depending on its redox state. Under homeostatic conditions, HMGB1 functions as a DNA scaffolding protein in all nucleated cells. Normal nuclear functions occur under reducing conditions; therefore, nuclear HMGB1 is in its fully reduced, “all-thiol” redox state [4, 5]. Damaged epithelial cells, including hepatocytes, passively release their intracellular HMGB1 into

the extracellular space [6-9]. HMGB1 has been shown to undergo oxidation that modulates various aspects of its function, including subcellular localization and pro-inflammatory chemokine or cytokine activity by signaling through TLR4 [10-12]. Active secretion of the partially oxidized, "disulfide" redox form of HMGB1 by monocytes and macrophages has been described, in which shuttling of the protein into the cytosol and/or prevention of nuclear import or reentry of HMGB1 is required [4], and disulfide-HMGB1 is exclusively responsible for HMGB1-TLR4 signaling, leading to further pro-inflammatory cytokine secretion [12]. Posttranslational modification, in the form of hyperacetylation on lysine residues within one or both nuclear localization sequences, is responsible for this cytoplasmic accumulation [5]. Because HMGB1 does not contain a leader sequence, the protein is released by a non-classical secretory pathway involving specialized lysosomal-associated membrane glycoprotein 1-positive (LAMP1+) vesicles of the endolysosomal compartment [13]. Secreted disulfide-HMGB1 can then potentially mediate a positive feedback loop by binding to TLR4 and initiating a downstream pro-inflammatory signaling cascade, which can further induce cell death [14, 15].

Because liver IRI has been shown to trigger HMGB1 release[16], which then signals through TLR4 [17] in mouse models, we hypothesized that disulfide-HMGB1-producing macrophages promote IRI in human OLT through TLR4. We used blood and liver biopsies from a large cohort of 92 OLT recipients with and without biopsy-proven IRI and identified the contribution of macrophage-derived disulfide-HMGB1 to the generation and perpetuation of pro-inflammatory macrophages in patients with IRI. Notably, the histone acetyltransferase (HAT), general transcription factor IIIC subunit 4 (GTF3C4), was significantly increased whereas histone deacetylase 5 (HDAC5) was significantly decreased in biopsies from IRI+ patients compared to

IRI− patients, providing a molecular mechanism for therapeutic targeting to mitigate downstream effects of IRI and improve overall OLT clinical outcomes. Additionally, GTF3C4 and/or HDAC5 expression levels could serve as a biomarker of IRI across multiple clinical situations, such as stroke, sepsis, myocardial infarction, or vascular surgery, as well as solid organ transplantation.

2.3 MATERIALS AND METHODS

2.3.1 Study design and sample collection

Adult primary OLT recipients were recruited between May 10, 2013 and July 28, 2018 (Tables 1-3). Routine standard-of-care and immunosuppressive therapy were administered as specified by University of California–Los Angeles (UCLA) liver transplantation (LT) protocols. All studies described were reviewed and approved by the UCLA Institutional Research Board (IRB; #13-000143). Patients gave written informed consent before their participation in the study. Study data were collected and managed using REDCap electronic data capture tools hosted at UCLA [18]. Donor organs were procured from both donation after brain death (DBD) and donation after circulatory death (DCD) donors using standardized techniques. No donor organs were obtained from executed prisoners or other institutionalized persons. Organs were perfused with and stored in cold University of Wisconsin solution (ViaSpan; Bristol-Myers Squibb Pharma, Garden City, NY). Cold ischemia time was defined as the time from perfusion of the donor with preservation solution to removal of the liver from cold storage. Tru-Cut needle biopsies were taken of donor allografts ~2 hours before transplantation (PRE biopsies). Recipient venous blood was collected with acid-citrate-dextrose anticoagulant during two main phases relative to the transplant: preoperative (PO) and postoperative at 1 day, 1 week, and 1 month. Intraoperative portal blood was collected from the recipient portal vein before reperfusion and as it was first flushed through

the vena cava of the donor liver during reperfusion (LF). Protocol Tru-Cut needle biopsies were taken from the left lobe intraoperatively after complete revascularization of the allograft (2 hours post-reperfusion; POST biopsies) before surgical closing of the abdomen and graded for IRI as described [2].

2.3.2 OLT recipient and donor characteristics

Ninety-two OLT recipients were scored for IRI by histopathology using intraoperative post-reperfusion biopsies of the liver allograft. Demographic data and clinical parameters of the recipients are shown in Table 1, donors are shown in Table 2, and combined recipient/donor parameters for the transplant are shown in Table 3. Sub-cohort selection was necessary in some assays, as described in the figure legends, because of limited patient sample quantities. For correlation between demographic data and IRI, the Student t test was used for continuous variables, and Fisher's exact test was used for categorical variables. There was no correlation between IRI status and any of the parameters for the overall cohort or any sub-cohorts used except bilirubin levels at the opening of the post-transplant phase, ~8 hours post-reperfusion, which were significantly increased in IRI+ patients (Table 1).

2.3.3 HMGB1 detection in patient plasma samples

HMGB1 enzyme-linked immunosorbent assay (ELISA; IBL International, Hamburg, Germany) was performed according to the manufacturer's instructions. To determine the redox state of HMGB1, OLT patient LF samples were run undiluted using gel electrophoresis and detected with anti-HMGB1 polyclonal antibody (Ab; Abcam, Cambridge, MA). The ratio of 25-kD band (bottom band, disulfide-HMGB1) to 28-kD band (top band, all-thiol HMGB1) was quantified

using ImageJ (NIH, Bethesda, MD). The ratio of all-thiol/disulfide-HMGB1 determined by western blotting analysis was used to extrapolate the amount of each redox form of HMGB1 present in patient LF samples by dividing the total HMGB1 content (as determined by ELISA) by each redox form's relative amount for each patient sample.

2.3.4 Human primary monocyte isolation, immune phenotyping, and functional cytokine assay

Monocytes were enriched from healthy donor blood using negative selection with RosetteSep technology (StemCell Tech, Vancouver, Canada) at a final purity of >92.6%. For monocyte stimulation, 30,000 cells were exposed to either RPMI-1640 media with 10% fetal bovine serum alone or 10 ng/mL of macrophage colony-stimulating factor (R&D Systems, Minneapolis, MN), 50 ng/mL of lipopolysaccharide (LPS; Invivogen, San Diego, CA), 200 ng/mL of all-thiol HMGB1 (HMGBiotech, Milan, Italy), 200 ng/mL of disulfide-HMGB1 (HMGBiotech), or with 10% patient LF samples and incubated at 37°C for 2, 4, 8, or 24 hours or 3 days.

Tumor necrosis factor alpha (TNFα) ELISA (R&D systems) was performed, according to the manufacturer's instructions, on supernatants from monocytes stimulated with purified HMGB1 in either the all-thiol or disulfide redox state and compared to the well-characterized canonical TLR4-ligand, LPS, to determine the HMGB1-mediated timing of monocyte activation and TNFα secretion **(Fig. 2-S5A)** and the functional threshold of disulfide-HMGB1 (**Fig. 2-S5B**).

For confocal microscopy, cells were incubated with primary antibodies for CD68 (BioLegend, San Diego, CA), HMGB1, LAMP1, or acetyl-lysine (a-K; Abcam), then appropriate fluorescence-

conjugated secondary antibodies and 4′,6-diamidino-2-phenylindole (DAPI). Cells were imaged in optically clear wells (Ibidi, Fitchburg, WI), with liquid mounting media (Ibidi).

Monocyte phenotypes were assessed by flow cytometry using fluorochrome-labeled detection antibodies: CD14/Brilliant Violet 785 (clone M5E2),CD16/Brilliant Violet 510 (clone 3G8), CD11b–planar cell polarity/cyanine 5 (clone ICRF44), CD68-PE (phycoerythrin)/cyanine 7 (clone Y1/82A), CD86/Brilliant Violet 605 (clone IT2.2), human leukocyte antigen (HLA)-DR/Brilliant Violet 650 (clone L243), galectin-9 (Gal-9)/fluorescein isothiocyanate (clone 9M1-3), T-cell immunoglobulin mucin-3 (TIM3)/allophycicyanin (clone F38-2E2), and T-cell immunoglobulin mucin-4 (TIM4)-PE (clone 9F4) from BioLegend; CD66a/Alexa Fluor 700 (clone COL-1) from Novus Biologicals; and CD80-APC/H7 (clone L307.4) and programmed death-ligand 1 (PDL1)/PE-CF594 (clone MIH1) from BD Biosciences (San Jose, CA). Samples were run on an LSR Fortessa (BD Biosciences) within 7 days of fixation. Data were acquired with FACSDiva software (BD Biosciences, San Jose, CA) and analyzed using FlowJo software (TreeStar, Ashland, OR).

2.3.5 TLR4-activation functional assay

Human TLR4 (hTLR4)-specific HEK-Blue reporter cells (InvivoGen) were grown, maintained, and used as described [3]. Neutralizing Abs (InvivoGen) were added for 1 hour before cell stimulation with patient LF to block the function of TLR4, CD14, and/or myeloid differentiation protein 2 (MD2).

2.3.6 Hierarchical clustering analysis

Abundances irrespective of conditions were normalized using robust Z-scaling with median and median absolute deviation. Then, medians of scaled values for each group were color-coded and plotted in heatmaps. Unsupervised hierarchical clustering was performed on rows and columns using Euclidean distance as the similarity measure with Ward's linkage.

2.3.7 Immunohistochemical and immunofluorescence staining of allograft biopsies

For immunohistochemical staining, formalin-fixed, paraffin-embedded biopsy sections were stained with primary Ab to CD68, detected using labeled horseradish peroxidase (Agilent, Santa Clara, CA), and visualized with diaminobenzidine, then counterstained with hematoxylin. Whole stained slides were converted to high-resolution digital brightfield images using an Aperio ScanScope AT high-throughput scanning system (Leica Biosystems, Buffalo Grove, IL). Images were then acquired using Aperio ImageScope software (Leica Biosystems), and analysis was performed using Tissue Studio software (Definiens).

For immunofluorescence (IF) staining, allograft biopsies were fixed in phosphate-buffered 4% paraformaldehyde (PFA), then impregnated with 30% sucrose. Samples were embedded in gelatin blocks, then optimum cutting temperature (OCT) embedded and cryosectioned. IF of tissue sections was performed as described [19, 20]. Sections were then incubated with primary Abs for CD68 (BioLegend), HMGB1 (Abcam), LAMP1 (Abcam), or a-K (Abcam), then incubated with appropriate fluorescence-conjugated secondary Abs and DAPI. Sections were mounted on a glass slide with Prolong Gold Antifade, coverslipped, and allowed to dry/cure overnight.

2.3.8 Confocal laser scanning microscopy of IF staining

Samples were observed and imaged using three-dimensional confocal laser scanning microscopy as described [19, 20]. In brief, IF images were acquired using a scanning confocal laser scanning microscope (LSM 880; Zeiss, Oberkochen, Germany), using Zen Black 2009 software.

2.3.9 Reconstructing HMGB1 subcellular localization within macrophages in three dimensions

The three-dimensional structure of macrophages in the allograft was reconstructed from confocal z-stacks using Imaris software (version 9.2; Bitplane AG, Zürich, Switzerland). Digital isolation of macrophages present in the tissue sample was performed for each image as described [19, 20]. To verify localization of labeled proteins at the subcellular level, liver biopsy sections were counterstained with the nuclear dye, DAPI, and/or the lysosomal marker, LAMP1, and nuclear or cytoplasmic/lysosomal localization of HMGB1 was determined based on colocalization with contents of the DAPI+ and/or LAMP1+ compartment remodeled in three dimensions as described in **Fig. 2-S3**.

2.3.10 RNA sequencing analysis

RNA sequencing (RNAseq) testing was performed by the UCLA Technology Center for Genomics and Bioinformatics and analyzed as described [2]. Transcript abundances are expressed as transcripts per million [21] log2 scale. Data have been deposited in the National Center for Biotechnology Information's Gene Expression Omnibus (GEO) and are accessible through GEO series accession number GSE15 1648.

2.3.11 Statistical analysis

Two-way analysis of variance (ANOVA) with Sidak's multiple comparisons test was used to determine differences among time and/or IRI status, unless otherwise indicated. A P value <0.05 was considered significant.

2.4 RESULTS

2.4.1 HMGB is released from donor hepatic tissue into patient portal blood following reperfusion

To understand when HMGB1 release occurs in the setting of solid organ transplantation, we performed an ELISA on 10 OLT patient blood samples (five IRI−, five IRI+), obtained at various key time points pre-transplant (PO), intraoperative (PV and LF), and post-transplant (day 1, week 1, week 2, week 3, and month 1) for levels of total HMGB1 (**Fig. 2-1**). HMGB1 was found to be <10 ng/mL in circulating systemic blood at all timepoints evaluated (**Fig. 2-1A**). Recipient PV obtained just before reperfusion showed slightly elevated levels of HMGB1, which were significantly increased immediately upon reperfusion through the donor allograft (LF; **Fig. 2-1A**). We then performed ELISA for HMGB1 on paired PV and LF samples for the full cohort of 92 OLT recipients (n = 92; 46 IRI−, 46 IRI+; Tables 1-3). Although overall HMGB1 levels were not significantly different between IRI+/– groups at either time point (**Fig. 2-1B**), HMGB1 levels increased significantly more over time in IRI+ patients than IRI− (**Fig. 2-1C**).

2.4.2 IRI status of OLT patients reflects oxidation state of HMGB1 in portal blood

Because HMGB1 presence in LF alone did not predict IRI status, we investigated the redox state of HMGB1, in OLT patient LF samples (**Fig. 2-2**). It has been shown that all-thiol HMGB1 is a

chemoattractant whereas disulfide-HMGB1 is the form that results in cytokine-inducing activity [12]; therefore, we reasoned that IRI+ patients may be differentially stimulating TNFα secretion from monocytes attributed to varying content of disulfide or all-thiol HMGB1. Gel electrophoresis can separate the two redox forms of HMGB1 attributable to the disulfide form running slightly faster than the all-thiol form [12]. We performed western blotting on LF samples from OLT patients with HMGB1 levels >400 ng/mL, the detectable limit in our assay (n = 77; 43 IRI−, 44 IRI+), to determine the ratio of disulfide to all-thiol HMGB1 in the LF (**Fig. 2-2A**). We then combined this information with the concentrations obtained in the HMGB1 ELISA assay from **Fig. 2-1** to extrapolate the concentration of all-thiol and disulfide-HMGB1 in patient LF samples (**Fig. 2-2B**). As suspected, IRI+ patients had statistically increased disulfide-HMGB1 than IRI− patients in their LF blood. Additionally, stratifying by IRI severity revealed that disulfide-HMGB1 levels steadily increase as histopathological IRI increases (**Fig. 2-2C**).

We added patient LF to monocytes and compared TNFα secretion from cells cultured with samples from 40 OLT patients (20 IRI−, 20 IRI+; **Fig. 2-2D**). LF from IRI+ recipients activated monocytes to secrete significantly more TNFα than IRI− patient LF samples at the 8-hour time point, both of which were abrogated upon pretreatment with a neutralizing anti-TLR4 monoclonal antibody (mAb), suggesting the HMGB1 found in IRI+ patients is in the disulfide redox state. Additionally, we were able to confirm that LF samples from IRI+ recipients containing high levels of disulfide-HMGB1 stimulated strong TNFα secretion from monocytes through TLR4 activation whereas IRI− patient LF did not (**Fig. 2-2E**).

2.4.3 OLT-IRI+ recipient blood activates macrophages toward pro-inflammatory phenotype through TLR4

HMGB1 signals through TLR4 only when it is partially oxidized into its disulfide redox form [12]. Our previous studies indicated that OLT-IRI+ patient LF samples were significantly more capable of signaling through TLR4 when examining a panel of commercially available hTLR-transfected HEK-293 cell lines [3]. Of note, a significant increase in IRI+ patient HMGB1 in LF relative to its PV baseline occurred (**Fig. 2-1C**), which mirrored the pattern observed in TLR4 activation in these same samples [3]. Therefore, we sought to determine whether patient liver macrophages sense HMGB1 through TLR4 similar to peripheral third-party monocytes, given that macrophages are the primary TLR4+ responders to HMGB1 in the liver by their TNFα production [22]. TLR4 transcripts are present in pre-reperfusion donor allografts and increased in post-reperfusion allografts (**Fig. 2-3A**), and IRI+ patients have increased transcripts compared to IRI− patients at both time points, despite the number of CD68+ cells in biopsies from OLT patients being similar (**Fig. 2-S1A,B**). IF staining of the biopsies for macrophages showed they are positive for TLR4 that colocalizes to HMGB1 (**Fig. 2-3B**).

To investigate whether HMGB1 requires the same cofactors as LPS to signal through TLR4, we pretreated HEK-293 cells transfected with hTLR4 with neutralizing antibodies to TLR4, CD14, and/or MD2, then added patient LF and checked for activation of TLR4 (**Fig. 2-3C**). As expected, pretreatment with anti-TLR4 mAb abolished TLR4 activation by patient LF regardless of whether it was from an IRI− or IRI+ patient. IRI− patient blood was less capable of activating TLR4 when CD14 activity was neutralized, but lack of MD2 signaling did not significantly affect TLR4 activation. Surprisingly, IRI+ patient LF activation of TLR4 was unaffected by absence of CD14

or MD2. Control disulfide-HMGB1 was only partially affected by CD14 and/or MD2 absence (**Fig. 2-S7C**), suggesting that although it can signal through TLR4 by these cofactors, they are not required. Overall, the effect observed in patients is a combination of ligand and receptor differences.

2.4.4 IRI+ OLT recipients have disulfide-HMGB1-producing macrophages in their allografts that increase after reperfusion

To determine the effect of IRI on the subcellular localization of HMGB1, IF staining was performed. Consistent with other observations [17], HMGB1 was almost exclusively localized in the nucleus of hepatocytes in pre-transplant livers of IRI− patients with no injury (**Fig. 2-S2**). In patients with IRI, the intensity of pre-transplant HMGB1 staining was increased diffusely throughout the cytoplasm of some hepatocytes, whereas others were depleted of HMGB1 entirely. Active secretion of the disulfide redox form of HMGB1 by monocytes and macrophages requires cytoplasmic translocation as well as loading into LAMP1+ cytoplasmic vesicles [4]. IF staining of patient allografts revealed CD68+ macrophages in clusters among healthy hepatocytes in both IRI− and IRI+ biopsies (**Fig. 2-S2**), but appeared to have most of their HMGB1 translocated into cytoplasmic vesicles in only IRI+ patient allografts (**Fig. 2-S2, bottom row**). Therefore, we characterized the subcellular localization of HMGB1 of macrophages to determine its redox state using three-dimensional reconstruction of high-resolution confocal laser scanning microscopy images of human OLT allografts (**Fig. 2-4**), as described in **Fig. 2-S3**. We found that HMGB1 translocated into the cytoplasm of macrophages in the allografts of IRI+ patients (**Fig. 2-4A, arrows**), which was significantly different (**Fig. 2-4B**) than macrophages found in IRI− allografts (**Supporting Videos S1 and S2**). Furthermore, we found that the majority of cytoplasmic HMGB1

was restricted within LAMP1+ vesicles of CD68+ macrophages in allografts of IRI+ patients, but not IRI− recipients, at both time points (**Fig. 2-4C, E**). These findings suggest that the protective effect occurring in IRI− patients is, at least in part, caused by the prevention of disulfide-HMGB1 formation and release by macrophages.

2.4.5 Increased GTF3C4 and decreased HDAC5 contribute to hyperacetylation of macrophage-HMGB1 in IRI+ OLT patients

Given that acetylation of HMGB1 is known to influence its subcellular localization and partial oxidation into secretable disulfide-HMGB1 in macrophages [23], we investigated the acetylation status at lysine residues of HMGB1 in OLT recipient biopsies by IF and confocal microscopy. We found that HMGB1 in IRI+ recipients colocalized predominantly with staining for acetylated lysine residues (**Fig. 2-5A, B**), indicating that translocation of HMGB1 observed in macrophages from these patient allografts (**Fig. 2-4**) was mediated by hyperacetylation. Along these lines, only a small percentage of acetylated lysine staining colocalized to HMGB1 in macrophages from IRI− biopsies (**Fig. 2-5A, B**).

Hyperacetylation of nuclear proteins, including HMGB1, is performed by HATs and balanced by the activity of histone deacetylases (HDACs). Because we observed a difference in hyperacetylation of HMGB1 that corresponded to recipient IRI status, we analyzed the expression of HATs and HDACs by RNAseq (**Fig. 2-5C, D**) in OLT recipient biopsies. Of 12 genes encoding HATs whose expression was detected in OLT patient biopsies (**Fig. 2-S4**), seven were differentially expressed between pre-reperfusion and post-reperfusion time points. Interestingly, GTF3C4, a gene encoding an HAT also known as KAT12, had increased transcripts in IRI+

allografts obtained post-reperfusion (**Fig. 2-5C**). Furthermore, of the 12 genes encoding HDACs found to be expressed in OLT recipient biopsies (**Fig. 2-S5**), six were differentially expressed from pre-reperfusion to post-reperfusion, yet only HDAC5 was decreased in IRI+ patient biopsies as compared to IRI− (**Fig. 2-5D**), and this occurred at the same time point that GTF3C4 transcripts were decreased.

2.4.6 Disulfide-HMGB1+ LF triggers monocytes to translocate nuclearHMGB1 into LAMP1+ vesicles and become more pro-inflammatory

It has been reported that HMGB1 is selectively internalized by infiltrating mononuclear phagocytes [24]. Furthermore, HMGB1 has been proposed to perpetuate inflammatory amplification loops in other disease settings, such as infection [25]. We found a significant increase in disulfide-HMGB1-producing macrophages in the post-reperfusion biopsies over the pre-reperfusion samples; therefore, we speculated that this uptake of HMGB1 by newly arriving myeloid cells could stimulate them to become disulfide-producing macrophages within the allograft. To investigate this possibility, we stimulated monocytes with either HMGB1-containing patient LF or commercially available purified all-thiol HMGB1 or disulfide-HMGB1 as controls. We found that IRI+ LF stimulated monocytes to translocate their own HMGB1 into their cytoplasm and package it into lysosomal vesicles within 2 hours (**Fig. 2-6A, B**), similar to results obtained with control disulfide-HMGB1 (**Fig. 2-S6A, B**), whereas IRI− LF (**Fig. 2-6A, B**) and all-thiol HMGB1 (**Fig. 2-S6A, B**) did not induce this change. Additionally, disulfide-HMGB1-containing IRI+ LF stimulated a change in phenotype of monocytes in culture for 3 days (**Fig. 2-6C**) to become more pro-inflammatory and invasive, upregulating HLA-DR, CD80, CD86, and CD11b while simultaneously down-regulating molecules that were increased in monocytes

cultured with IRI− LF, including carcinoembryonic antigen-related cell adhesion molecule 1 (biliary glycoprotein), TIM3, TIM4, and programmed death-ligand 1 (PD-L1), molecules involved in anti-inflammatory and pro-resolution as well as T-cell exhaustion.

2.5 DISCUSSION

IRI is a pathophysiological process in which hypoxic organ damage is accentuated following return of blood flow and oxygen delivery. Liver IRI consists of direct hepatocellular damage as the result of the ischemic insult, as well as delayed dysfunction and damage that result from activation of innate inflammatory pathways. Innate immune cells are activated after ischemic injury to initiate the tissue repair processes needed to regain homeostasis and provide defense against microbial invasion. However, excessive activation can lead to exaggerated local and systemic inflammation that may extend the tissue damage. HMGB1 is an early mediator of inflammation and cellular injury after IRI, and its pro-inflammatory actions have been shown to require TLR4 in liver IRI mouse models [16, 26, 27]. Our human studies have confirmed liver IRI to be TLR4-driven [3]; therefore, we sought to determine whether pro-inflammatory HMGB1 was mobilized in response to IRI in LT patients. Similar to earlier reports [28], we found that HMGB1 levels are increased following reperfusion in OLT (LF sample); however, this did not correlate to biopsy-proven patient IRI status. We provide evidence that in human OLT, IRI+ recipient LF contained a significantly increased amount of disulfide-HMGB1, which corresponded to the degree of IRI severity, the amount of TNFα secreted by LF-stimulated macrophages, as well as activation of TLR4. Therefore, we propose that the partially oxidized disulfide-HMGB1 redox form is a more relevant mechanistic biomarker and therapeutic target than total HMGB1 in OLT-IRI and, likely, other clinical states involving sterile inflammation.

Our data show that TLR4 is increased in IRI+ liver grafts and is co-localized with HMGB1 in the cytoplasmic vesicles of macrophages within the allograft. However, the precise mechanism of TLR4 activation by HMGB1 remains to be clarified. Direct binding of HMGB1 to TLR4 [14] or LPS-mediated binding [29] are observed with CD14 [15], or MD2 proposed to be necessary [30, 31] for the latter. Interestingly, in our human studies, HMGB1 did not require either MD2 or CD14 or even LPS, given that the addition of polymyxin B did not alter the ability of patient LF or control disulfide-HMGB1 to activate TLR4 [3] or stimulate TNFα from monocytes. Despite these conflicting results, the affinity between HMGB1 and TLR4 is very low [14], indicating that one or more binding partners are required to enhance this association. It is possible that there is an alternate high-affinity receptor (or co-receptor) for HMGB1 on the surface of macrophages for TLR activation, and scavenger receptors have been proposed in this capacity [32], specifically class A scavenger receptors macrophage scavenger receptor 1 and macrophage receptor with collagenous structure (MARCO) [24]. TLR4 signals that are activated by HMGB1/scavenger receptors or HMGB1 with other co-receptors may be different in OLT-IRI than those activated by LPS, given that it was shown that MARCO uptake of HMGB1 led to neuroprotection by the M2 macrophages generated, whereas uptake by TLR4 alone resulted in the generation of M1 macrophages secreting pro-inflammatory cytokines [32]. Our study uncovers the role of the disulfide-HMGB1/TLR4/TNFα axis in driving the OLTIRI- generated sterile inflammation response toward an adaptive immunity, but further characterization of the precise molecules involved in this pathway is warranted.

A limitation of this clinical study is that we were unable to determine the originating cellular source, or specific timing and/or localization of HMGB1 oxidation. It is well established that IR-

stressed hepatocytes translocate their nuclear HMGB1 into the cytoplasm [7], and we observed this effect in patient allografts as well. Therefore, it is reasonable to speculate that injured hepatocytes are a major cellular source of extracellular HMGB1 found in patient blood. However, we found no evidence to support disulfide-HMGB1 originating from within hepatocytes, given that cytoplasmic HMGB1 found in hepatocytes was diffuse rather than localized into LAMP1+ vesicles. We also cannot exclude the possibility that non-disulfide HMGB1 originating from damaged hepatocytes is partially oxidized into disulfide-HMGB1 in the extracellular space by reactive oxygen species generated under IRI. However, high oxidative environments such as this have been shown to produce a terminally oxidized, sulfonyl, non-immunogenic form of HMGB1 [11], making this more likely to be a mechanism for initiation of IRI rather than a mechanism for driving IRI once it has begun.

We found that pre-transplant donor allografts contained CD68+ myeloid cells with HMGB1 restricted primarily in LAMP1+ cytoplasmic vesicles rather than the nucleus, indicating that these cells were generated initially as a response to ischemic conditions resulting from organ procurement. Disulfide-HMGB1-containing CD68+ cells were significantly increased in IRI+ allografts post-reperfusion, suggesting that IRI+ recipient blood flow into the organ amplified the initial ischemic response. HMGB1 is important in perpetuating inflammatory amplification loops in other disease settings such as infection [25]; therefore, it is possible that disulfide-HMGB1, either alone or in concert with other binding partners, induces a self-perpetuating cycle in OLT-IRI by activating macrophages to secrete more disulfide-HMGB1. In agreement with this concept, the addition of exogenous disulfide-HMGB1 to freshly isolated monocytes caused them to translocate hyperacetylated HMGB1 into cytoplasmic vesicles within 2 hours, whereas the

addition of all-thiol HMGB1 did not initiate any further translocation out of the nuclear compartment. We also found macrophages in donor allografts of IRI+ patients with translocated HMGB1 in their LAMP1+ vesicular compartment that increased after reperfusion, indicating that these macrophages are differentially activated from those found in IRI− patient biopsies that predominantly contained nuclear HMGB1. Because our in vitro experiments with monocytes treated with LF from IRI+ patients resulted in the up-regulation of several pro-inflammatory molecules, including HLA-DR, CD80, and CD86, it is reasonable to presume a comparable liver graft macrophage activation profile following stimulation with patient LF over the course of the first week post-transplant. Attenuating the activities of these specific cells may be a preferable therapeutic approach toward mitigating hepatic IRI and improving LT clinical outcomes.

Release of HMGB1 by LPS-challenged macrophages is dependent on the activation of poly [ADPribose] polymerase 1 [33], which ultimately regulates the translocation of HMGB1 to the cytoplasm through up-regulating the acetylation of HMGB1 by elevating the activity ratio of HATs to HDACs, which can catalyze acetylation and deacetylation of HMGB1 [23]. GTF3C4 can act as an HAT by interacting with histone H3 [34], a level of epigenetic control which was shown to regulate T-helper cell differentiation into effector phenotypes [35]. Our RNAseq analysis identified increased expression of GTF3C4 in IRI+ patient allografts, making this a potential regulator of IRI and downstream effector differentiation of CD4+ T cells by HMGB1 hyperacetylation in macrophages in which HMGB1 has also been described as having a role in histone H3 activity, and these two proteins are likely to be in regular close contact. Histone deacetylase 4 (HDAC4) and HDAC5 [36, 37] have been implicated in ischemic brain injury, and our mouse studies have suggested that the HDAC, sirtuin 1 (Sirt1), plays a role in mediating liver

IRI [38]. In our screening of RNAseq results for HDACs related to human OLT-IRI, HDAC5 was found to be increased in IRI+ patients post-reperfusion, whereas HDAC4 was significantly decreased and Sirt1 was similarly expressed between IRI+/– OLT recipients. These data indicate that, in human OLT recipients, HDAC5 is the major HDAC needed to deacetylate HMGB1 and constrain it within the nuclear compartment for regaining cellular homeostasis. A larger cohort with more representative cases across all IRI severities will be necessary to assess correlation with IRI severity. Taken together, these results indicate that the combined effect of increased GTF3C4 and decreased HDAC5 contribute to overall hyperacetylation of HMGB1 in macrophages of IRI+ patients, which drives it into cytoplasmic vesicles for secretion as a pro-inflammatory cytokine capable of self-perpetuating clinical or subclinical levels of inflammation and, possibly, an initiation of adaptive immune responses by TLR4 signaling.

Ischemia-reperfusion injury is not limited to solid organ transplantation, with aspects of the condition occurring in many other surgical situations and health conditions. However, it is currently an unavoidable consequence of the transplantation procedure, allowing us the unique opportunity to investigate the mechanisms of HMGB1-stimulated pro-inflammatory macrophage activation in a powered patient cohort. We found that the disulfide redox state of HMGB1 is responsible for mediating IRI and its subsequent switch from innate to adaptive immune activation through TLR4 signaling in macrophages found in the allograft. Furthermore, this redox state of HMGB1 stems from macrophages activated to hyperacetylate HMGB1, thereby resulting in its translocation from the nucleus into the cytoplasmic vesicles for secretion upon further stimulation. The histone acetyltransferase, GTF3C4, and deacetylase, HDAC5, appear to work in concert to promote translocation and partial oxidation of HMGB1. Therefore, disulfide-HMGB1, GTF3C4,

and HDAC5 comprise a group of molecules that could not only serve as putative mechanistic biomarkers, but also as targets for future therapeutic development aimed at decreasing the occurrence of IRI in the human OLT setting as well as other types of sterile inflammatory conditions.

2.6 ABBREVIATIONS

Ab, antibody

a-K, acetyl-lysine

ANOVA, analysis of variance

DAMP, danger-associated molecular pattern

DAPI, 4′,6-diamidino-2-phenylindole

ELISA, enzyme-linked immunosorbent assay

Gal-9, galectin-9

GTF3C4, general transcription factor IIIC subunit 4

HAT, histone acetyltransferase

HDACs, histone deacetylases

HDAC5, histone deacetylase 5

HLA, human leukocyte antigen

HMGB1, high-mobility group box 1

hTLR4, human TLR4

IF, immunofluorescence

IRI, ischemia-reperfusion injury

LAMP1+, lysosomal-associated membrane glycoprotein 1-positive

LF, liver flush

LPS, lipopolysaccharide

LT, liver transplantation

mAb, monoclonal antibody

MD2, myeloid differentiation protein 2

OCT, optimum cutting temperature

OLT, orthotopic liver transplantation

PRR, pattern recognition receptor

PD-L1, programmed death-ligand 1

PE, phycoerythrin

PFA, paraformaldehyde

PO, preoperative

PV, portal vein blood

RNAseq, RNA sequencing

TIM3, T-cell immunoglobulin mucin-3

TIM4, T-cell immunoglobulin mucin-4

TLR, Toll-like receptor

TNFα, tumor necrosis factor alpha

UCLA, University of California–Los Angeles.

2.7 ACKNOWLEDGMENTS

We acknowledge the BSCRC Imaging Core, as well as thank Gregg Kunder, Stephanie Younan, and the liver transplant team who go above and beyond to collect patient samples for this

project. We hereby express our thanks for all of the organ donors and their families, for giving the gift of life and the gift of knowledge, by their generous donation.

Table 2-1. Recipient Characteristics.

Clinical and Demographic Data	(n = 92)	IRI⁻ (n = 46)	IRI⁺ (n = 46)	
Recipient:				
Characteristic	Value	Value	Value	*P* Value*
Age, years, mean ± SD	56 ± 11	57 ± 11	54 ± 10	0.21
Sex, n (%)				0.52
Female	36 (39)	20 (43)	16 (35)	
Male		56 (61)	26 (57)	30 (65)
Race, n (%)				0.97
Asian		8 (9)	4 (9)	4 (9)
Black	5 (5)	3 (7)	2 (4)	
White	47 (51)	24 (52)	23 (50)	
Other		32 (35)	15 (33)	17 (37)
Ethnicity, n (%)				0.50
Hispanic/Latino	38 (41)	16 (35)	22 (48)	
Non-Hispanic/Latino	51 (55)	28 (61)	23 (50)	
Unknown/not reported	3 (3)	2 (4)	1 (2)	
Liver disease etiology, n (%)				0.12
Alcohol-associated	23 (25)	7 (15)	16 (35)	
HBV		6 (7)	3 (7)	3 (7)
HCV		33 (36)	18 (39)	15 (33)
NAFLD/NASH	15 (16)	10 (22)	5 (11)	
AIH		4 (4)	2 (4)	2 (4)
PBC		2 (2)	2 (4)	0 (0)
PSC		4 (4)	2 (4)	2 (4)
ALF		2 (2)	2 (4)	0 (0)
Other		3 (3)	0 (0)	3 (7)
HCC, n (%)	26 (28)	16 (35)	10 (22)	0.25
MELD, at list, mean ± SD	26 ± 12	25 ± 12	28 ± 11	0.21
MELD, at transplant, mean ± SD	36 ± 6	36 ± 5	36 ± 6	0.67
Transplant(s), n (%)				0.39
Isolated liver	78 (85)	41 (89)	37 (80)	
Liver-kidney	14 (15)	5 (11)	9 (20)	
Split liver, n (%)	1 (1)	1 (2)	0 (0)	>0.99
LFTs, opening, mean ± SD				
ALT	553 ± 559	505 ± 466	602 ± 559	0.37
AST	1,127 ± 1,086	1,040 ± 980	1,214 ± 1,188	0.45
Bilirubin	8.3 ± 6.5	6.9 ± 4	9.7 ± 8.1	0.04*
INR	1.4 ± 0.2	1.4 ± 0.2	1.5 ± 0.3	0.4

*P Value <0.05. Abbreviations: HBV, hepatitis B virus; HCV, hepatitis C virus; NAFLD, nonalcoholic fatty liver disease; NASH, nonalcoholic steatohepatitis; AIH, autoimmune hepatitis; PBC, primary biliary cirrhosis; PSC, primary sclerosing cholangitis; ALF, acute liver failure; HCC, hepatocellular carcinoma; MELD, Model for End-Stage Liver Disease; LFTs, liver function

tests; ALT, alanine aminotransferase; AST, aspartate aminotransferase; INR, international normalized ratio.

Table 2-2. Donor Characteristics.

Clinical and Demographic Data	(n = 92)	IRI⁻ (n = 46)	IRI⁺ (n = 46)	
Donor:				
Characteristic	Value	Value	Value	*P* Value*
Age, years, mean ± SD	40 ± 17	40 ± 17	40 ± 16	0.97
Sex, n (%)				0.68
Female	41 (45)	22 (48)	19 (41)	
Male		51 (55)	24 (52)	27 (59)
Race, n (%)				0.27
Asian		8 (8.7)	2 (4.4)	6 (13)
Black	8 (9)	4 (9)	4 (9)	
White	46 (50)	27 (59)	19 (41)	
Other		30 (33)	13 (28)	17 (37)
Ethnicity, n (%)				0.37
Hispanic/Latino	29 (31.5)	12 (26)	17 (37)	
Non-Hispanic/Latino	62 (67)	33 (72)	29 (63)	
Other		1 (1)	1 (2)	0 (0)
Status, n (%)				0.40
DBD		67 (73)	31 (67)	36 (78)
DCD		4 (4)	3 (7)	1 (2)
Unknown	21 (23)	12 (26)	9 (20)	
Warm ischemia, min, mean ± SD	53 ± 14	52 ± 12	54 ± 17	0.40
Cold ischemia, h, mean ± SD	7.4 ± 1.8	7.2 ± 1.6	7.6 ± 2.0	0.24
Cause of death, n (%)				0.61
Trauma	34 (37)	18 (39)	16 (35)	
CVS		29 (32)	13 (28)	16 (35)
Anoxia	27 (29)	13 (28)	14 (30)	
Other		2 (2)	2 (4)	0 (0)
DM, n (%)	9 (10)	4 (9)	5(11)	1.00
HTN, n (%)	23 (25)	10 (22)	13 (29)	0.48
CAD, n (%)	4 (4)	2 (4)	2 (4)	1.00
LFTs, at procurement, mean ± SD				
ALT	64 ± 116	42 ± 54	86 ± 152	0.07
Bilirubin	1.0 ± 0.7	0.9 ± 0.6	1.1 ± 0.8	0.12

*P Value <0.05. Abbreviations: CVS, cerebral vasospasm; DM, diabetes mellitus; HTN, hypertension; CAD, coronary artery disease; LFTs, liver function tests; ALT, alanine aminotransferase.

Table 2-3. Transplant Characteristics.

Clinical and Demographic Data	(n = 92)	IRI⁻ (n = 46)	IRI⁺ (n = 46)	
Recipient + Donor				
Characteristic	Value	Value	Value	*P* Value*
ABO, n (%)				>0.99
Identical	81 (88)	40 (87)	41 (89)	
Compatible	11 (12)	6 (13)	5 (11)	
Donor Risk Index, mean ± SD	1.5 ± 0.4	1.5 ± 0.3	1.5 ± 0.4	0.58
Sharing, n (%)				0.34
Local		52 (57)	25 (54)	27 (59)
Regional	37 (40)	18 (39)	19 (41)	
National	3 (3)	0 (0)	3 (7)	

*P Value <0.05

Figure 2-1A

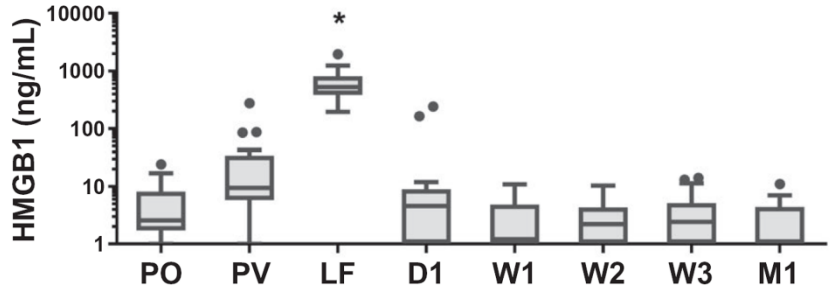

Figure 2-1B

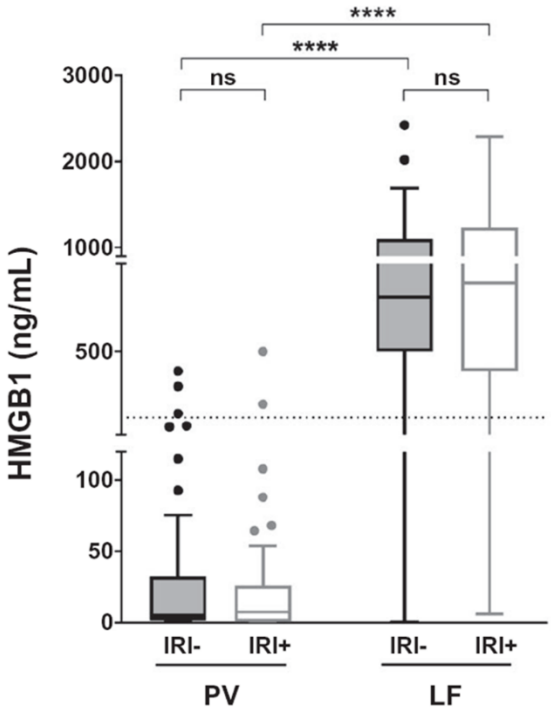

Figure 2-1C

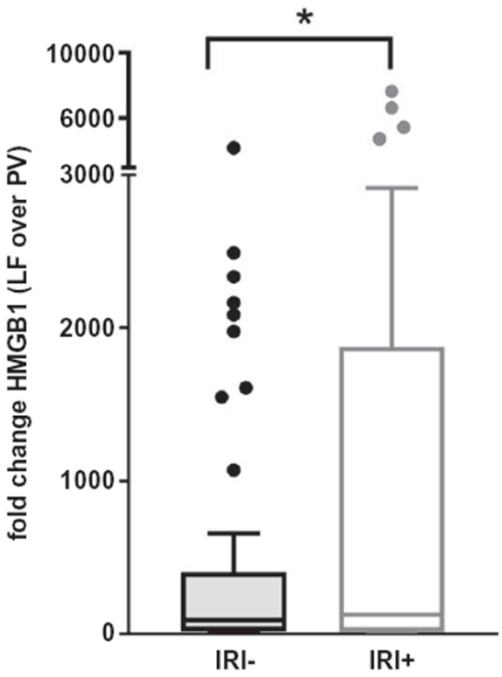

Figure 2-1. Longitudinal OLT recipient systemic and portal blood samples differ in HMGB1 content by time, but not patient IRI status.

A-B Patient plasma samples obtained at key time points pre-, intra-, or postoperative time points from either circulating systemic blood (PO, D1, W1-3, and M1) or portal blood

obtained before (PV) or after reperfusion through the donor allograft (LF) were assayed by ELISA for levels of HMGB1 present. Results were examined

A. across time, indicating that only PV and LF samples contain HMGB1 (n = 10; 5 IRI−, 5 IRI+), or

B. by patient IRI status in PV/LF only (n = 92; 46 IRI−, 46 IRI+). Dotted line indicates functional threshold of HMGB1 (200 ng/mL).

C. Paired analysis of fold change of HMGB1 levels in LF over those in PV for each patient by IRI status.

i. Data are presented as Tukey box-and-whisker plots: Whiskers are inner fences reaching 1.5 times the interquartile range, and boxes represent the interquartile ranges; dots indicate outlying values, and lines represent median values. *P < 0.05; ****P < 0.0001 by two-way ANOVA with Sidak's multiple comparisons test was used to determine differences among time and/or IRI status.

ii. Abbreviations: D1, day 1; LF, liver flush; M1, month 1; ns, not significant; PO, pre-operative; PV, portal vein blood; W1-3, weeks 1-3.

Figure 2-2A

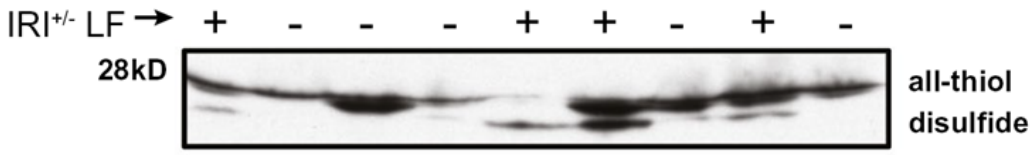

Figure 2-2B

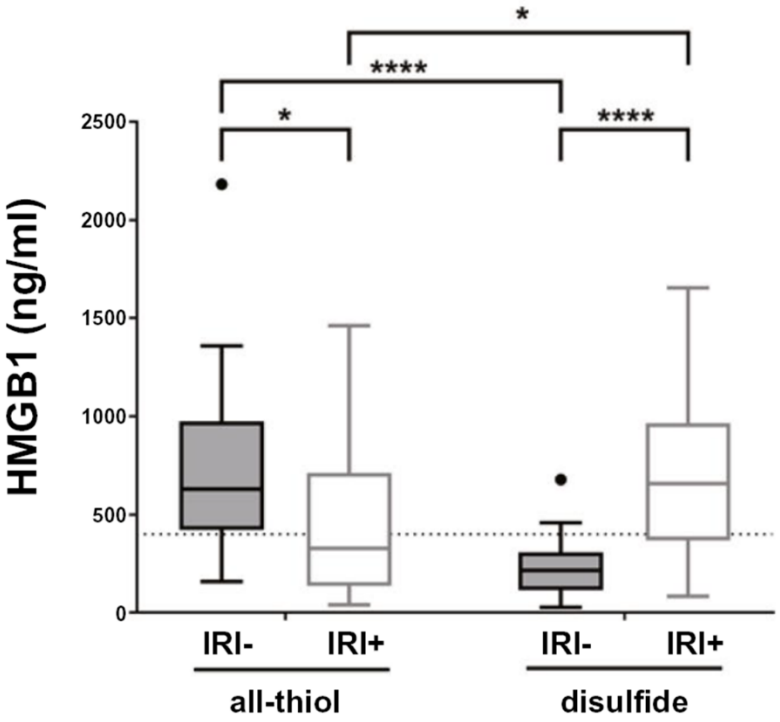

Figure 2-2C

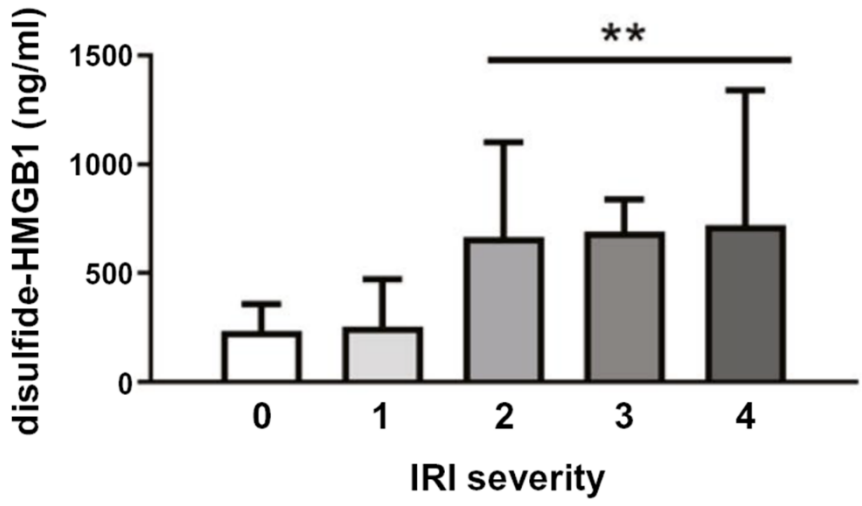

Figure 2-2D

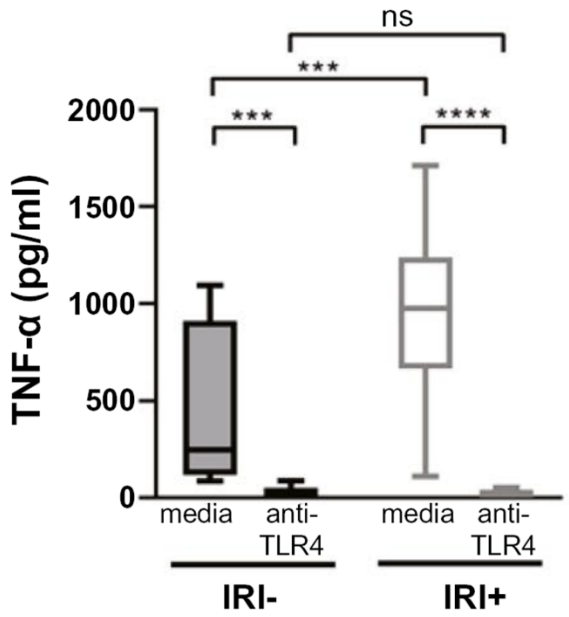
ns
***
***
****
2000
1500
1000
500
0
TNF-α (pg/ml)
media
anti-TLR4
media
anti-TLR4
IRI-
IRI+

Figure 2-2E

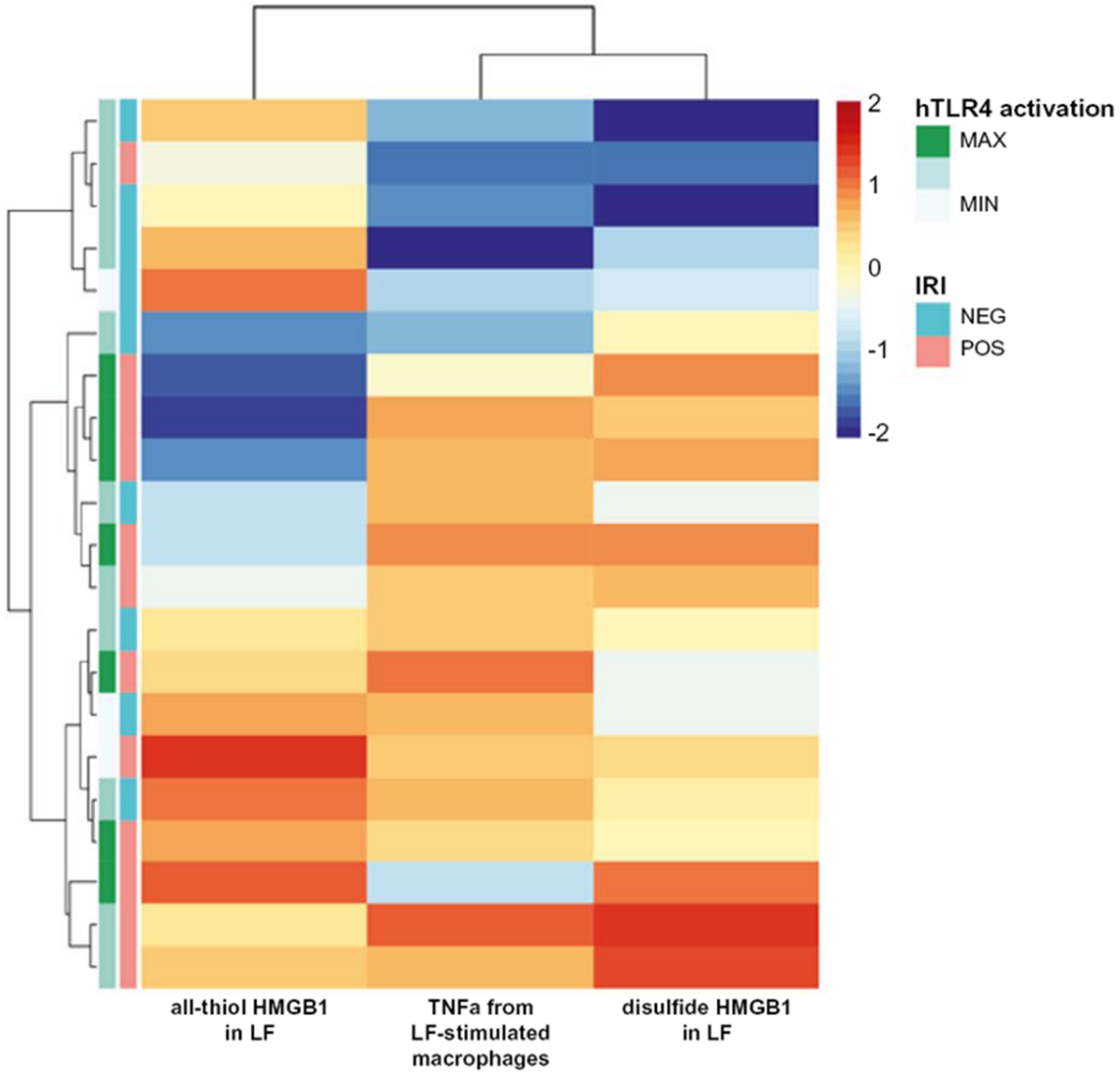

Figure 2-2. Redox state of HMGB1+ LF is disulfide in IRI+ and all-thiol in IRI− OLT patients. Patient LF samples obtained just after reperfusion through the donor allograft were assayed by immunoblotting to determine the ratio of disulfide to all-thiol HMGB1 for each patient.

A. Representative western blotting showing 28-kD bands that correspond to all-thiol HMGB1 and slightly lower bands at ~25 kD corresponding to disulfide-HMGB1 for samples from either IRI+ (+) or IRI− (−) patients.

B. Amount of all-thiol and disulfide-HMGB1 was extrapolated by dividing the total HMGB1 content per sample as determined by ELISA in **Fig. 2-1** by the ratio of HMGB1 redox forms determined by western blotting in **Fig. 2-3A** (IRI+, n = 27; IRI−, n = 31).

C. Disulfide-HMGB1 levels by IRI severity. Data shown as mean ± SD for each group. Thirty-one IRI−, 27 IRI+; IRI 0 (n = 4), 1 (n = 27), 2 (n = 18), 3 (n = 5), and 4 (n = 4).

D. HMGB1+ LF from 40 OLT patients (20 IRI−, 20 IRI+) was used to stimulate monocytes from healthy third-party donors for 8 hours (as determined in **Fig. 2-S5A** following pre-treatment for one hour with either media or anti-TLR4 mAb, and supernatant was assayed for secreted TNFα.

E. Comparison of TLR4 activation, disulfide-HMGB1 levels, and TNFα secretion by monocytes as determined by the common cohort of n = 21; 9 IRI−, 12 IRI+ from HEK assay, disulfide-HMGB1 levels and TNFα production from macrophages. Shown is a heatmap in which the rows represent patients, the columns represent the groups compared, and the colors represent normalized median values per assay (blue = low, red = high). The rows and columns are ordered based on the results of an unsupervised hierarchical clustering, with dendograms on the left side showing groups of IRI− (salmon) or IRI+ (aqua) OLT recipients with or without functional activation of HEK-Blue hTLR4 cells by their LF.

i. *P < 0.05; **P < 0.01; ****P < 0.0001 by two-way ANOVA with Sidak's multiple comparisons test was used to determine differences amongst HMGB1 redox state and/or IRI status.

ii. Abbreviations: MAX, maximum; MIN, minimum; NEG, negative; POS, positive; ns, not significant.

Figure 2-3A

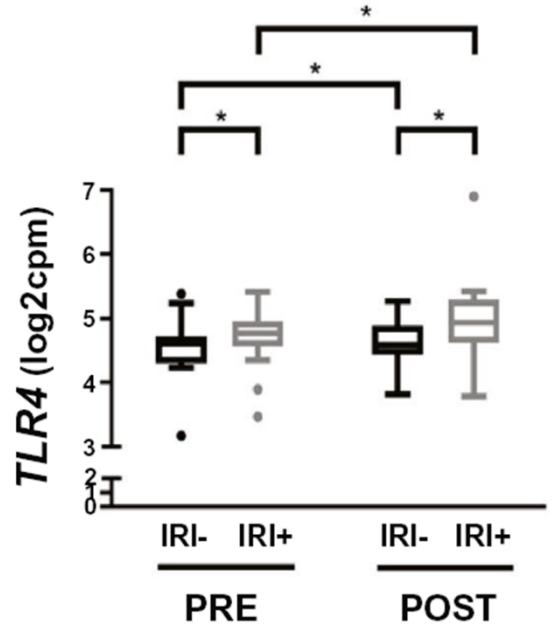

Figure 2-3B

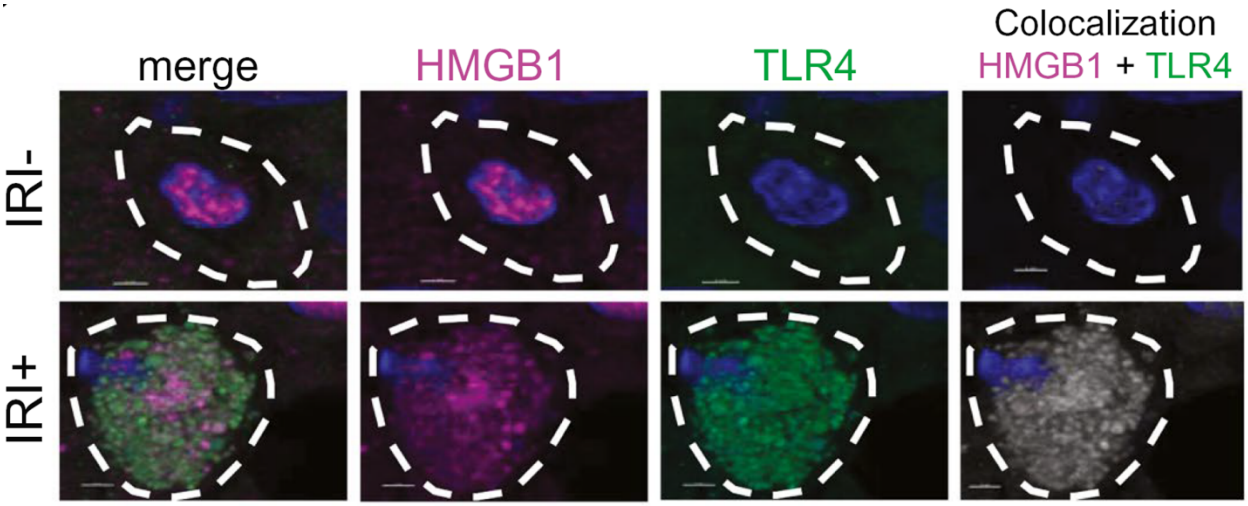

Figure 2-3C

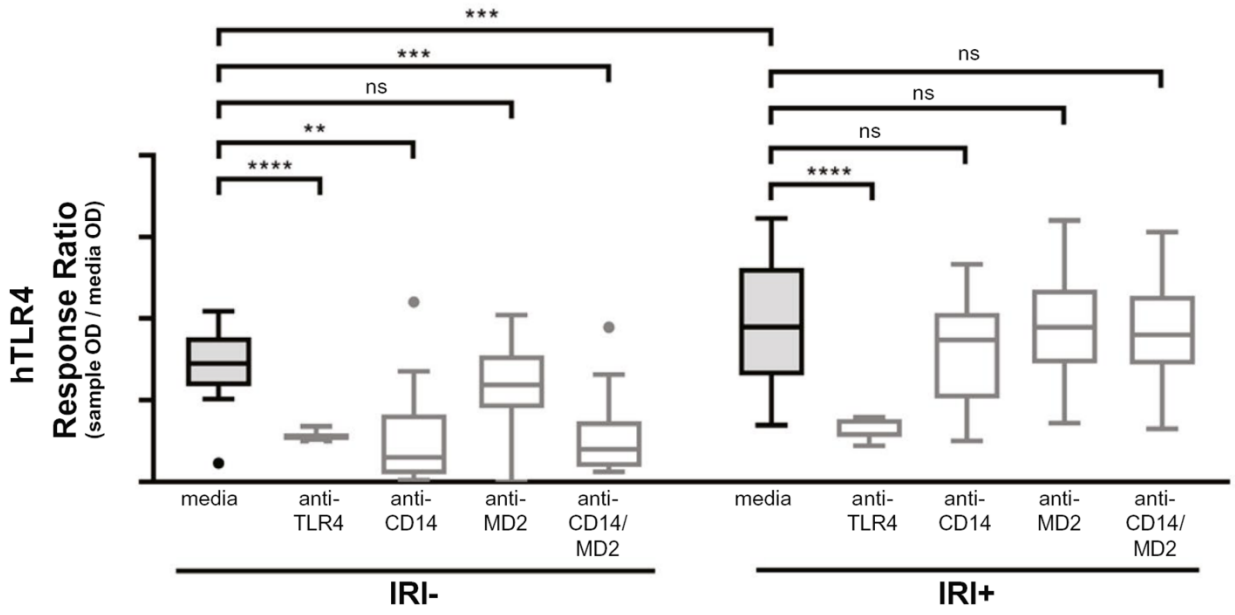

Figure 2-3. HMGB1+ LF from IRI+, but not IRI−, patients causes TNFα release from monocytes by TLR4.

A. Transcripts of the TLR4 gene are increased in donor allografts of IRI+ patients and over time. (n = 40; 20 IRI− and 20 IRI+).

B. IF staining for HMGB1 (pink) or TLR4 (green) along with the nuclear counterstain, DAPI (blue), show TLR4+ macrophages present in IRI+ allografts that are not present in macrophages of IRI− allografts. Importantly, TLR4 and HMGB1 are colocalized in IRI+ macrophages (last panel). Scale bars = 2 μm (top row), 3 μm (bottom row) as indicated (n = 20; 10 IRI− and 10 IRI+).

C. Patient LF was used to stimulate human HEK-Blue TLR4-transfected cell lines (hTLR4) pretreated with either media, anti-TLR4 mAb, anti-CD14 mAb, anti-MD2 mAb, or anti-CD14/anti-MD2 mAbs together and compared to responses achieved using the natural

control ligand, LPS, or media alone (**Fig. 2-S7C**) solid (LPS ECmax), dashed (LPS EC50), and dotted (media) lines (n = 27; 14 IRI−, 13 IRI+).

i. Data are presented as Tukey box-and-whisker plots: Whiskers are inner fences reaching 1.5 times the interquartile range, and boxes represent the interquartile ranges; dots indicate outlying values, and lines represent median values for each time point (A) or patient IRI status (B). *P < 0.05; **P < 0.01; ***P < 0.001; ****P < 0.0001 by two-way ANOVA with Sidak's multiple comparisons test was used to determine differences among time, mAb treatment, and/or IRI status.

ii. Abbreviations: OD, optical density; ns, not significant.

Figure 2-4A

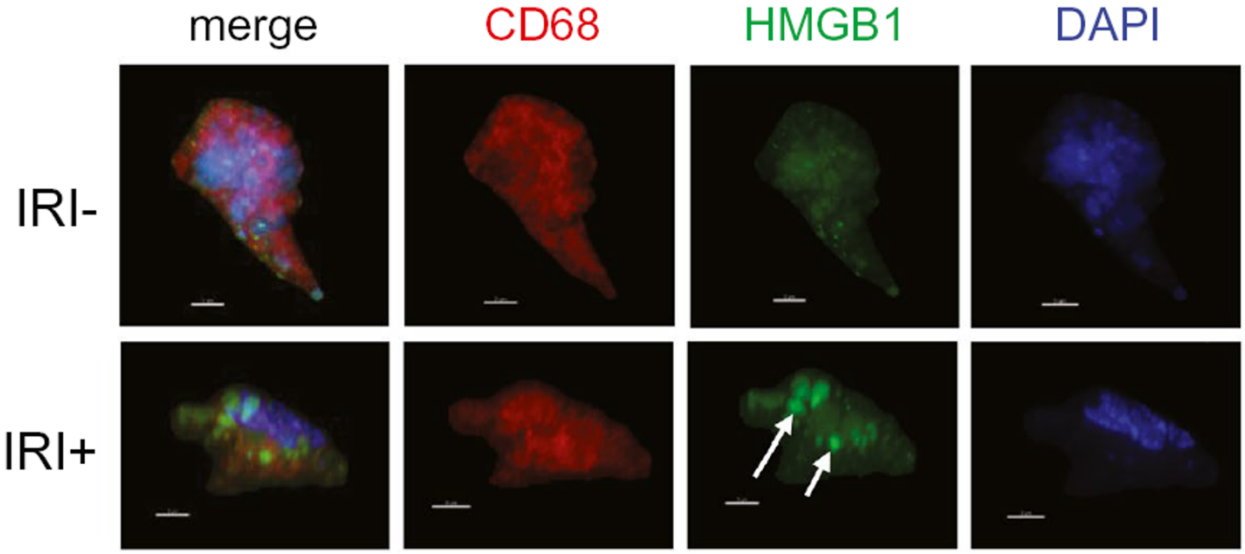

Figure 2-4B

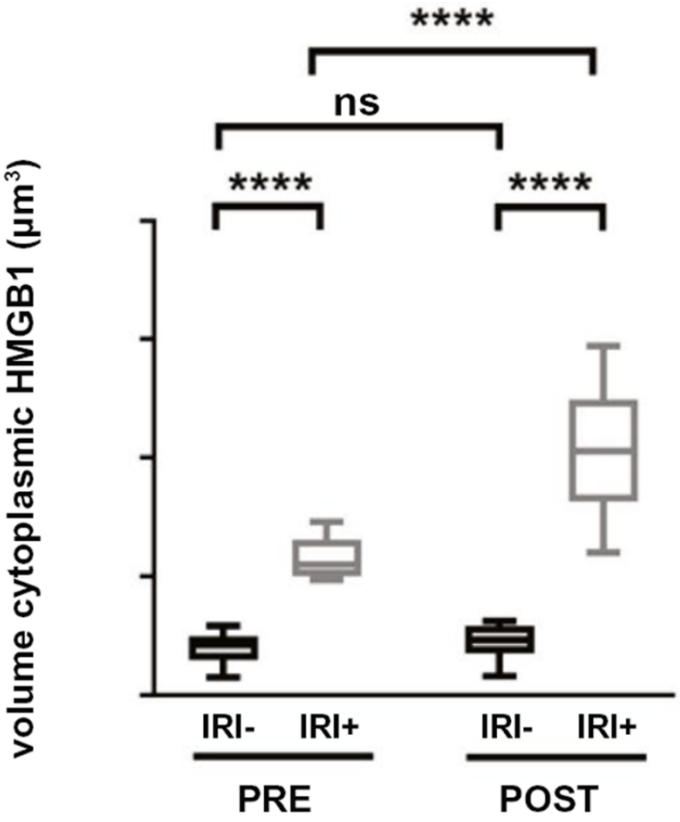

Figure 2-4C

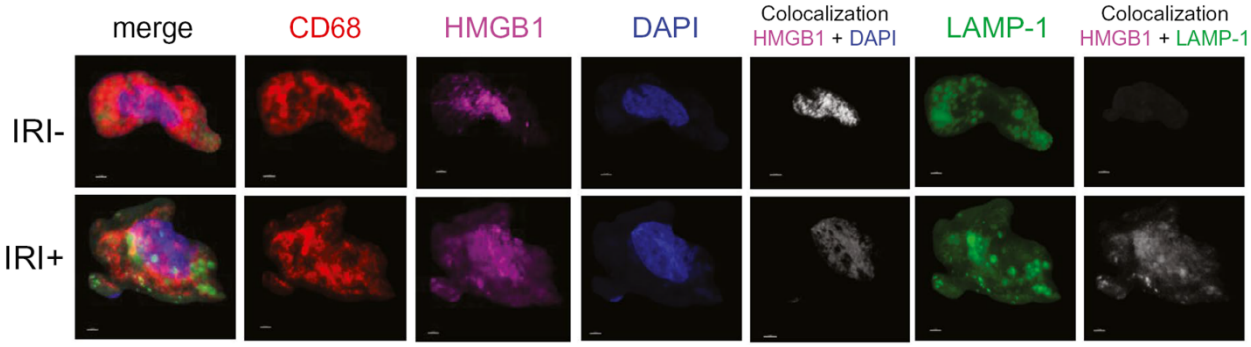

Figure 2-4D

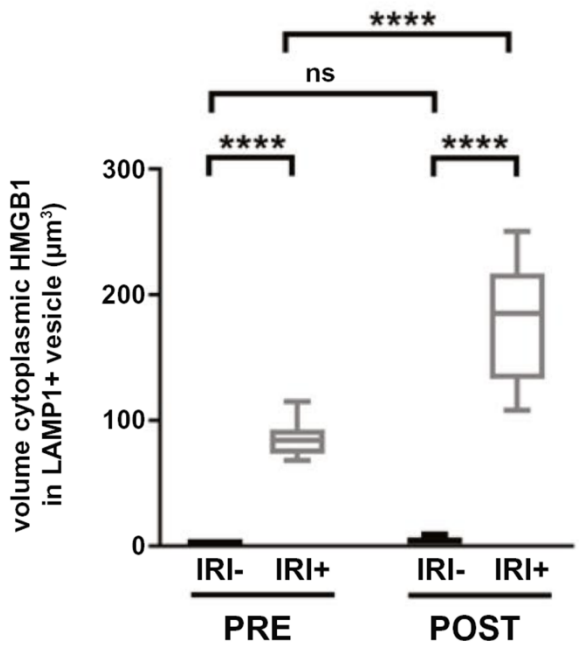

Figure 2-4E

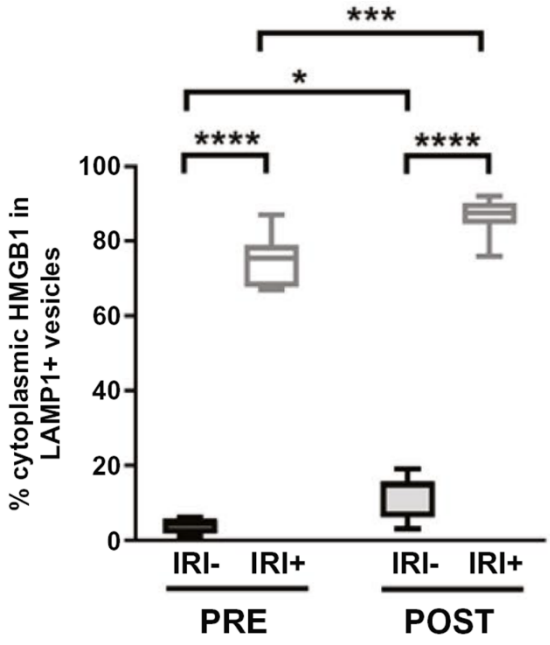

Figure 2-4. IRI+ biopsies contain disulfide-producing macrophages that increase over time. Allograft biopsies were obtained 2 hours pre-transplant (PRE) or 2 hours post-reperfusion (POST), fixed in 4% PFA, sucrose-impregnated, and embedded in gelatin and then OCT blocks for IF.

A. Ten- or 30-µm sections were stained for CD68 (red) and HMGB1 (green) and counterstained with DAPI to detect cellular nuclei (blue). Scale bars = 3 µm.

B. Quantification of macrophage-specific cytoplasmic HMGB1 from reconstructed confocal laser scanning microscopy Z-stacks as described in **Fig. 2-S4C**.

C. Sections were stained for CD68 (red), HMGB1 (pink), DAPI (blue), and LAMP1 (green). Localization of HMGB1 to the nuclear compartment (white, fifth panel of top and bottom rows) or LAMP1+ cytoplasmic vesicles (white, last panel of top and bottom rows) was determined using Imaris software (version 9.2; Bitplane AG, Zürich, Switzerland).

D. Quantification of macrophage-specific cytoplasmic HMGB1 constrained within LAMP1+ vesicles by volume (μm3). (E) Quantification of the percent of macrophage-specific cytoplasmic HMGB1 constrained within LAMP1+ vesicles.

i. Numbers shown in (B) and (D) represent the average volume of HMGB1 found within the cytoplasm or LAMP1+ cytoplasmic vesicles of ≥3 randomly selected macrophages per patient for n = 20 patients; IRI− = 10 and IRI+ = 10. Numbers shown in (E) represent the percent of cytoplasmic HMGB1 found within LAMP1+ vesicles of ≥3 macrophages per tissue slice for n = 20 patients; IRI− = 10 and IRI+ = 10. *P < 0.05.

ii. Data are presented as Tukey box-and-whisker plots: Whiskers are inner fences reaching 1.5 times the interquartile range, and boxes represent the interquartile ranges; dots indicate outlying values, and lines represent median values. *P < 0.05; ***P < 0.001; ****P < 0.0001 by twoway ANOVA with Sidak's multiple comparisons test was used to determine differences among HMGB1 redox state and/or IRI status.

iii. Abbreviation: ns, not significant.

Figure 2-5A

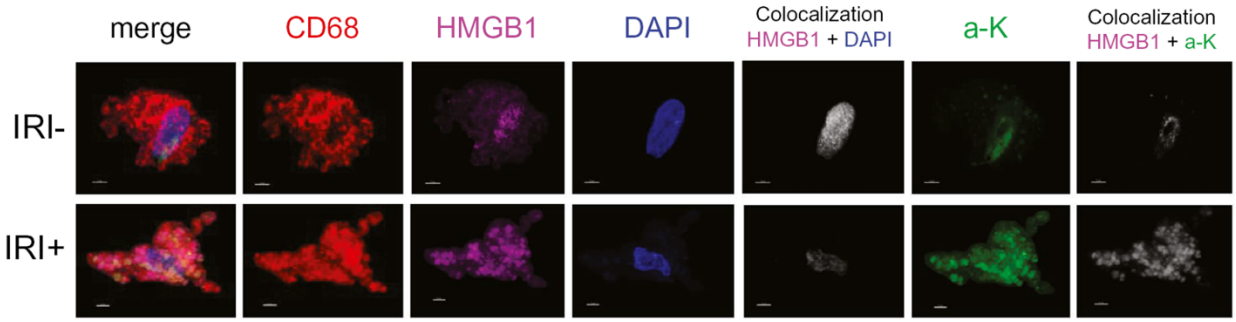

Figure 2-5B

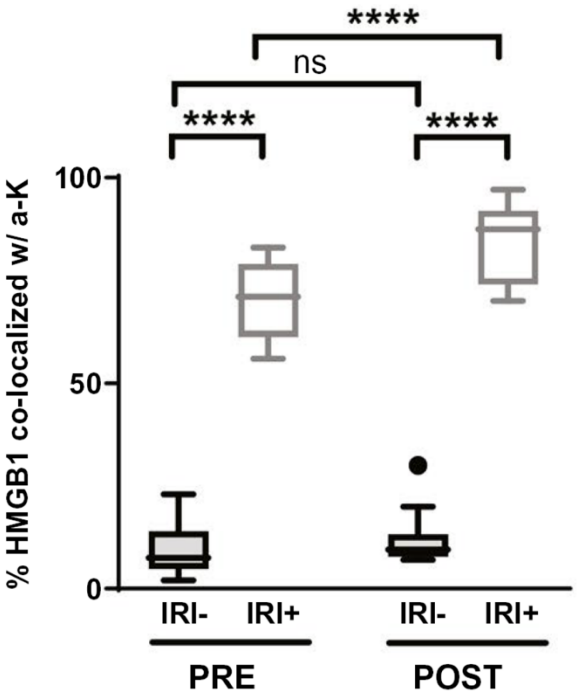

Figure 2-5C **Figure 2-5D**

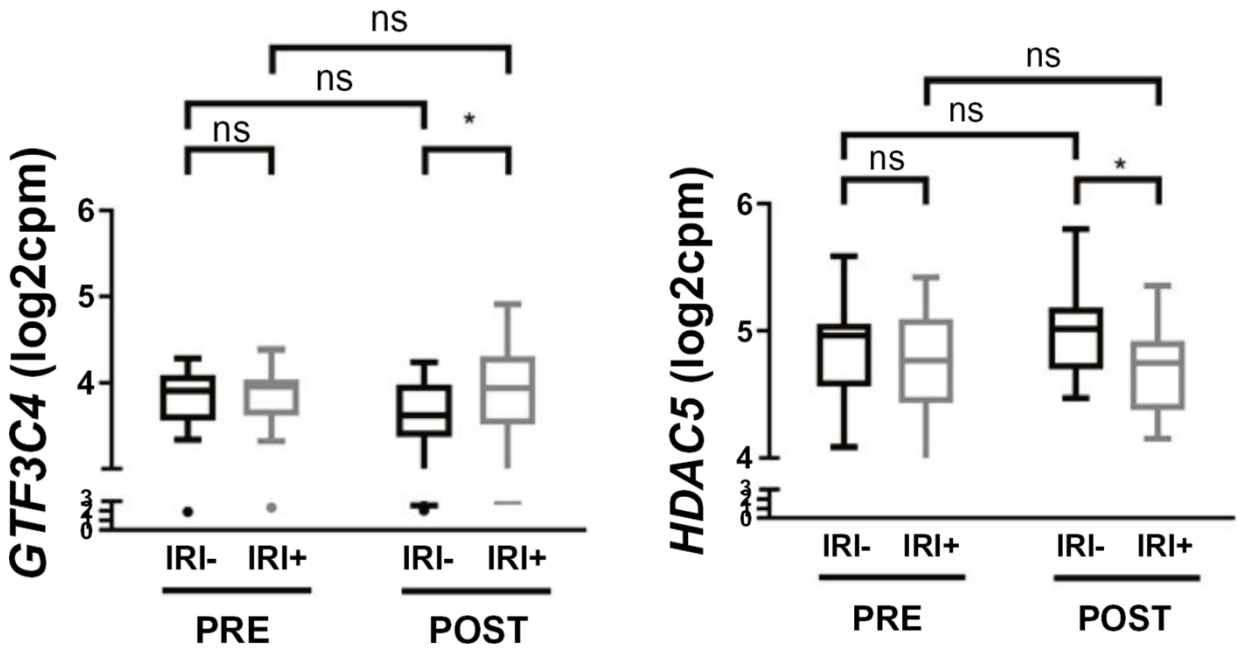

Figure 2-5. Increased GTF3C4 and decreased HDAC5 contribute to hyperacetylation of macrophage HMGB1 in IRI+ OLT patients.

A. Allograft biopsies were obtained 2 hours pre-transplant (PRE) or 2 hours post-reperfusion (POST), fixed in 4% PFA, sucrose-impregnated, and embedded in gelatin and then OCT blocks for IF. Ten- or 30-μm sections were stained for CD68 (red), HMGB1 (pink), DAPI (blue), and acetylated lysine residues (green; a-K). Images were acquired by confocal microscopy, and localization of HMGB1 to the nuclear compartment (white, fifth panel of top and bottom rows) or a-K (white, last panel of top and bottom rows) was determined using Imaris software (Bitplane). Scale bars = 3 μm.

B. Quantification of the percent of macrophage-specific HMGB1 (pink) which colocalized to a-K (green; colocalization, white) from reconstructed confocal laser scanning microscopy Z-stacks (n = 20; 10 IRI− and 10 IRI+).

Gene expression (transcripts per million; log2 CPM) of

C. GTF3C4, an HAT encoding gene, or

D. HDAC5, an HDAC encoding gene, in PRE/POST biopsies from IRI+ and IRI− OLT recipients by RNAseq (n = 40; 20 IRI− and 20 IRI+).

i. Data are presented as Tukey box-and-whisker plots: Whiskers are inner fences reaching 1.5 times the interquartile range, and boxes represent the interquartile ranges; dots indicate outlying values, and lines represent median values for each time point. *P < 0.05 by two-way ANOVA with Sidak's multiple comparisons test was used to determine differences among HMGB1 redox state and/or IRI status.

ii. Abbreviations: log2cpm, log2 counts per million; ns, not significant.

Figure 2-6A

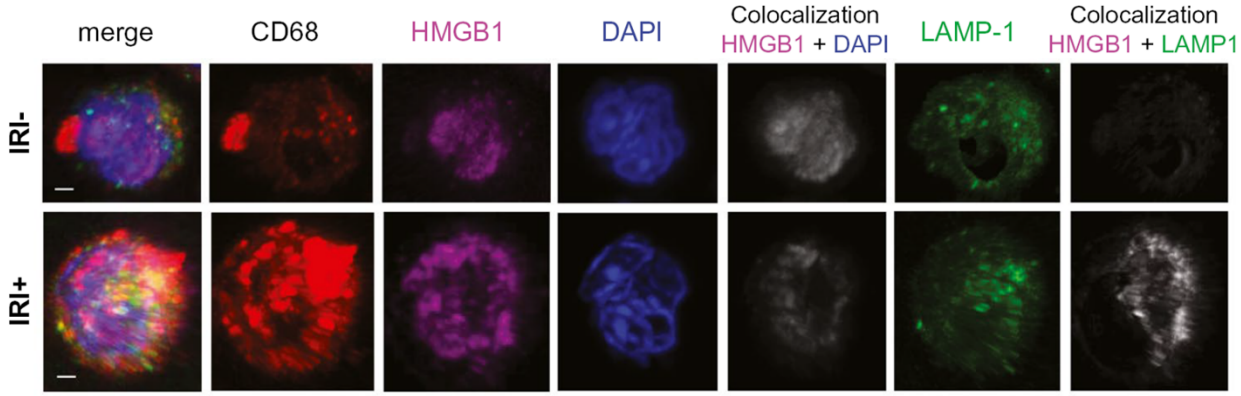

Figure 2-6B

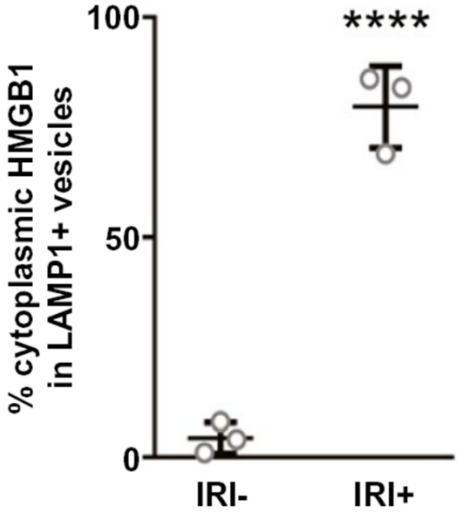

Figure 2-6C

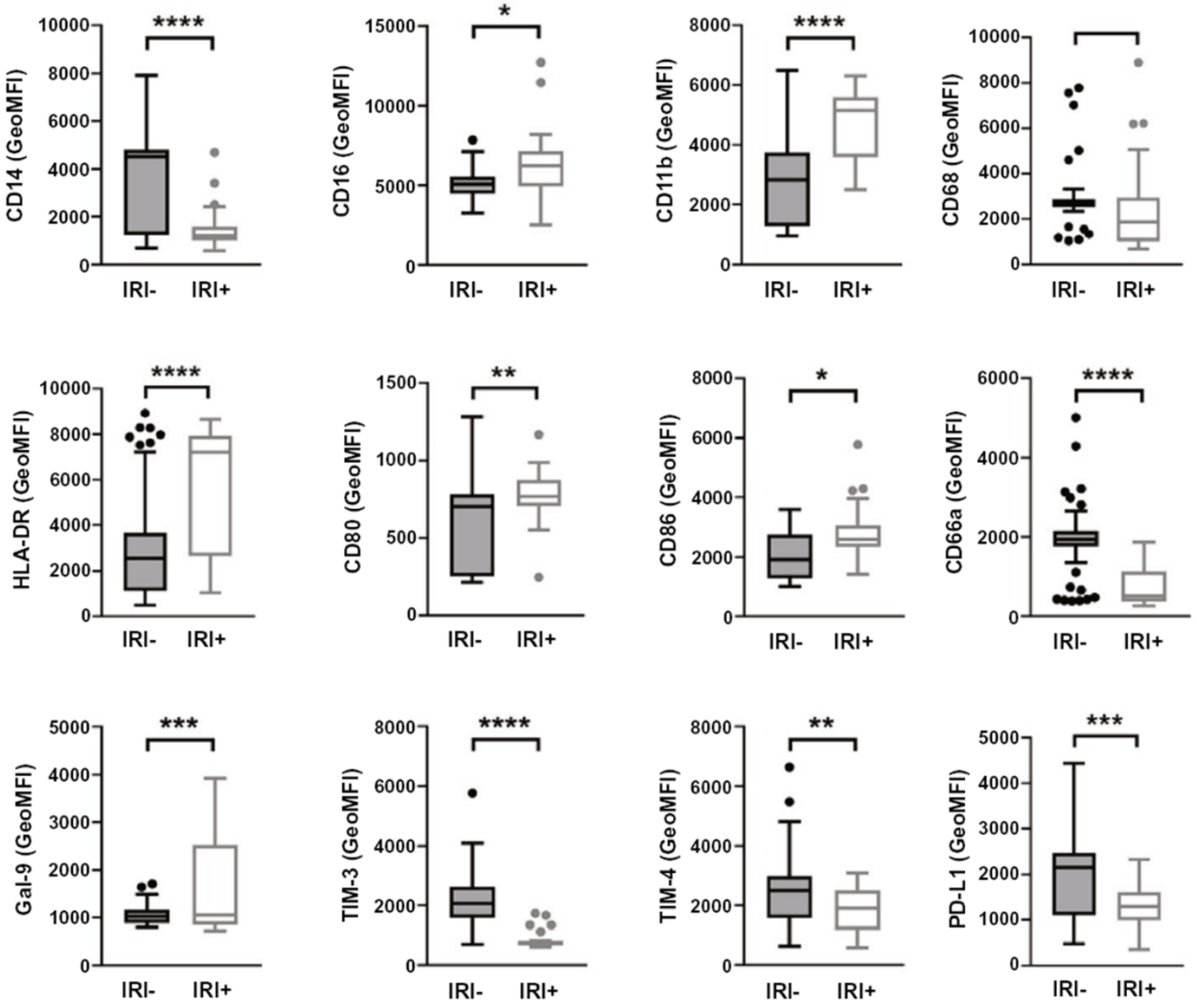

Figure 2-6. Disulfide-HMGB1+IRI+ patient LF activates monocytes to translocate nuclear HMGB1 into cytoplasmic vesicles and become more pro-inflammatory. PBMC-derived monocytes from healthy, third-party donors were cultured with patient LF (n = 6; 3 IRI−, 3 IRI+) for 2 hours to determine HMGB1 localization by confocal microscopy or 3 days to determine functional phenotype by flow cytometry.

A. Representative images of monocytes stained by multicolor IF for CD68 (red), HMGB1 (pink), DAPI (blue), and LAMP1 (green) and z-stack images were acquired by confocal

microscopy and reconstructed in Imaris software (Bitplane AG, Zürich, Switzerland). Scale bars = 2 μm.

B. Quantification of monocyte-specific cytoplasmic HMGB1 in LAMP1+ vesicles from reconstructed confocal laser scanning microscopy Z-stacks. Data are presented as dots for each of three separate experiments, with long lines indicating mean.

C. Stimulated monocytes were multiplex stained with a panel of directly labeled antibodies and run on a flow cytometer to determine surface expression levels of CD14, CD16, CD11b, CD68, HLA-DR, CD80, CD86, CD66a, Gal-9, TIM-3, TIM-4, and PD-L1. GeoMFI for the respective surface marker on cells stimulated by n = 77; 43 IRI− versus 34 IRI− LF are shown.

i. Data are presented as Tukey box-and-whisker plots: Whiskers are inner fences reaching 1.5 times the interquartile range, and boxes represent the interquartile ranges; dots indicate outlying values, and lines represent median values. *P < 0.05; **P < 0.01; ***P < 0.001; ****P < 0.0001 by Student t test.

ii. Abbreviations: GeoMFI, geometric mean fluorescence intensity; ns, no significance; PBMC, peripheral blood mononuclear cell.

Figure 2-S1A

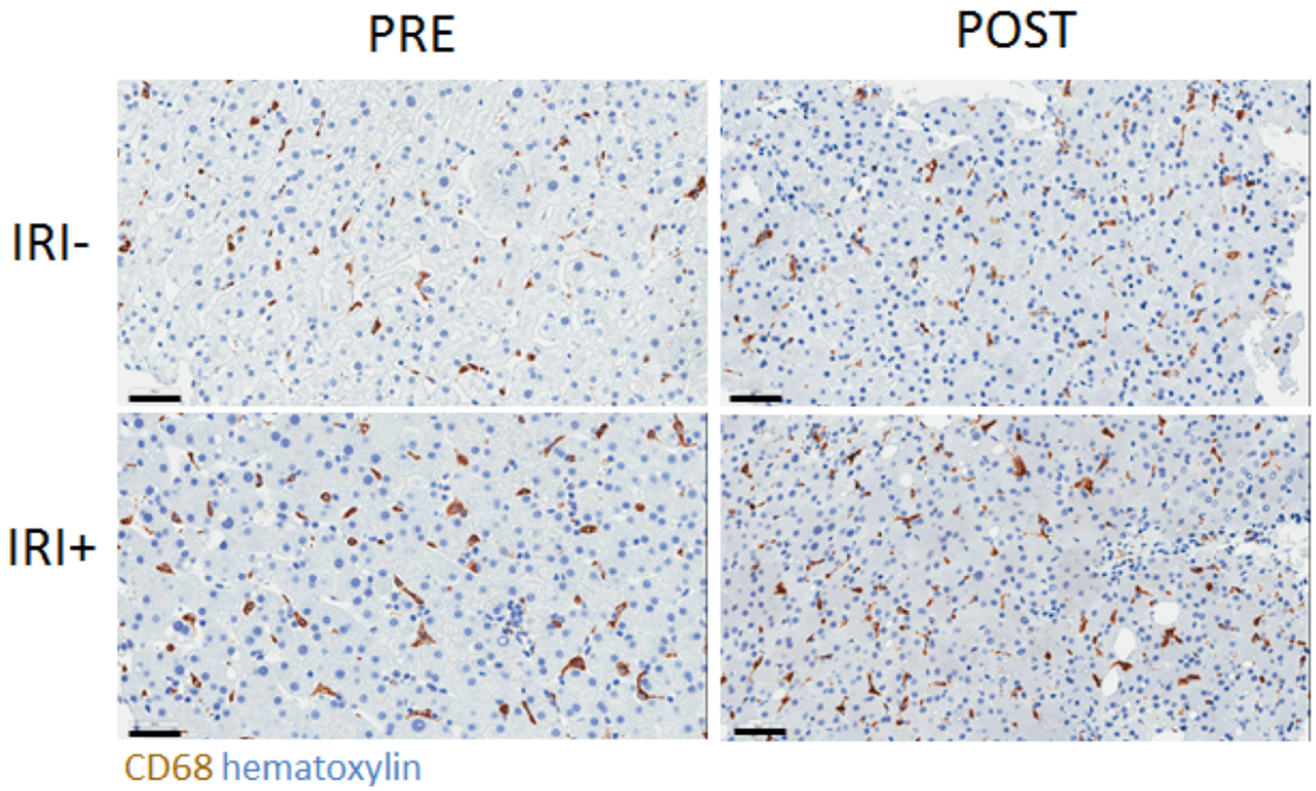

Figure 2-S1B

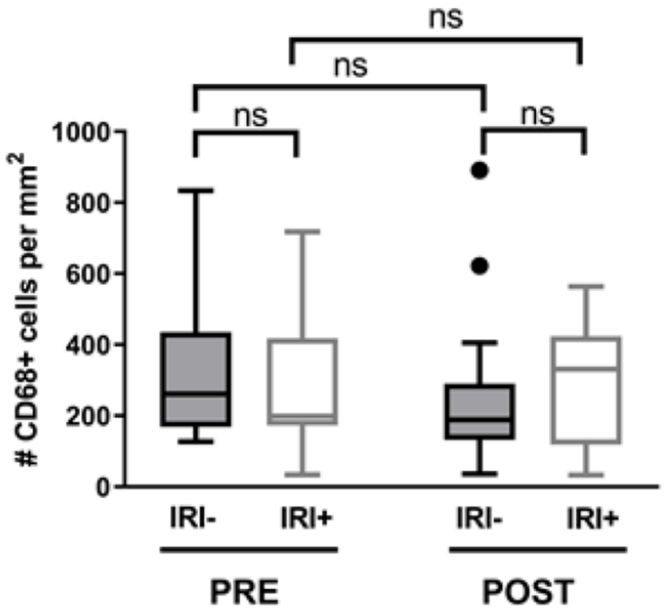

Supplementary Figure 2-S1. Numbers of CD68+ macrophages do not change over time or by patients IRI status. Allograft biopsies were obtained 2 hrs pre-transplant (PRE) or 2 hrs post-reperfision (POST), formalin-fixed and then paraffin-embedded for immunohistochemistry (IHC).

A. 3um sections were stained for CD68 (brown) and counterstained for hematoxylin (blue). Shown are representattive images from one IRI- and IRI+ patient. Scale bars = 50um
B. Numbers of CD68+ cells were quantified usign Definiens software on digitally scanned slides and are shorn as the average number of CD68+ cells per mm^2 tissue area for n= 40 patients, with IRI+=20 and IRI-= 20 patients.

i. Data are presented as Tukey box-and-whisker plots: whiskers are inner fences reaching 1.5 times the interquantile range and boxes represent the interquartile ranges, dots indicate outlying values and lines represent median values. ns = not significant by two-way analysis of variance (ANOVA) with Sidak's multiple comparrisons test to determine differences amongst patient IRI status and time.

Figure 2-S2

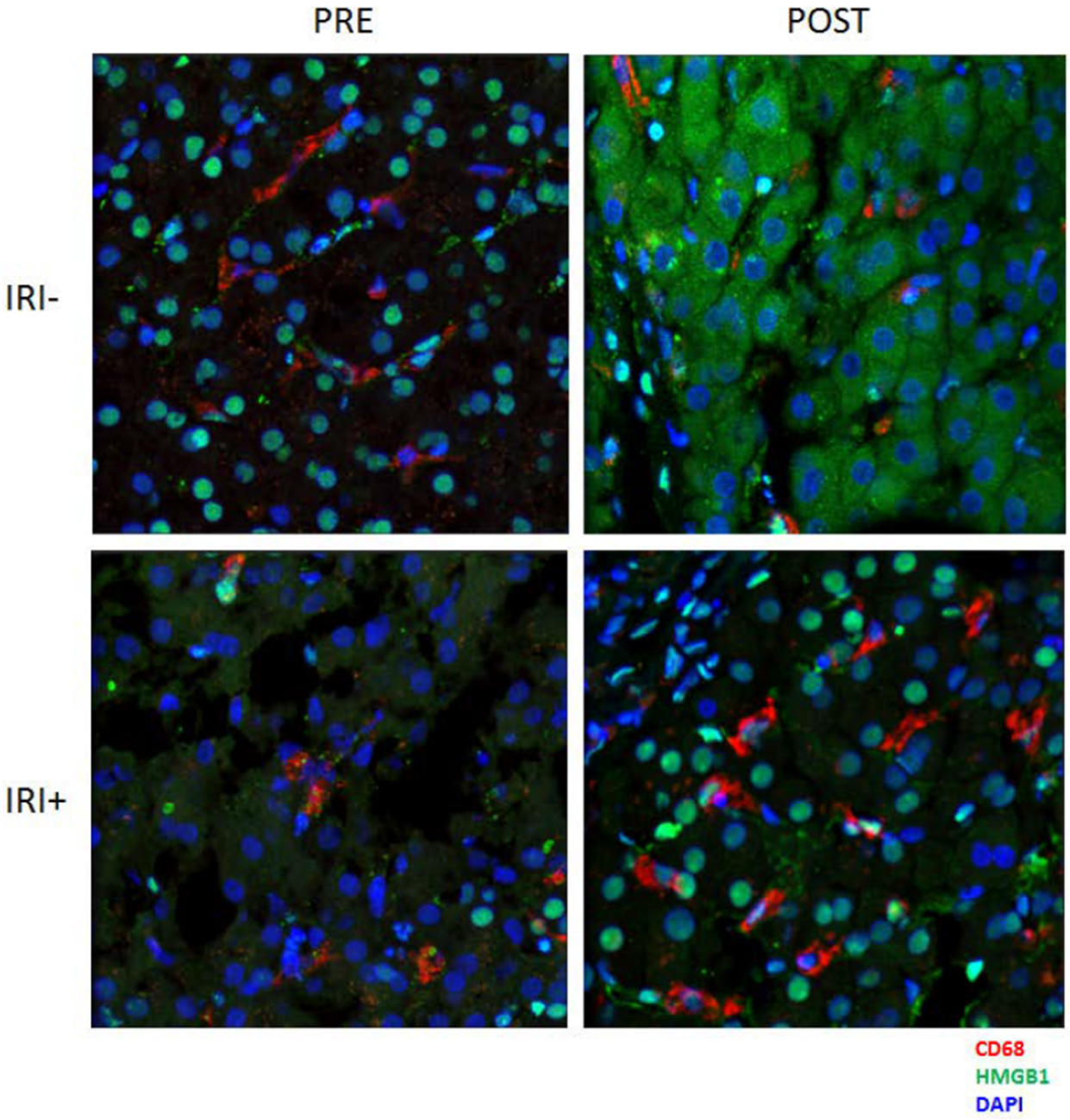

Supplementary Figure 2-S2. Hepatocytic HMGB1 in OLT recipient allografts. Allograft biopsies were obtained 2 hrs pre-reperfusion (PRE) or 2 hrs post-reperfusion (POST), fixed in 4% PFA, sucrose-impregnated in gelatin then OCT blocks for immunofluorescence (IF). 10 or 30um sections were stained for CD68 (red), HMGB1 (green), and counterstained with DAPI to detect cellular nuclei (blue). IRI- allografts show strong nuclear staining in pre-transplant

biopsies as expected in healthy donor livers, and subsequent hepatocyte translocation of HMGB1 into the cytoplasmic compartment following the relatively mild damage occurring during IRI in these patients. In contrast, IRI+ allografts have many hepatocytes lacking HMGB1 entirely, which has been reported before for organs experiencing more severe damage during IRI. Post-allograft biopsies for these patients have large aggregations of macrophages near hepatocytes that do not have nuclear HMGB1, suggesting they may be actively damaging healthy hepatocytes further.

Figure 2-S3

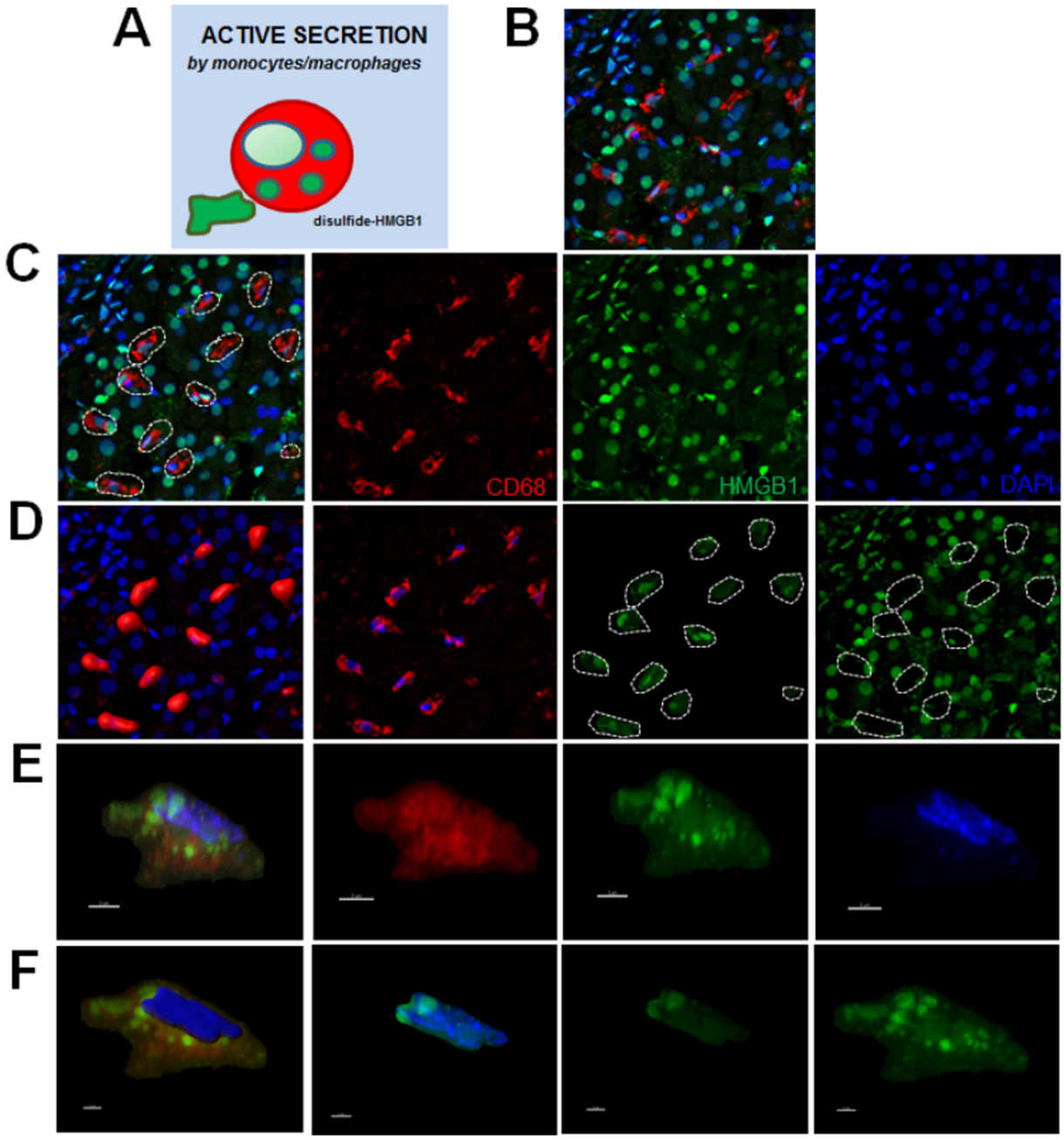

Supplementary Figure 2-S3. 3D reconstruction of subcellular compartments in macrophages from liver biopsy samples.

A. Model showing subcellular localization of disulfide-HMGB1 production in monocytes/macrophages.

B. Raw, unedited 3-color confocal image with IF staining for CD68 (red) HMGB1 (green), and nuclei (DAPI, blue). Image used in this example is from IRI+ POST individual from **Figure 2-S2** and IRI+ isolated macrophage from **Figure 2-4A**.

C. Merged image from **(B)** split into separate channels as indicated. Far left panel highlights cells of interest (dashed line).

D. Reconstructed images from Imaris showing 3D "surface object" applied to the red channel, which contains cell-surface staining of CD68 in activated macrophages within the allograft (far left panel). Second panel from the left shows digitally isolated macrophages using only the blue and red signals coming from within the surface objects creased in the far left panel, as accomplished using the "mask" tool to set the values outside the mask for that channel to 0, leaving only the signal inside the mask. Third panel shows digitally isolated macrophage-specific HMGB1, created using only the green signal coming from within the surface objects created in the far left panel by again using the mask tool to isolate those specific signals.

E. Merged and separated channels from a single macrophage after digital isolation as described in **A-D**.

F. 3D reconstruction and digital isolation of subcellular compartments within the digitally isolated macrophage shown in **(E)**. First panel shows digital reconstruction of the nuclear compartment using a surface object on the blue channel with DAPI staining. Second panel from the left shows all channels with all non-nuclear signal masked (all values outside of nuclear surface object set to 0). Third panel shows HMGB1 signal in green channel from within the nuclear compartment only. Final panel shows HMGB1 signal

that is non-nuclear but within the constraints of the macrophage, which equals all HMGB1 within the cytoplasmic compartment of the cell.

Figure 2-S4

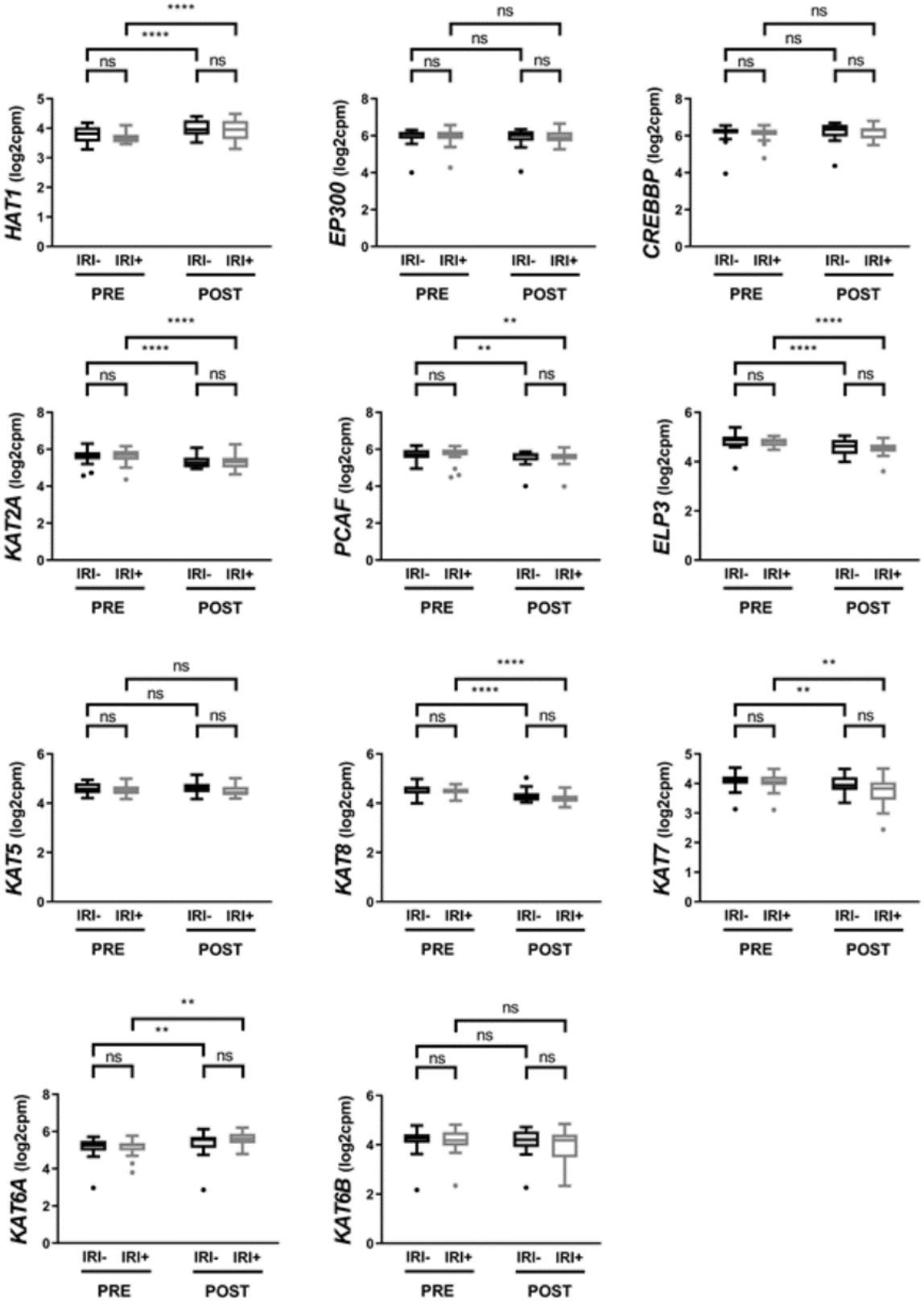
HAT1 (log2cpm)
EP300 (log2cpm)
CREBBP (log2cpm)
KAT2A (log2cpm)
PCAF (log2cpm)
ELP3 (log2cpm)
KAT5 (log2cpm)
KAT8 (log2cpm)
KAT7 (log2cpm)
KAT6A (log2cpm)
KAT6B (log2cpm)
IRI- IRI+ IRI- IRI+
PRE POST
ns
**
****

Supplementary Figure 2-S4. RNAseq analysis of HAT genes. Gene expression (transcripts per million, $\log_2$ CPM) histone acetyltransferase (HAT)-encoding genes, in PRE/POST biopsies from IRI+ and IRI- OLT recipients by RNAseq. Data are presented as Tukey box-and-whisker plots: whiskers are inner fences reaching 1.5 times the interquartile range and boxes represent the interquartile ranges, dots indicate outlying values and lines represent median values for each time point. n=40; 20 IRI- and 20 IRI+. *$p<0.05$ by two-way analysis of variance (ANOVA) with Sidak's multiple comparisons test was used to determine differences amongst time and/or IRI status.

Figure 2-S5

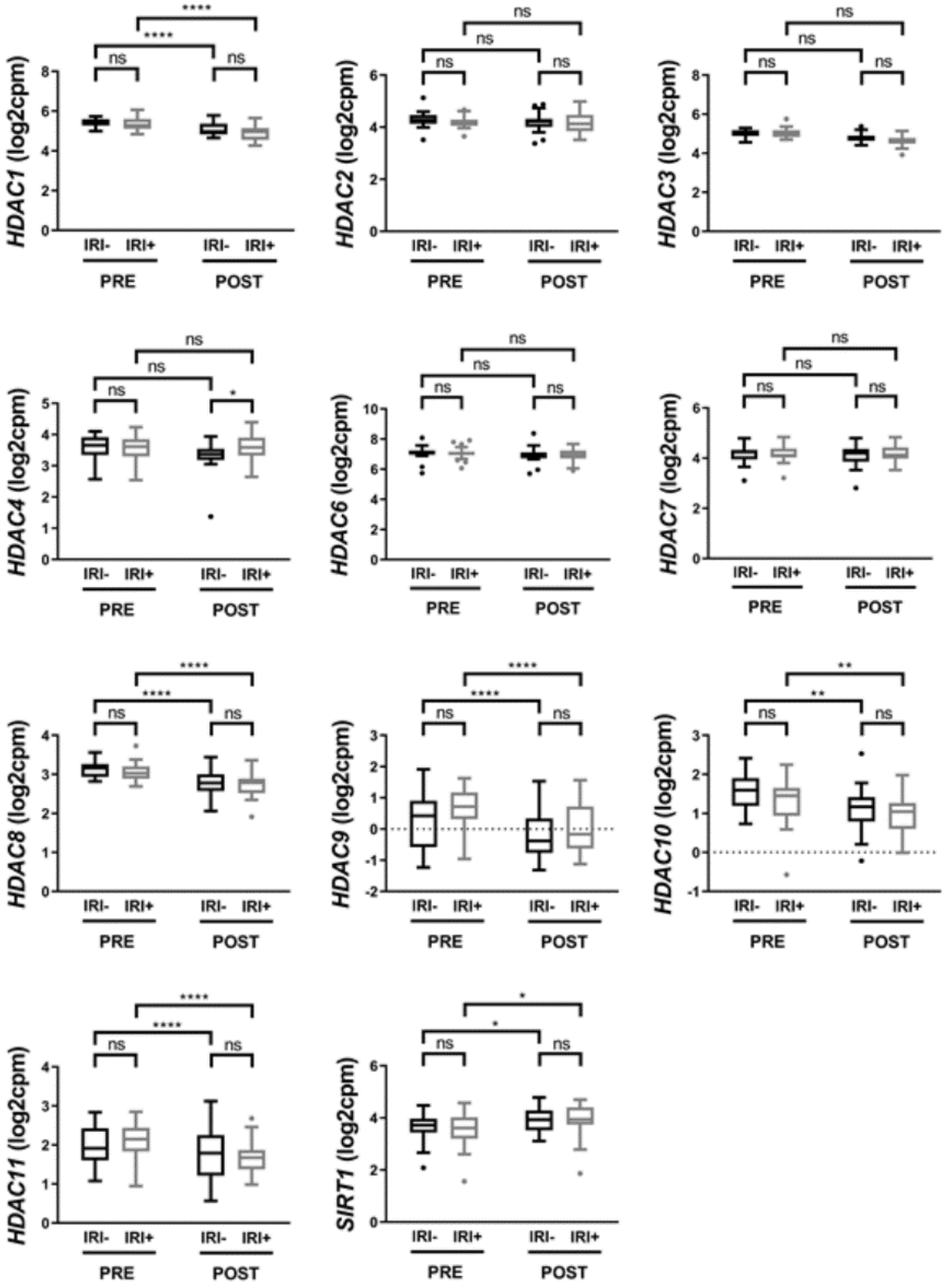
HDAC1 (log2cpm)
HDAC2 (log2cpm)
HDAC3 (log2cpm)
HDAC4 (log2cpm)
HDAC6 (log2cpm)
HDAC7 (log2cpm)
HDAC8 (log2cpm)
HDAC9 (log2cpm)
HDAC10 (log2cpm)
HDAC11 (log2cpm)
SIRT1 (log2cpm)
IRI- IRI+ IRI- IRI+
PRE POST

Supplementary Figure 2-S5. RNAseq analysis of HAT genes. Gene expression (transcripts per million, $\log_2$ CPM) histone deacetylase (HDAC)-encoding genes, in PRE/POST biopsies from IRI+ and IRI- OLT recipients by RNAseq. Data are presented as Tukey box-and-whisker plots: whiskers are inner fences reaching 1.5 times the interquartile range and boxes represent the interquartile ranges, dots indicate outlying values and lines represent median values for each time point. n=40; 20 IRI- and 20 IRI+. *$p<0.05$ by two-way analysis of variance (ANOVA) with Sidak's multiple comparisons test was used to determine differences amongst time and/or IRI status.

Figure 2-S6A

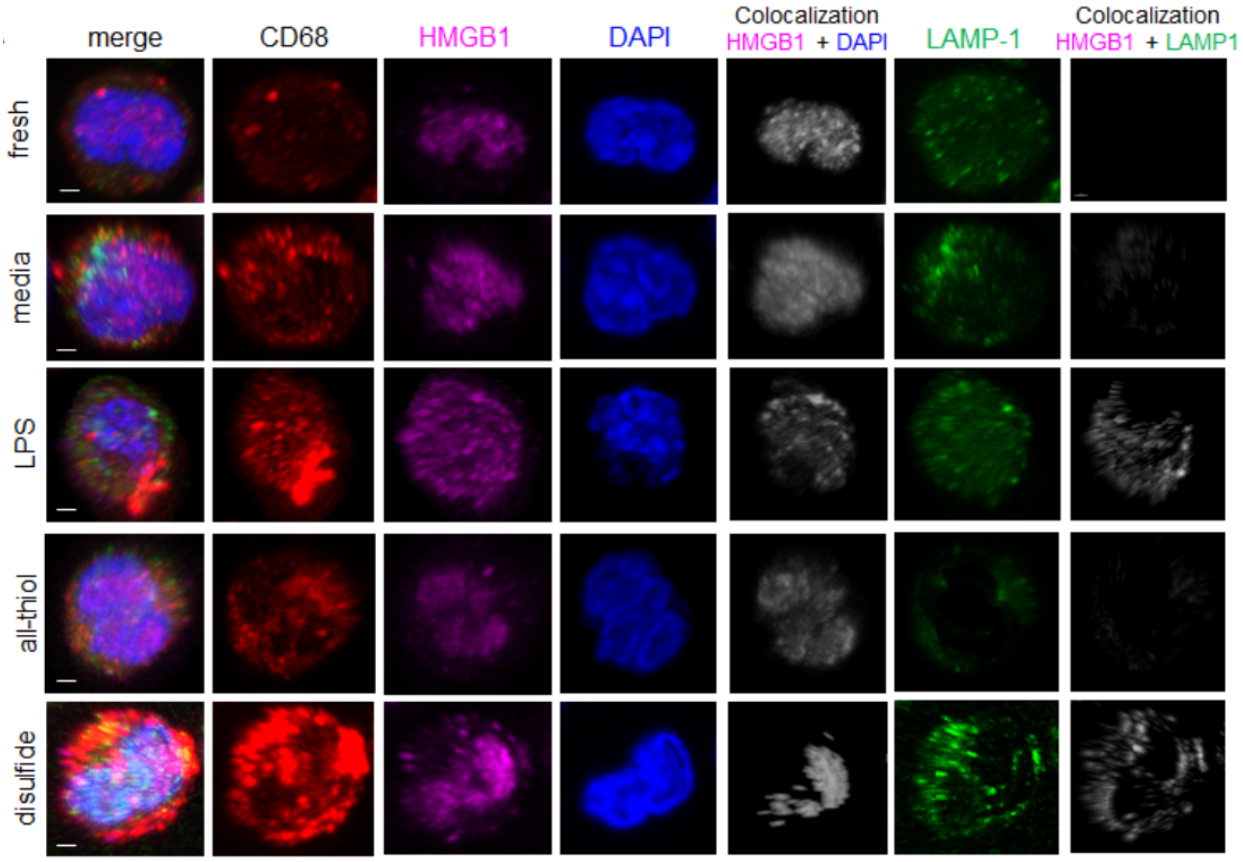

Figure 2-S6B

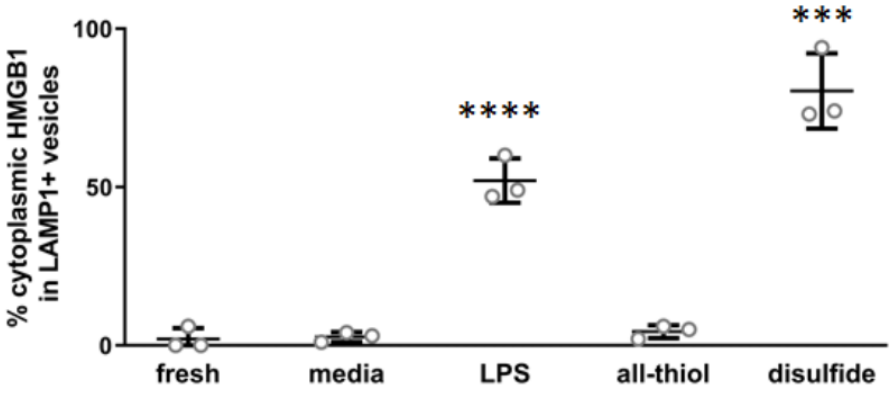

Supplementary Figure 2-S6. Disulfide-HMGB1+IRI+ patient LF activates monocytes to translocate nuclear HMGB1 into cytoplasmic vesicles and become more pro-inflammatory.

PBMC-derived monocytes from healthy, third-party donors were freshly isolated (fresh) or

cultured with control media, LPS, all-thiol HMGB1 or disulfide HMGB1 for 2 hours to determine HMGB1 localization by confocal microscopy or 3 days to determine functional phenotype by flow cytometry.

A. Representative images of monocytes stained by multicolor IF for CD68 (red), HMGB1 (pink), DAPI (blue), and LAMP1 (green), and z-stack images were acquired by confocal microscopy and reconstructed in Imaris. Scale bars = 2um.

B. Quantification of monocyte-specific cytoplasmic HMGB1 in LAMP1+ vesicles from reconstructed confocal laser-scanning microscopy Z-stacks.

i. Data are presented as dots for each of three separate experiments with long lines indicating means. ns = no significance; ****$p<0.0001$; by Student's t-test as compared to freshly isolated cells.

Figure 2-S7A

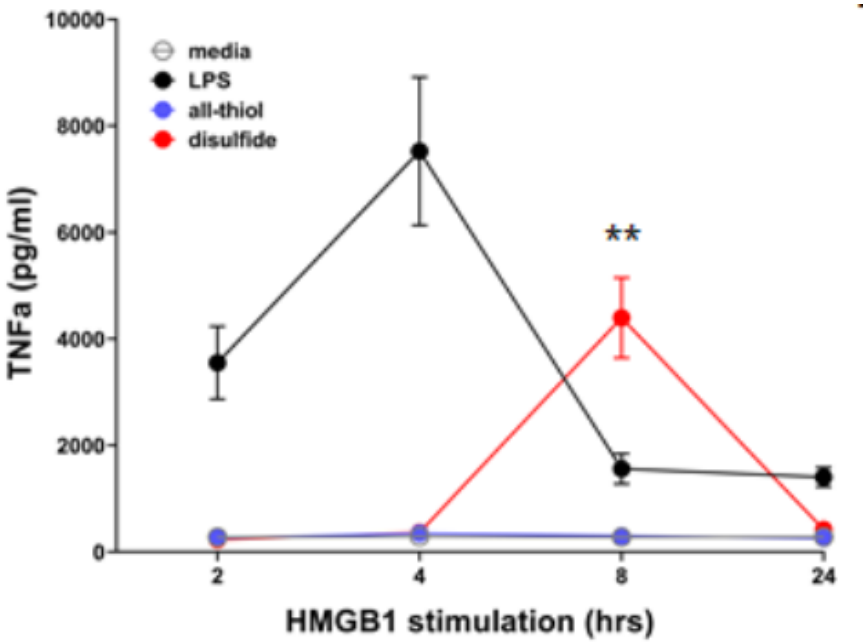

Figure 2-S7B

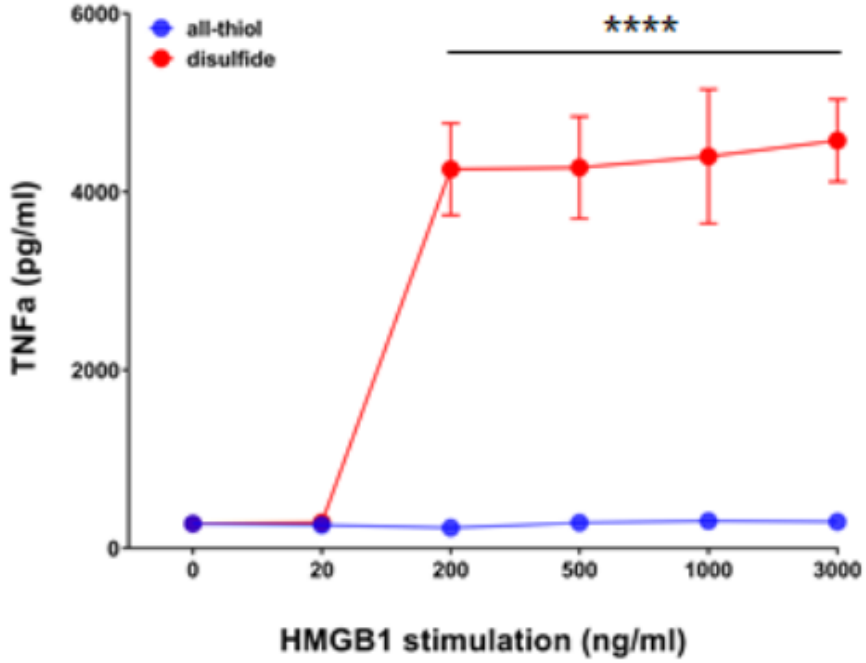

Figure 2-S7C

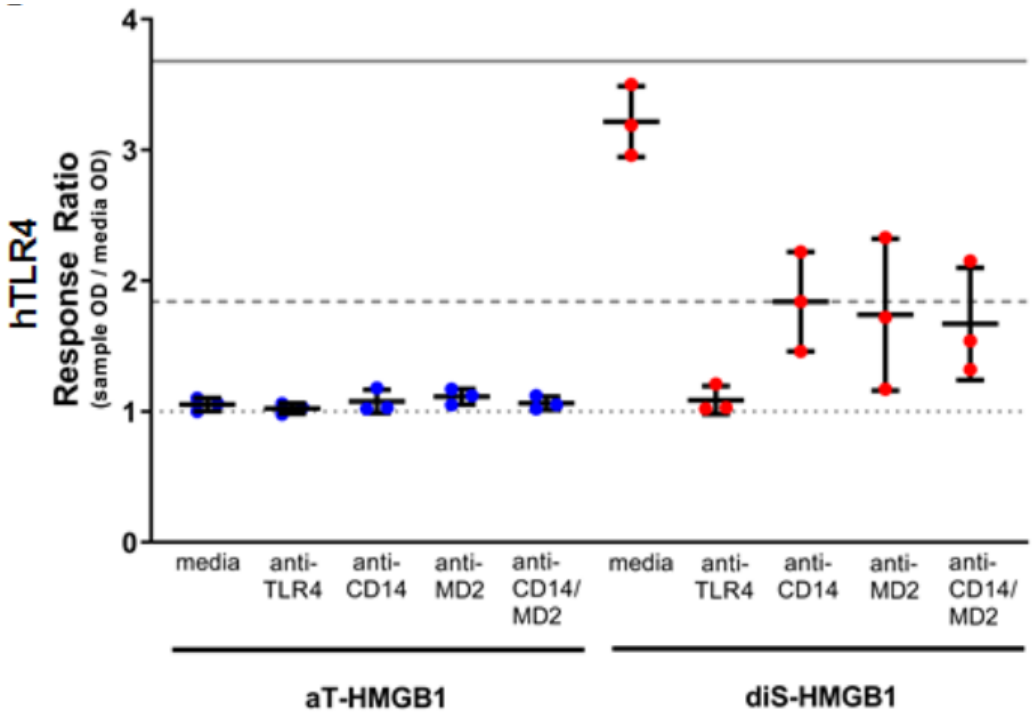

Supplementary Figure 2-S7. Disulfide-HMGB1 stimulates TNAa release from monocytes in 8 hours.

A. Four controls were used to stimulate PBMC-derived monocytes from third-party healthy donors for 2-24 hours and supernatant was assayed for secreted TNFa to determine timing of disulfide-HMGB1-stimulated TNFa release, which peaked at 8 hours.

B. All-thiol- or disulfide-HMGB1 were added at increasing concentrations to determine the optimal concentration for use in experiments (200 ng/ml)

C. All-thiol- or disulfide-HMGB1 was used to stimulate HEK-Blue TLR4-transfected cell lines pre-treated with either media (hTLR4), anti-TLR4 mAb, anti-CD14 mAb, anti-MD2 mAb or anti-CD14/anti-MD2 mAbs together, and compared to ECmax (solid line) and EC_{50} (dashed line) responses achieved using the natural control ligand LPS, as well as media alone (dotted line set to 1).

i. Data in A and B are presented as line graphs with dot showing average from three separate experiments ± SD. *$p<0.05$, ****$p<0.0001$ by two-way analysis of variance (ANOVA) with Sidak's multiple comparisons test.

Supplemental Video 2-S1: available at
https://aasldpubs.onlinelibrary.wiley.com/doi/abs/10.1002/hep.31324

Supplemental Video 2-S2: available at
https://aasldpubs.onlinelibrary.wiley.com/doi/abs/10.1002/hep.31324

2.8 REFERENCES

[1] Matzinger P. Tolerance, danger, and the extended family. Annual Review of Immunology 1994;12:991-1045.

[2] Sosa RA, Zarrinpar A, Rossetti M, Lassman CR, Naini BV, Datta N, et al. Early cytokine signatures of ischemia/reperfusion injury in human orthotopic liver transplantation. JCI Insight 2016;1:e89679.

[3] Sosa RA, Rossetti M, Naini BV, Groysberg VM, Kaldas FM, Busuttil RW, et al. Pattern Recognition Receptor-reactivity Screening of Liver Transplant Patients: Potential for Personalized and Precise Organ Matching to Reduce Risks of Ischemia-reperfusion Injury. Ann Surg 2018.

[4] Hoppe G, Talcott KE, Bhattacharya SK, Crabb JW, Sears JE. Molecular basis for the redox control of nuclear transport of the structural chromatin protein Hmgb1. Exp Cell Res 2006;312:3526-3538.

[5] Bonaldi T, Talamo F, Scaffidi P, Ferrera D, Porto A, Bachi A, et al. Monocytic cells hyperacetylate chromatin protein HMGB1 to redirect it towards secretion. EMBO J 2003;22:5551-5560.

[6] Scaffidi P, Misteli T, Bianchi ME. Release of chromatin protein HMGB1 by necrotic cells triggers inflammation. Nature 2002;418:191-195.

[7] Huang H, Nace GW, McDonald KA, Tai S, Klune JR, Rosborough BR, et al. Hepatocyte-specific high-mobility group box 1 deletion worsens the injury in liver ischemia/reperfusion: a role for intracellular high-mobility group box 1 in cellular protection. Hepatology 2014;59:1984-1997.

[8] Hosakote YM, Brasier AR, Casola A, Garofalo RP, Kurosky A. Respiratory Syncytial Virus Infection Triggers Epithelial HMGB1 Release as a Damage-Associated Molecular Pattern Promoting a Monocytic Inflammatory Response. J Virol 2016;90:9618-9631.

[9] Wakabayashi A, Shimizu M, Shinya E, Takahashi H. HMGB1 released from intestinal epithelia damaged by cholera toxin adjuvant contributes to activation of mucosal dendritic cells and induction of intestinal cytotoxic T lymphocytes and IgA. Cell Death Dis 2018;9:631.

[10] Leavy O. HMGB1-mediated inflammatory cell recruitment. Nature Reviews Immunology 2012;12:232-232.

[11] Yang H, Lundback P, Ottosson L, Erlandsson-Harris H, Venereau E, Bianchi ME, et al. Redox modification of cysteine residues regulates the cytokine activity of high mobility group box-1 (HMGB1). Mol Med 2012;18:250-259.

[12] Venereau E, Casalgrandi M, Schiraldi M, Antoine DJ, Cattaneo A, De Marchis F, et al. Mutually exclusive redox forms of HMGB1 promote cell recruitment or proinflammatory cytokine release. J Exp Med 2012;209:1519-1528.

[13] Gardella S, Andrei C, Ferrera D, Lotti LV, Torrisi MR, Bianchi ME, et al. The nuclear protein HMGB1 is secreted by monocytes via a non-classical, vesicle-mediated secretory pathway. EMBO reports 2002;3:995.

[14] Yang H, Hreggvidsdottir HS, Palmblad K, Wang H, Ochani M, Li J, et al. A critical cysteine is required for HMGB1 binding to Toll-like receptor 4 and activation of macrophage cytokine release. Proc Natl Acad Sci U S A 2010;107:11942-11947.

[15] Kim S, Kim SY, Pribis JP, Lotze M, Mollen KP, Shapiro R, et al. Signaling of high mobility group box 1 (HMGB1) through toll-like receptor 4 in macrophages requires CD14. Mol Med 2013;19:88-98.

[16] Tsung A, Sahai R, Tanaka H, Nakao A, Fink MP, Lotze MT, et al. The nuclear factor HMGB1 mediates hepatic injury after murine liver ischemia-reperfusion. J Exp Med 2005;201:1135-1143.

[17] Tsung A, Klune JR, Zhang X, Jeyabalan G, Cao Z, Peng X, et al. HMGB1 release induced by liver ischemia involves Toll-like receptor 4 dependent reactive oxygen species production and calcium-mediated signaling. J Exp Med 2007;204:2913-2923.

[18] Harris PA, Taylor R, Thielke R, Payne J, Gonzalez N, Conde JG. Research electronic data capture (REDCap)--a metadata-driven methodology and workflow process for providing translational research informatics support. J Biomed Inform 2009;42:377-381.

[19] Sosa RA, Murphey C, Robinson RR, Forsthuber TG. IFN-gamma ameliorates autoimmune encephalomyelitis by limiting myelin lipid peroxidation. Proc Natl Acad Sci U S A 2015;112:E5038-5047.

[20] Sosa RA, Murphey C, Ji N, Cardona AE, Forsthuber TG. The kinetics of myelin antigen uptake by myeloid cells in the central nervous system during experimental autoimmune encephalomyelitis. J Immunol 2013;191:5848-5857.

[21] Li B, Ruotti V, Stewart RM, Thomson JA, Dewey CN. RNA-Seq gene expression estimation with read mapping uncertainty. Bioinformatics 2010;26:493-500.

[22] Chen X-L, Sun L, Guo F, Wang F, Liu S, Liang X, et al. High-Mobility Group Box-1 Induces Proinflammatory Cytokines Production of Kupffer Cells through TLRs-Dependent Signaling Pathway after Burn Injury. PLoS ONE 2012;7.

[23] Yang Z, Li L, Chen L, Yuan W, Dong L, Zhang Y, et al. PARP-1 mediates LPS-induced HMGB1 release by macrophages through regulation of HMGB1 acetylation. J Immunol 2014;193:6114-6123.

[24] Shichita T, Ito M, Morita R, Komai K, Noguchi Y, Ooboshi H, et al. MAFB prevents excess inflammation after ischemic stroke by accelerating clearance of damage signals through MSR1. Nat Med 2017;23:723-732.

[25] Gougeon ML, Melki MT, Saidi H. HMGB1, an alarmin promoting HIV dissemination and latency in dendritic cells. Cell Death Differ 2012;19:96-106.

[26] Zhai Y, Shen XD, O'Connell R, Gao F, Lassman C, Busuttil RW, et al. Cutting edge: TLR4 activation mediates liver ischemia/reperfusion inflammatory response via IFN regulatory factor 3-dependent MyD88-independent pathway. J Immunol 2004;173:7115-7119.

[27] Oyama J, Blais C, Jr., Liu X, Pu M, Kobzik L, Kelly RA, et al. Reduced myocardial ischemia-reperfusion injury in toll-like receptor 4-deficient mice. Circulation 2004;109:784-789.

[28] Ilmakunnas M, Tukiainen EM, Rouhiainen A, Rauvala H, Arola J, Nordin A, et al. High mobility group box 1 protein as a marker of hepatocellular injury in human liver transplantation. Liver Transpl 2008;14:1517-1525.

[29] Youn JH, Oh YJ, Kim ES, Choi JE, Shin JS. High mobility group box 1 protein binding to lipopolysaccharide facilitates transfer of lipopolysaccharide to CD14 and enhances lipopolysaccharide-mediated TNF-alpha production in human monocytes. J Immunol 2008;180:5067-5074.

[30] Yang H, Wang H, Ju Z, Ragab AA, Lundback P, Long W, et al. MD-2 is required for disulfide HMGB1-dependent TLR4 signaling. J Exp Med 2015;212:5-14.

[31] Troseid M, Lind A, Nowak P, Barqasho B, Heger B, Lygren I, et al. Circulating levels of HMGB1 are correlated strongly with MD2 in HIV-infection: possible implication for TLR4-signalling and chronic immune activation. Innate Immun 2013;19:290-297.

[32] Komai K, Shichita T, Ito M, Kanamori M, Chikuma S, Yoshimura A. Role of scavenger receptors as damage-associated molecular pattern receptors in Toll-like receptor activation. Int Immunol 2017;29:59-70.

[33] Davis K, Banerjee S, Friggeri A, Bell C, Abraham E, Zerfaoui M. Poly(ADP-ribosyl)ation of high mobility group box 1 (HMGB1) protein enhances inhibition of efferocytosis. Mol Med 2012;18:359-369.

[34] Hsieh YJ, Kundu TK, Wang Z, Kovelman R, Roeder RG. The TFIIIC90 subunit of TFIIIC interacts with multiple components of the RNA polymerase III machinery and contains a histone-specific acetyltransferase activity. Mol Cell Biol 1999;19:7697-7704.

[35] Falvo JV, Jasenosky LD, Kruidenier L, Goldfeld AE. Epigenetic control of cytokine gene expression: regulation of the TNF/LT locus and T helper cell differentiation. Adv Immunol 2013;118:37-128.

[36] He M, Zhang B, Wei X, Wang Z, Fan B, Du P, et al. HDAC4/5-HMGB1 signalling mediated by NADPH oxidase activity contributes to cerebral ischaemia/reperfusion injury. J Cell Mol Med 2013;17:531-542.

[37] Evankovich J, Cho SW, Zhang R, Cardinal J, Dhupar R, Zhang L, et al. High mobility group box 1 release from hepatocytes during ischemia and reperfusion injury is mediated by decreased histone deacetylase activity. J Biol Chem 2010;285:39888-39897.

[38] Nakamura K, Zhang M, Kageyama S, Ke B, Fujii T, Sosa RA, et al. Macrophage heme oxygenase-1-SIRT1-p53 axis regulates sterile inflammation in liver ischemia-reperfusion injury. J Hepatol 2017;67:1232-1242.

Chapter 3:

Disulfide-HMGB1 signals through TLR4 and TLR9 to induce inflammatory macrophages capable of innate-adaptive crosstalk in human liver transplantation

3.1 ABSTRACT

Ischemia-reperfusion injury (IRI) during orthotopic liver transplantation (OLT) contributes to graft rejection and poor clinical outcomes. The disulfide form of high mobility group box 1 (diS-HMGB1), an intracellular protein released during OLT-IRI, induces pro-inflammatory macrophages. How diS-HMGB1 differentiates human monocytes into macrophages capable of activating adaptive immunity remains unknown. We investigated if diS-HMGB1 binds TLR4 and TLR9 to differentiate monocytes into pro-inflammatory macrophages that activate adaptive immunity and promote graft injury and dysfunction. Assessment of 106 clinical liver tissue and longitudinal blood samples revealed that OLT recipients were more likely to experience IRI and graft dysfunction with increased diS-HMGB1 released during reperfusion. Increased diS-HMGB1 concentration also correlated with TLR4/TLR9 activation, polarization of monocytes into pro-inflammatory macrophages, and production of anti-donor antibodies. *In vitro*, healthy volunteer monocytes stimulated with purified diS-HMGB1 had increased inflammatory cytokine secretion, antigen presentation machinery, and ROS production. TLR4 inhibition primarily impeded cytokine/chemokine and costimulatory molecule programs, whereas TLR9 inhibition decreased HLA-DR/ROS production. diS-HMGB1-polarized macrophages also showed increased capacity to present antigens and activate T memory cells. In murine OLT, diS-HMGB1 treatment potentiated IR-mediated hepatocellular injury, accompanied by increased serum alanine transaminase levels. This translational study identifies the diS-HMGB1/TLR4/TLR9 axis as potential therapeutic targets in OLT-IRI recipients.

3.2 INTRODUCTION

Orthotopic liver transplantation (OLT) is a life-saving treatment for end-stage liver diseases [1, 2]. During the transplant process, the donor liver is at risk of ischemia-reperfusion injury (IRI), which is associated with increased incidence of rejection episodes and lower graft and patient survival [3, 4]. IRI involves a complex sterile inflammatory response, accompanied by the release of damage-associated molecular patterns (DAMPs) into the extracellular environment [5-7]. Liver resident macrophages expressing pattern recognition receptors (PRRs) bind DAMPs, become activated, and produce cytokine/chemokine programs that recruit recipient-derived inflammatory cells. Recruited host monocytes undergo distinct alterations in response to IR stress that drive their activation and differentiation into monocyte-derived macrophages (MDMs) [8]. PRR activation also links innate and adaptive immunity, as their signals improve the antigen presenting capacity of macrophages to host T cells [9]. The mechanism by which OLT-IRI immune cascades regulate human MDM recruitment/enhancement of antigen presentation remains to be elucidated.

The function of high mobility group box 1 (HMGB1), an ubiquitously-expressed DNA binding protein classified as a DAMP, is determined by the oxidation of three cysteine residues. Fully-reduced all-thiol HMGB1 (aT-HMGB1) acts as a chemoattractant, partially-oxidized disulfide HMGB1 (diS-HMGB1) induces pro-inflammatory cytokine secretion in monocytes/macrophages, and terminally-oxidized all-sulfonyl HMGB1 (aS-HMGB1) is thought to be non-immunogenic [10-12]. We reported that post-reperfusion portal vein blood (liver flush, LF) from IRI+ OLT patients contains increased concentrations of diS-HMGB1 compared to IRI- patients [13]. IRI+ pre-reperfusion biopsies comprise macrophages with hyperacetylated, lysosomal diS-HMGB1 that increased post-reperfusion [13]. This suggests that diS-HMGB1 secreted from

macrophages induces a self-perpetuating cycle of inflammation in OLT-IRI by activating infiltrating macrophages. Although our data supports the idea that diS-HMGB1 has the potential to function as a main driver of OLT injury [13], definitive evidence showing diS-HMGB1's ability to worsen liver IRI and the hepatocellular damage is lacking.

HMGB1 has multiple receptors [14] with diS-HMGB1 reported to bind toll-like receptor (TLR) 4 [12]. HMGB1 can also bind unmethylated DNA fragments and be endocytosed by the receptor for advanced glycation end products (RAGE) to trigger activation of intracellular TLR9, but the oxidative state of HMGB1 activating TLR9 is unknown [15]. Both TLR4 and TLR9 serve as HMGB1 sensors that exacerbate the innate immune response in murine hepatic IRI [16, 17]. Post-reperfusion portal LF from IRI+ OLT patients containing increased concentrations of diS-HMGB1 induces higher activation of both TLR4- and TLR9-transfected reporter cells [13, 18], suggesting a dual role for these PRRs in diS-HMGB1 pro-inflammatory signaling. However, the definitive mechanism(s) underpinning how diS-HMGB1 differentiates monocytes into pro-inflammatory macrophages that promote graft inflammation and prime alloreactive T cells in human OLT are unknown. We hypothesized that diS-HMGB1 binds TLR4 and/or TLR9 causing monocyte differentiation into pro-inflammatory sentinel, which stimulate alloimmunity through cytokine secretion and alloantigen presentation in OLT-IRI.

3.3 MATERIALS AND METHODS

3.3.1 Study design, sample and data collection

One-hundred-and-six adult primary OLT recipients were recruited into a study approved by the UCLA Institutional Research Board (IRB #13-000143) (**Table 3-1**). Patients were recruited

between May 2013 and September 2020 and provided informed consent in writing. All research was conducted in accordance with the Declaration of Helsinki. Routine standard-of-care and immunosuppressive therapy were administered as previously described [19]. Donor and recipient clinical information, sample collection, and dataset collection and analysis details were obtained as described previously: histopathological features and IRI scoring (IRI+ or IRI-) of 2-hour post-reperfusion biopsies, clinical liver function tests (LFTs: ALT, AST, bilirubin, INR) for post-operative Day 1–Day 7 (D1–D7) [4]; PRR activation by LF samples [18], and macrophage immunophenotyping after culture with LF patient samples [13].

3.3.2 Animals

C57BL/6 male mice at 8–10 weeks of age were used (Jackson Laboratory, Bar Harbor, ME). Animals were housed in a UCLA animal facility under specific pathogen-free conditions and received humane care according to the criteria outlined in the "Guide for the Care and Use of Laboratory Animals" [20]. All studies were reviewed and approved by the UCLA Animal Research Committee (ARC #1999-094).

3.3.3 Mouse liver transplantation

We used an established liver IRI mouse model of *ex vivo* hepatic cold storage (18 hours) followed by syngeneic OLT [21]. To mimic the "marginal" human OLT setting, donor livers were stored in University of Wisconsin (UW) solution at 4°C for 18 hours prior to transplantation into syngeneic mice. diS-HMGB1 (100 ng/gm) was directly injected into the portal vein immediately following liver reperfusion (diS-OLT). The dose of diS-HMGB1 administered to recipient mice was determined using the equivalent concentration found in

human LF from IRI+ patients. Animals were sacrificed at 6 h post-reperfusion, the peak of hepatocellular damage in this model, and liver and serum samples were collected. The sham group underwent the same procedures except for OLT. Formalin-fixed paraffin-embedded liver sections (5 μm) were stained with hematoxylin and eosin (H&E) for Suzuki's scoring. Cell death was assessed by terminal deoxynucleotidyl transferase dUTP nick end labeling (TUNEL) immunofluorescence. Graft function was assessed by serum ALT levels. All three analyses were performed as described [21].

3.3.4 Non-reducing HMGB1 western blot

HMGB1 western blots were performed as previously described [13]. Briefly, undiluted mouse samples (PBS use to flush storage solution out of cold ischemic mouse livers immediately preceding transplantation and serum collected 6 hours after reperfusion) or human OLT patient post-reperfusion LF plasma samples were treated with non-reducing loading buffer, run on a non-reducing SDS-PAGE gel, and transferred to a membrane for blotting with an anti-HMGB1 antibody (Abcam, Cambridge, UK). Densitometry analysis was performed with ImageJ (NIH, Bethesda, MD) and used to calculate the ratio of the bottom band (partially-oxidized disulfide HMGB1, diS-HMGB1, 25 kD) to the top band (fully-reduced all-thiol, aT-HMGB1, 28 kD) in each sample.

3.3.5 Disulfide-HMGB1 quantification

diS-HMGB1 was quantified by combining ELISA quantification and Western Blot densitometry, as described [13]. Briefly, total HMGB1 concentration in the OLT patient post-reperfusion LF samples was analyzed by ELISA (Tecan, Switzerland) according to manufacturer's instructions.

The same plasma sample was run on a non-reducing SDS-PAGE gel as described above. The ratio of lower band (disulfide) to top band (reduced) HMGB1 was combined with the total HMGB1 concentration from ELISA data to determine the concentration of diS-HMGB1 in each plasma sample. Antibody information is shown in **Table 3-S3**.

3.3.6 Human primary monocyte isolation and culture with diS-HMGB1, inhibitors, and controls

Human monocytes were isolated from healthy volunteer donor peripheral blood (IRB #10-001689) via negative selection with RosetteSep following the manufacturer's protocol (Stemcell, Vancouver Canada). Recovered monocytes were plated at $0.5x10^5$/well for immunophenotyping or $1x10^5$/well for antigen presentation assays and cultured in RPMI with 2% heat-inactivated fetal bovine serum (HI-FBS) (Omega, Tarzana, CA) and 1% Penicillin/Streptomycin for 24 hours or 5 days containing the following stimuli: diS-HMGB1 (600ng/ml; Tecan, Switzerland), aS-HMGB1 (600ng/ml; Tecan, Switzerland), LPS (10ng/ml; Invivogen, CA), or ODN2216 (2.5 μM; Invivogen, CA). diS-HMGB1-stimulted cells were cultured in the presence or absence of inhibitors and respective controls: for TLR4: TAK-242 (TLR4i; stored in DMSO) 10 μg/ml or DMSO (TLR4c) 1:1000 dilution (to match TLR4i dilutions); for TLR9: oligonucleotides ODN2088 (TLR9i) and ODN2088 control (TLR9c) (both from Invivogen, CA) 5 μM; for diS-HMGB1 neutralization: neutralizing HMGB1 antibody (αHMGB1, clone 3E8) or isotype control (mIgG) 2.25 ng/ml (both from Biolegend, CA). For 5-day cultures, 25% of original media volume was added to replenish nutrients on Day 3. TLR4i, TLR4c, αHMGB1, and mIgG were optimized for our culture system and each added 1 hour before diS-HMGB1. Cells were cultured at 37°C and 5% CO2. TLR9i or TLR9c was added immediately before diS-HMGB1 stimulation following manufacturer recommendations. Antibody information is shown in **Table 3-S3**.

3.3.7 Human primary CD4+ T cell isolation

Human CD4+ T cells were isolated from healthy volunteer donor peripheral blood (IRB #10-001689) via negative selection with RosetteSep following the manufacturer's protocol (Stemcell, Vancouver, Canada) and frozen in 90% HI-FBS (Omega, Tarzana, CA) and 10% DMSO until required for co-culture experiments. Blood donors were confirmed to be vaccinated against SARS-CoV-2.

3.3.8 CD4+ T memory cell assay

On experimental Day 0, human primary monocytes and CD4+ T cells were isolated from the same healthy volunteer donor as described above. On Day 0, $1.0x10^5$ monocytes were stimulated with 600ng/ml diS-HMGB1 or aS-HMGB1 and cultured for 5 days as described above. CD4+ T cells were frozen on Day 0, thawed on experimental Day 4, and cultured in resting media (complete advanced RPMI, 5% Human AB serum, 1% Pen/Strep) overnight at 37°C and 5% CO_2. On experimental Day 5, MDMs were washed with 1x sterile PBS and co-cultured with CD4+T cells at a 1:1 ratio in stimulation media (complete advanced RPMI, 5% Human AB serum, 50 μM β-mercaptoethanol, 1X L-glutamine (200mM)) in the presence of SARS-CoV-2 spike protein peptides at a final concentration of 1 μg/ml (kind gift from Dr. A. Sette) [22]. Cells were co-cultured for 24 hours at 37°C with 5% CO_2. After 16 hours of co-culture, brefeldin-A and monancin (Biolegend, San Diego, CA) were added to 1X concentration to prevent secretion of intracellular proteins. After the remaining 8 hours of co-culture, T cells were stained for surface marker and intracellular protein expression and analyzed by flow cytometry.

3.3.9 HLA antibody testing

Sera were treated with DTT and tested for HLA antibodies using the IgG-SAB Assay from One Lambda/Thermo Fisher (Canoga Park, CA) as previously described [23]. Antibodies were considered positive if the MFI was greater than 1000 for HLA-A, -B, -DR, -DQ or greater than 2000 for HLA-C and -DP.

3.3.10 Surface marker and intracellular cytokine flow cytometry

MDMs were phenotyped using anti-human CD16 (BUV737), anti-human CD64 (AF488), anti-human CD86 (BV650), anti-human HLA-DR (BV711), anti-human PD-L1 (PE-CF594), anti-human TIM-3 (BV510). T cells were phenotyped using anti-human CD3 (AF700), anti-human CD4 (PerCP-Cy5.5), anti-human CD8 (BUV737), anti-human IFNγ (PE), anti-human Ki67 (BUV395). Exclusion channel antibodies (BUV496) for T cell experiments included anti-human CD14 and anti-human CD16. Live-Dead Fixable Blue stain (BUV496, Thermo Fisher, Waltham, MA) was used for all flow experiments to exclude dead cells from analysis. Samples were run on an LSR Fortessa (BD Bioscience, San Jose, CA) within 7 days of fixation. Data were acquired with FACSDiva software (BD Biosciences, San Jose, CA) and analyzed using FlowJo software (TreeStar, Ashland, OR). Antibody information is shown in **Table 3-S3**. Representative images of gating strateges are shown in **Fig. 3-S4**.

3.3.11 Cytokine analysis

Cell culture supernatants were collected 24 hours after stimulation of monocytes with diS-HMGB1, controls, and inhibitors and stored at -80°C. Human 38-plex magnetic cytokine/chemokine kits (EMD Millipore, HCYTMAG-60K-PX38) were used per manufacturer's

instructions and as previously described [4]. 24/38 cytokines were analyzed for the manuscript. The remaining 14 molecules were excluded due to no known secretion by monocytes/macrophages or experimental replicates were all under the lower limit of detection for the assay.

3.3.12 Reactive Oxygen Species (ROS) detection

MDMs stimulated with LPS, ODN2216, or diS-HMGB1 with inhibitors or controls were stained on Day 5 with CellROX DeepRed (5 μM) (Thermo Fisher, Waltham, MA) for 30 minutes at 37°C. Cells were washed 3 times with 1x PBS and fixed with 4% paraformaldehyde. Samples were analyzed by flow cytometry within 2 hours of fixing. All procedures were performed as suggested by the manufacturer.

3.3.13 Statistical analyses

Recipient, donor, and transplant characteristics were summarized using means (± standard deviations) for continuous variables and frequencies (percentages) for discrete variables. **Table 3-1** displays the statistics as well as p-values from univariate correlation analyses – either simple linear regression or ANOVA models for continuous and categorical responses, respectfully – between the demographic data and diS-HMGB1 concentrations in patients' post-reperfusion LF samples. **Fig. 3-S1** shows data for the four characteristics trending or significantly associated with diS-HMGB1 concentration. Additional regression models were used to determine the significance and r2 values of correlations between patient clinical and functional datasets and corresponding patient diS-HMGB1 concentrations. Here, however, some analyses required sub-cohort selection due to limited patient sample quantities as noted by their numbers in figure legends. All p-values

were two-sided with values less than 0.05 considered significant. No adjustments were made for multiplicity due to the discovery nature of the study.

Tensor factorization: LFT measurements were restructured into a three-dimensional array with patients, collection time, and LFT as each dimension. Prior to factorization, LFT measurements were z-score normalized so that the LFT measurements across collection times for each patient had zero mean and unit variance. Using TensorLy [24], the LFT tensor was factored using canonical polyadic (CP) decomposition using alternating least squares with four components [25]. Disulfide concentrations from LF samples were then regressed against the resulting patient CP factors via multiple linear regression using the statsmodels package [26, 27]. Regression coefficients and the corresponding 95% confidence intervals were recorded for each CP component. The CP factors can be inspected like other dimensionality reduction methods, such as principal component analysis, where each factor plot indicates the association of that component with each feature. For instance, component 1 (**Fig. 3-1D**) is strongly associated with an increase in bilirubin and is sustained over time.

In vitro experiments used one-sample or paired t-tests for datasets with normal distributions and Mann-Whitney or Wilcoxon ranked tests for datasets with non-normal distributions. *In vitro* analyses were performed in GraphPad Prism 9 or with the one-sample t-test base function in R. Numbers of biological replicates per group are noted in figure legends. P-values less than 0.05 were considered significant.

3.4 RESULTS

3.4.1 Disulfide-HMGB1 released during liver reperfusion correlates with hepatocellular injury, graft dysfunction and polarizes pro-inflammatory macrophages in human OLT recipients

To determine if diS-HMGB1 levels correlated with post-OLT clinical outcomes, we retrospectively analyzed the correlation between diS-HMGB1 levels in human OLT LF samples and clinical outcomes in a cohort of 106 OLT patients (**Fig. 3-1A**). The recipient, donor, and transplant characteristics are shown (**Table 3-1**). IRI+ (n=47) patients had higher diS-HMGB1 compared with IRI- patients (n=59) (*P*=.0001; **Table 3-2, Fig. 3-S1A**). OLT recipients were 2.4-times more likely to experience IRI for every 333 ng/ml of diS-HMGB1 released during reperfusion (*P*=.001). Younger recipient age weakly correlated with higher diS-HMGB1 levels (*P*=.06; **Table 3-2, Fig. 3-S1B**). Increased donor hypertension weakly associated with (*P*=.06) and longer donor warm ischemia time positively correlated with *(P*=.04) diS-HMGB1 concentration (**Table 3-2, Fig. 3-S1C,D**). No other recipient or donor factors correlated with LF diS-HMGB1 concentration (**Table 3-S1, 3-S2**).

To determine if diS-HMGB1 levels associate with hepatocellular injury in human OLT, we correlated diS-HMGB1 concentration in LF samples from 106 OLT recipients to: 1) histological features on 2-hour post-reperfusion liver biopsies, and 2) liver function tests (LFTs) from peripheral blood draws for the first seven days post-transplant. Indeed, higher concentrations of diS-HMGB1 in recipient LF correlated with the severity of hepatocellular necrosis (0-4 score: *P*=.0001; negative vs positive for feature: *P*<.0001; **Fig. 3-1B**) and sinusoidal congestion (0-4 score: *P*=.0797; negative vs positive for feature: *P*=.0049; **Fig. 3-1C**). To identify common patterns across LFTs in the first week post-transplant and their relationship with diS-HMGB1, we

applied a dimensionality reduction technique called canonical polyadic (CP) decomposition (**Fig. 3-1D**, see supplemental methods). The first four CP contributed to ~85% of dataset variance and were therefore analyzed further (**Fig. 3-S2**). Component 1 positively correlated with diS-HMGB1 (β= 1.00, 95% CI [0.25, 1.75]) and was associated with high bilirubin and low international normalization ratio (INR), whereas component 2 negatively correlated with diS-HMGB1 (β= -1.01, 95% CI [-1.89, -0.30]) and was associated with high INR. Components 1 and 2 demonstrated sustained association to each post-transplant day, indicating the pattern did not have a temporal relationship. However, components 3 (β= 0.28, 95% CI [-0.61, 1.17]) and 4 (β= 0.03, 95% CI [-0.47, 0.53]) demonstrated stronger positive associations to earlier post-transplant days, suggesting transient and resolving high LFT values did not strongly correlate with diS-HMGB1. Therefore, histology and LFT results across time suggest that diS-HMGB1 correlates with the hepatocellular damage and inflammation that does not resolve within the first week post-OLT.

Next, we investigated whether diS-HMGB1 concentration correlates with the ability of LF samples to activate TLR-transfected HEK-293 reporter cell lines. diS-HMGB1 concentration in LF positively correlated with TLR4 (r^2=0.22, *P*=.0004) and TLR9 (r^2=0.11, *P*=.01) activation (**Fig. 3-1E**). Based on these findings, we questioned if diS-HMGB1 present in LF could alter the phenotype of monocytes in three-day cultures (n=69) (**Fig. 3-1F**). Lower diS-HMGB1 concentrations correlated with the expression of proteins associated with dampening innate and adaptive immune responses, including CD14 (r^2=0.05, *P*=.06), CD66a (r^2=0.15, *P*=.001), TIM-3 (r^2=0.15, *P*=.008), and PD-L1 (r^2=0.07, *P*=.03). In contrast, higher concentrations of diS-HMGB1 associated with expression of the pro-inflammatory markers CD11b (r^2=0.04, *P*=.12), CD16 (r^2=0.05, *P*=.07), and CD86 (r^2=0.05, *P*=.06). These results support the hypothesis that generation

of diS-HMGB1 during OLT-IRI can drive macrophage polarization to a pro-inflammatory profile in recipients via TLR4 and TLR9 signaling.

3.4.2 Disulfide-HMGB1 increases human monocyte cytokine production through TLR4 and TLR9 signaling

To elucidate the role of diS-HMGB1 in pro-inflammatory MDM polarization, we developed an *in vitro* culture system to model the stimulation of OLT recipient infiltrating monocytes by diS-HMGB1 released from the donor allograft upon reperfusion. Monocytes were cultured with purified diS-HMGB1 or the non-immunogenic, all-sulfonyl form of HMGB1 (aS-HMGB1) at 600 ng/ml, the mean value of diS-HMGB1 previously detected in IRI+ patient LF samples [13]. After 24-hour stimulation with diS-HMGB1 or aS-HMGB1, we analyzed culture supernatant cytokines and chemokines by multiplex Luminex. diS-HMGB1-stimulated monocytes showed an increase in nine pro-inflammatory cytokines, two anti-inflammatory cytokines, seven chemokines, and four growth factors (**Fig. 3-2A**). Most increases trended or reached statistical significance, including pro-inflammatory cytokines IL-1β (P=.05), IL-6 (P=.05), and TNFα (P=.08); anti-inflammatory cytokines IL-10 (P=.02) and IL-1RA (P=.02); chemokines IL-8 (P=.11), MDC (P=.03), and MCP-1 (P=.05); and growth factors EGF (P=.03), GM-CSF (P=0.05) and IL-7 (P=.05). These data show that diS-HMGB1 triggers monocyte-derived inflammatory soluble mediators that can induce a local pro-inflammatory environment, recruit myeloid cells into the liver, and support myeloid/lymphoid cell differentiation and activation.

As TLR4 and TLR9 are diS-HMGB1 receptors and elevated concentrations of diS-HMGB1 elaborated from the allograft into LF positively correlated with TLR4 and TLR9 activation, we

examined the requirement for one or both PRRs in the diS-HMGB1-induced cytokine/chemokine profile. Monocytes were stimulated for 24 hours with diS-HMGB1 with/without the following TLR4 or TLR9 pharmacologic inhibitors: TAK-242 (a TLR4 small-molecule inhibitor; TLR4i), ODN-2088 (a TLR9 antagonist oligonucleotide; TLR9i), both inhibitors in combination (TLR4+9i), or controls (TLR4c, TLR9c, TLR4+9c) (**Fig. 3-2B**). Production of 19/24 cytokines were altered by TLR4 and/or TLR9 inhibition. TLR4i decreased IL-1β (*P*=.05), IL-6 (*P*=.04), IFNγ (*P*=.006), TNFα (*P*=.05), IL-1RA (*P*=.05), IL-8 (*P*=.05), MDC (*P*=.02), MIP-1a (*P*=.03), EGF (*P*=.03), Flt-3 (*P*=.03), and IL-7 (*P*=.01). TLR9i decreased MDC (*P*=.002) and increased MIP-1a (*P*=.01), MCP-3 (*P*=.04), and IP-10 (*P*=.04). Combined TLR4i+9i treatment increased MIP-1a (*P*=.02), decreased IL-1α (*P*=.02), IFNa2 (*P*=.03), and IL-10 (*P*=.01), and decreased MDC (*P*=.0002). These data confirm that TLR4 and TLR9 are the principal PRRs regulating the diS-HMGB1-induced pro-inflammatory macrophage secretome.

3.4.3 Disulfide-HMGB1 triggers macrophage polarization to a pro-inflammatory phenotype and function through TLR4 and TLR9 signaling

Having established that TLR4 and TLR9 control the cytokine profile of diS-HMGB1-stimulated monocytes, we next asked if diS-HMGB1 regulates MDM polarization through TLR4, TLR9 or both. We first cultured monocytes with diS-HMGB1 or aS-HMGB1 for 5 days and assessed their T cell activation molecules (HLA-DR, CD86), T cell inhibitory molecules (PD-L1, TIM-3) and Fc receptors (CD16, CD64) by flow cytometry. diS-HMGB1 increased expression of HLA-DR (*P*=.06), CD86 (*P*=.02), and CD64 (*P*=.02) and decreased PD-L1 (*P*=.04) (**Fig. 3-3A**). TIM-3 and CD16 expression did not differ between aS-HMGB1 and diS-HMGB1 stimulation. Further, diS-HMGB1's ability to upregulate HLA-DR, CD86 and CD64 while suppressing PD-L1 was blocked

by neutralizing HMGB1 antibodies (αHMGB1, **Fig. 3-3B**; HLA-DR: *P*<0.0001; CD86: *P*=.0007; CD64: *P*=.0002; PD-L1: *P*=.001). These data reveal diS-HMGB1 can enhance MDM-mediated recipient innate-adaptive crosstalk through upregulated antigen presentation machinery and Fc receptors and downregulation of inhibitory molecules.

We next investigated the specific roles of TLR4 and TLR9 as essential regulators of diS-HMGB1 MDM polarization. We stimulated donor monocytes with diS-HMGB1 together with TLR4i, TLR9i, TLR4+9i, or respective controls. Surface marker expression was compared to MDMs from the same donor treated with diS-HMGB1 alone (**Fig. 3-3C**). Treatment with TLR4i decreased HLA-DR (*P*=.1) and CD86 (*P*=.02) while TLR9i decreased HLA-DR (*P*=.008) and CD64 (*P*<.0001). Combined TLR4+9i decreased HLA-DR (P=.003), CD86 (*P*=<.0001) and CD64 (*P*<.0001) to levels below either inhibitor alone. TLR4+9c also decreased HLA-DR (*P*=.02), CD86 (*P*=.01), and CD64 (*P*=.01). Upon further analysis, combined inhibitors induced lower expression of these molecules compared to combined controls (HLA-DR *P*=.02, CD86 P=.04, CD64 P=.01), confirming the regulatory role of TLR4 and TLR9 on their expression. Interestingly, PD-L1 expression remained unchanged by TLR inhibitor treatment (TLR4i: *P*=.34; TLR9i: *P*=.37; TLR4+9i: *P*=.79), suggesting its regulation through a currently unknown mechanism. These data reveal TLR4 and TLR9 each have unique, yet cooperative, impacts on diS-HMGB1-induced expression of CD86, HLA-DR, and CD64 and therefore both contribute to diS-HMGB1-mediated innate-adaptive interactions.

3.4.4 Disulfide-HMGB1 increases human macrophage ROS production through TLR9 signaling

Macrophages produce reactive oxygen species (ROS) that can damage parenchymal liver cells, promoting alloreactivity through the release of donor HLA antigens [28, 29]. To examine if diS-HMGB1-polarized MDMs produce ROS via TLR4 and/or TLR9, we stimulated monocytes with diS-HMGB1, LPS, or TLR9 agonist ODN2216 on Day 0 and cultured cells for 5 days (**Fig. 3-4A**). diS-HMGB1 stimulated higher ROS production compared to both LPS (P=.002) and ODN2216 (P=.0096). We then assessed diS-HMGB1-mediated ROS production in the presence of TLR4i, TLR9i, or respective controls (**Fig. 3-4B, C**). TLR9i decreased ROS production (P=.003) but TLR4i had no effect (P=.29). Neutralizing diS-HMGB1 decreased ROS production (P=.0003; **Fig. 3-4D**) to levels equivalent to TLR9i treatment (P=.5) (**Fig. 3-4E**). These data suggest that diS-HMGB1 induction of ROS production by MDMs is mediated through TLR9.

3.4.5 Disulfide-HMGB1-polarized human macrophages have increased capacity to present antigens and activate T cells

To address if diS-HMGB1-polarized macrophages are poised to stimulate an adaptive immune response, we cultured monocytes with patient LF samples and analyzed their PD-L1:CD86 ratio, a measurement that reflects macrophage capacity to suppress or activate T cells [30]. LF from IRI+ patients induced a lower PD-L1:CD86 ratio than the corresponding IRI- LF samples (P=.001) (**Fig. 3-5A**). Notably, regardless of patient IRI status, higher diS-HMGB1 concentrations in LF correlated with a lower PD-L1:CD86 ratio (r^2=0.0841, P=.02) (**Fig. 3-5B**), suggesting that increased diS-HMGB1 leads to greater capacity for MDMs to activate T cells. To determine if this lower ratio is linked to increased post-OLT alloimmunity, we compared the LF-induced PD-

L1:CD86 ratio to the presence of post-transplant donor-specific HLA antibodies (DSA) in OLT patients. LF from post-transplant DSA producers (n=15) stimulated a lower PD-L1:CD86 ratio on macrophages compared to the LF from patients who did not have post-OLT DSA (n=26) (*P*=.04) (**Fig. 3-5C**). To confirm diS-HMGB1's capacity to upregulate co-stimulation/co-inhibitory molecules, we compared the PD-L1:CD86 ratio of macrophages stimulated with purified diS-HMGB1 and aS-HMGB1. Consistent with patient LF, diS-HMGB1 stimulated a lower PD-L1:CD86 ratio compared to aS-HMGB1-stimulated macrophages from the same donor (*P*=.02) (**Fig. 3-5D**).

Collectively, our data support the notion that diS-HMGB1-polarized MDMs have increased capacity to present antigens and activate T cells that can then influence antibody production and class-switching in B cells. To investigate this possibility, we developed a co-culture assay modeling indirect allorecognition, where recipient MDMs present donor peptides to recipient alloreactive memory T cells. Human CD4+ T cells were co-cultured with diS-HMGB1- or aS-HMGB1-derived MDMs and SARS-CoV-2 spike protein peptide pools for 24 hours. diS-HMGB1-stimulated MDMs induced higher Ki67 (*P*=.02) and interferon-γ (IFNγ, *P*=.02) expression in CD4+T cells compared to their aS-HMGB1-stimulated counterparts (**Fig. 3-5E**). These data indicate that diS-HMGB1 can directly influence adaptive immune activation.

3.4.6 Disulfide-HMGB1 increases hepatocellular injury in a murine OLT-IRI model

To determine if diS-HMGB1 mediates hepatocellular injury, we used an OLT murine model of IRI with extended 18-hour cold storage that mimics the marginal human OLT setting [21]. We collected the PBS used to flush the cold-stored liver immediately before the transplant surgery

(PBS liver flush) and blood 6 hours post-reperfusion (post-OLT) (**Fig. 3-6A**). diS-HMGB1 was the principal form of HMGB1 present at both pre- and post-reperfusion phases compared to aT-HMGB1 (PBS *P*=.01; post-OLT *P*=.05) (**Fig. 3-6B, C**). The diS-HMGB1 to aT-HMGB1 ratio also increased between the end of cold storage (2.9±0.4) and 6 hours post-reperfusion (5.5±1.0) (*P*=.01). To determine if diS-HMGB1 potentiates the severity of hepatic IRI, recipient mice (n=6/group) were conditioned with diS-HMGB1 (100ng/gm; portal vein) immediately following reperfusion (**Fig. 3-6D**) and compared to OLT without diS-HMGB1 adjunct (diS-OLT vs OLT). At 6 hours post-reperfusion, diS-HMGB1-treated IR-stressed OLT displayed augmented hepatocellular injury compared to controls (**Fig. 3-6E**). These correlated with increased Suzuki's grading of liver IRI (OLT= 5±1.3 vs diS-OLT= 7±1.8; *P*=.05; **Fig. 3-6F**); frequency of TUNEL+ cells (OLT= 49.17±12.27 vs diS-OLT= 85.83±18.15; *P*=.002; **Fig. 3-6G, H**) and hepatocellular damage (serum ALT: OLT= 4,436±1,349 vs diS-OLT= 10,161±5,950 IU/L; *P*=.04; **Fig. 3-6I**).

3.5 DISCUSSION

This translational study aimed to test the hypothesis that diS-HMGB1 is a key mediator of myeloid cell inflammation and alloimmunity in OLT-IRI through TLR4 and/or TLR9. diS-HMGB1 levels corresponded with increased hepatocellular necrosis, congestion, and graft dysfunction that failed to resolve during the first week post-transplant, and heightened immune activation in human OLT-IRI. TLR4 and TLR9 were key innate immune receptors driving diS-HMGB1-mediated human MDM polarization to a pro-inflammatory phenotype capable of promoting graft inflammation and T cell priming. TLR4 and TLR9 inhibition impaired macrophage commitment toward the pro-inflammatory phenotype induced by diS-HMGB1 alone – TLR4 ablation abrogated costimulatory molecule expression and cytokine production, whereas TLR9 silencing downregulated HLA class

II expression, and chemokine/ROS production. Given the increase of costimulatory molecules, MHC class II and downregulation of co-inhibitory molecules, diS-HMGB1-polarized MDMs were more efficient in driving antigen-specific memory T cell activation. These *in vitro* data highlight the novel function of the diS-HMGB1/TLR4/TLR9 axis in myeloid cell regulation, capacity for antigen presentation and capability to drive T cell-mediated alloimmunity in the mechanism of liver IRI. We also provide what we believe is the first direct evidence that administration of diS-HMGB1 exacerbated IR-mediated hepatocellular injury in a clinically-relevant murine OLT model. As such, diS-HMGB1 and its TLR4/TLR9 cognate receptors may represent putative therapeutic targets for preventing IRI in solid organ transplants, and potentially more broadly in other disease states involving ischemic injury/sterile inflammation, such as stroke and myocardial infarction [15, 31-33].

diS-HMGB1 was present in murine circulation at 6 hours post-reperfusion in an *in vivo* model of hepatic cold ischemia that mimics marginal human OLT-IRI, consistent with the presence of diS-HMGB1 in human OLT-IRI [13]. Further, diS-HMGB1 augmented IR-induced histologic features of liver injury/graft dysfunction. Although prior studies reported that extracellular HMGB1 causes injury in a murine model of liver IRI via TLR4 signaling [17, 34], we believe this is the first report showing the importance of HMGB1 oxidation state in OLT damage. These results are consistent with the concept that diS-HMGB1 is a key driver of OLT inflammation/injury and support pre-clinical assessment for therapeutics dampening diS-HMGB1, such as HMGB1 neutralizing antibodies or TLR4/9 inhibitors [35].

The importance of diS-HMGB1 to clinical outcomes was corroborated by our findings in OLT patients. diS-HMGB1 concentration in reperfusion effluent correlated with severity of hepatocellular injury and early allograft dysfunction (EAD). Furthermore, OLT patient plasma containing diS-HMGB1 had greater potential to activate TLR4/TLR9 signaling in reporter cells and induce a pro-inflammatory macrophage phenotype. Similar to the L-GrAFT scoring system that uses the rate-of-change of aspartate transaminase (AST), bilirubin, and platelet counts and maximum INR value to assess EAD [36], diS-HMGB1 release in patient LF correlated with a low rate-of-change for bilirubin and INR, suggesting measuring its level could identify OLT recipients at risk for EAD.

Purified diS-HMGB1 was a potent driver of MDM polarization in macrophage phenotype/function, comparable to MDMs polarized with OLT patient plasma containing diS-HMGB1. These MDMs were characteristic of M1 macrophages expressing increased antigen presentation machinery and secreting greater amounts of inflammatory cytokines, chemokines and growth factors. Oxidative stress from ROS production also contributes to graft injury, as it is detrimental to liver parenchymal cell survival [29, 37, 38]. These results expand upon previous findings of M1 macrophages initiating and sustaining IRI pathology [17, 39].

Inhibition of TLR4 and TLR9 signaling impaired multiple facets of the diS-HMGB1-induced MDM phenotype. Consistent with previous studies, TLR4 regulated a broader cytokine/chemokine pro-inflammatory response while TLR9 mainly produced chemokines involved in leukocyte recruitment/ROS generation [13, 40, 41]. A number of transcriptional regulators downstream of TLR4 and TLR9 modulate the surface markers explored in this study. LPS and bacterial CpG-

DNA are capable of inducing a functional interaction of NF-κB with the promoter element of HLA-DRA to induce MHC-II gene expression in a TLR9-dependent manner [42]. Interestingly, expression of the immune checkpoint PD-L1 was not altered by either TLR inhibitor. TLR2, CXCR4, and other receptors bind HMGB1 making it possible that one of these molecules regulate myeloid PD-L1 expression [14]. Additionally, TLR9 controlled diS-HMGB1-induced ROS production, although evidence exists supporting both TLR4 and TLR9-mediated ROS production. CpG-DNA increases ROS production during intracellular infection of dendritic cells with *Salmonella,* a model for ROS production, while increasing presentation of *Salmonella* peptides [9]. *Salmonella* infection in $TLR9^{-/-}$ mice confirmed this pathway, supporting our TLR9-dependent ROS mechanism [43]. A separate study concluded that TLR4, not TLR9, contributes to macrophage *Salmonella*-induced ROS production *in vitro* [44]. Collectively, these data document the complex and divergent effects of diS-HMGB1-mediated TLR4 vs TLR9 signaling on MDM polarization and function.

An increasing body of data emphasize the importance of donor and recipient TLR-mediated signals in promoting alloreactive T/B cell responses and graft rejection [45]. Simultaneous deletion of TLR adaptor molecules MyD88 and Trif in donor skin prolonged allograft survival, diminished donor cell migration to draining lymph nodes and delayed graft infiltration by host T cells [46]. T cells stimulated by MyD88-silenced dendritic cells (DCs) increased the production of Th2-type cytokines, accompanied by decreased donor-specific alloreactivity [47]. Correspondingly, DCs treated with HMGB1 promoted T cell proliferation/differentiation, whereas HMGB1 blockade ameliorated chronic cardiac transplant vasculopathy and decreased T cell infiltration/pro-inflammatory cytokine production [48, 49]. Our data support TLR4 and TLR9 signaling in

enhancing antigen presenting activity of MDMs and their capacity to stimulate alloreactivity. MDMs exposed to diS-HMGB1 stimulated increased CD4+ T cell proliferation and IFNγ production, implying that IRI+ patients have increased ability to promote T cell- and B cell-mediated alloimmunity and that diS-HMGB1 promotes this activated state. In agreement with this concept, we found that higher diS-HMGB1 concentrations correlated with a lower PD-L1:CD86 ratio when monocytes were stimulated with either IRI+ LF or purified diS-HMGB1. Additionally, a lower PD-L1:CD86 ratio in LF correlated with post-transplant production of DSA. Therefore, it is reasonable to consider that diS-HMGB1 blockade would reduce alloreactivity and improve OLT outcomes.

A limitation of this study is the inherent property of diS-HMGB1 as a transient oxidative form of HMGB1 [13]. To account for this, we confirmed that a single dose of diS-HMGB1 on Day 0 and repeated doses of diS-HMGB1 through Day 5 showed comparable MDM phenotypes (**Fig. 3-S3**). A second limitation is the receptor repertoire of diS-HMGB1 extending beyond TLR4 and TLR9 [14]. As seen in our cytokine/phenotyping data, IL-12p40, IL-12p70, G-CSF, and GM-CSF secretion and PD-L1 expression were modified by diS-HMGB1 adjunct, but not TLR4 or TLR9 inhibition. Future studies should explore the effect of other receptors, such as TLR2 or CXCR4, individually or in concert with TLR4 and TLR9 pathways on MDM phenotypes [14].

In sum, our data is consistent with a model whereby interactions between diS-HMGB1, released from IR-stressed donor allografts, and TLR4/TLR9 molecules induce MDM polarization to an M1-like phenotype with increased expression of both pro-inflammatory cytokines and antigen presentation/co-stimulation molecules. Macrophage-derived ROS contributes to hepatocyte death,

likely generating donor HLA antigens processed and presented via indirect allorecognition by diS-HMGB1-polarized macrophages. These macrophages then go on to present donor-derived peptides to activate alloreactive T cells and DSA production. The current findings also provide a basis for using therapeutics to alter macrophage polarization and improve OLT outcomes, including anti-oxidants and TLR4/TLR9 neutralizing antibodies and/or small molecule antagonists [35, 50].

3.6 ABBREVIATIONS

ALT, alanine transaminase

aS-HMGB1, terminally-oxidized HMGB1

AST, aspartate transaminase

aT-HMGB1, fully-reduced HMGB1

Bili, bilirubin

CP, canonical polyadic component

DAMPs, damage-associated molecular patterns

DCs, dendritic cells

diS-HMGB1, partially-oxidized disulfide HMGB1

diS-OLT, mice undergoing cold ischemia transplants with 100ng diS-HMGB1 per 1g mouse weight injected into the portal vein during reperfusion

DSA, donor-specific HLA antibodies

EAD, early allograft dysfunction

H&E, hematoxylin and eosin

HMGB1, high mobility group box 1

IFNγ, interferon-gamma

INR, international normalized ratio

IRI, ischemia-reperfusion injury

LF, portal vein blood collected immediately following graft reperfusion from human OLT recipients

LFTs, liver function tests

LPS, lipopolysaccharide

MDMs, monocyte-derived macrophages

MFI, mean fluorescent intensity

ODN2216, oligonucleotide TLR9 agonist

OLT, orthotopic liver transplantation

PRR, pattern recognition receptor

RAGE, receptor for advanced glycation end products

ROS, reactive oxygen species

sALT, serum alanine transaminase

TLR, toll like receptor

TLR4c, TLR4 inhibitor control

TLR4i, TLR4 inhibitor

TLR4+9c, TLR4 inhibitor and TLR9 antagonist controls in combination

TLR4+9i, TLR4 inhibitor and TLR9 antagonist in combination

TLR9c, TLR9 antagonist control

TLR9i, TLR9 antagonist

TUNEL, terminal deoxynucleotidyl transferase dUTP nick end labeling

3.7 ACKNOWLEDGMENTS

This work was supported by NIH grants PO1 AI120944 (to JWKW and EFR), Ruth L. Kirschstein National Research Service Award T32CA009120 and L60 MD011903 (to RAS), and U01AI148119 (ASM). The authors thank Dr. A. Sette for the kind gift of the SARS-CoV-2 spike protein peptide pools used in this study. The authors hereby express their gratitude for all of the organ donors and their families, for giving the gift of life and the gift of knowledge, by their generous donation.

Table 3-1. Recipient, Donor, and Transplant Characteristics (n=106).

Recipient	
diS-HMGB1 [mean±SD]	413±333
Age, years [mean±SD]	57±11
Gender [n (%)]	
Female	45 (42%)
Male	61 (58%)
Race [n (%)]	
Asian	8 (7%)
Black/African American	5 (5%)
White/Caucasian	42 (40%)
Hispanic/Latino	48 (45%)
Other	3 (3%)
Liver disease etiology, n (%)	
AIH	5 (5%)
ALF	3 (3%)
ETOH	29 (27%)
HBV	4 (4%)
HCV	34 (32%)
NAFLD/NASH	19 (18%)
PBC	2 (2%)
PSC	4 (4%)
Other/unknown	6 (6%)
LFTs, opening [mean±SD]	
AST	1091±1007
ALT	545±492
Bilirubin	8±6.2
INR	1.5±0.3
Transplant liver type [n (%)]	
Liver/Kidney	11 (10%)
Split right triseg	1 (1%)
Whole Liver	94 (89%)
MELD at list [mean±SD]	26±11
MELD at txpt [mean±SD]	33±9

Donor	
Age, years [mean±SD]	39±16
Gender [n (%)]	
Female	48 (45%)
Male	58 (55%)
Race [n (%)]	
Asian	7 (7%)
Black/African American	8 (8%)
White/Caucasian	55 (52%)
Hispanic/Latino	33 (31%)
Other	3 (3%)
Status [n (%)]	
DBD	102 (96%)
DCD	4 (4%)
Warm ischemia, min [mean±SD]	52±11
Cold ischemia, h [mean±SD]	7.6±3.3
Cause of death [n (%)]	
Trauma	37 (35%)
CVS	32 (30%)
Anoxia	35 (33%)
Other	2 (2%)
DM [n (%)]	20 (12%)
HTN [n (%)]	35 (22%)
CAD [n (%)]	6 (4%)
LFTs at procurement [mean±SD]	
ALT	58±89
Bilirubin	.95±.69

Transplant, Recipient + Donor	
LIRI [n (%)]	
LIRI+	47 (44%)
LIRI-	59 (56%)
ABO [n (%)]	
Identical	95 (90%)
Compatible	11 (10%)
Donor Risk Index [mean±SD]	1.49±.36
Sharing [n (%)]	
Local	63 (59%)
Regional	41 (39%)
National	2 (2%)

Table 3-1. Recipient, Donor, and Transplant Characteristics. Abbreviations: AIH, autoimmune hepatitis; ALF, acute liver failure; ALT, alanine transaminase; AST, aspartate aminotransferase; CAD, coronary artery disease; CVS, cerebral vasospasm; DBD, donation after brain death; DCD, donation after cardiac death; DM, diabetes mellitus; EtOH, alcohol-associated; HBV, hepatitis B virus; HCC, hepatocellular carcinoma; HCV, hepatitis C virus; HTN, hypertension; INR, international normalization ratio; LFTs, liver functions tests; LIRI, liver ischemia-reperfusion injury; MELD, model for end-stage liver disease; NAFLD, non-alcoholic fatty liver disease; NASH, non-alcoholic steatohepatitis; PBC, primary biliary cirrhosis; PSC, primary sclerosing cholangitis

Table 3-2. Characteristics Correlated with diS-HMGB1 Concentration in LF Samples

Characteristic, Continuous	***r***	***P***
Recipient Age, years	-0.181	0.06
Donor Warm Ischemia, min	0.204	0.04*
Characteristic, Categorical	**diS-HMGB1, ng/ml [mean±SD]**	***P***
Donor HTN		0.06
HTN-	381±31	
HTN+	531±99	
LIRI		0.0001*
LIRI-	304±227	
LIRI+	549±392	

Table 3-2. Characteristics correlated with diS-HMGB1 concentration in LF samples. Four cohort characteristics trended or reached significance when analyzed for correlation with diS-HMGB1 in patient LF samples using simple linear regression or ANOVA models for continuous and categorical responses, respectfully. *r* values represent the correlation coefficients of continuous factors with diS-HMGB1. **P*<.05. Correlations of all other characteristics with diS-HMGB1 concentration were not significant and shown in **Tables S1, S2**. Abbreviations: HTN: hypertension; LIRI: liver ischemia-reperfusion injury.

Figure 3-1A

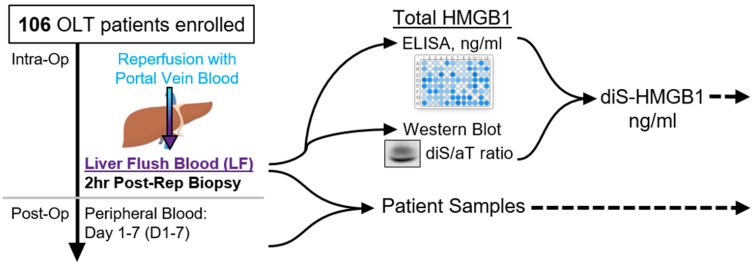

diS-HMGB1 Correlations

Assay/Clinical Parameters	Post-Tx Sample Analyzed
Histopathological features	2hr Post-rep Biopsy
LFT Values	Peripheral blood, D1-7
PRR Activation	LF plasma
Macrophage Phenotypes	LF plasma

Figure 3-1B

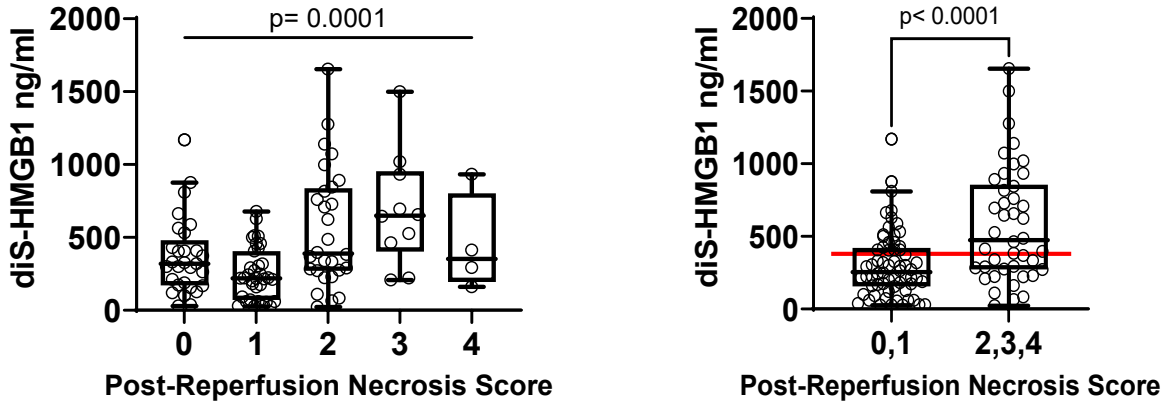

Figure 3-1C

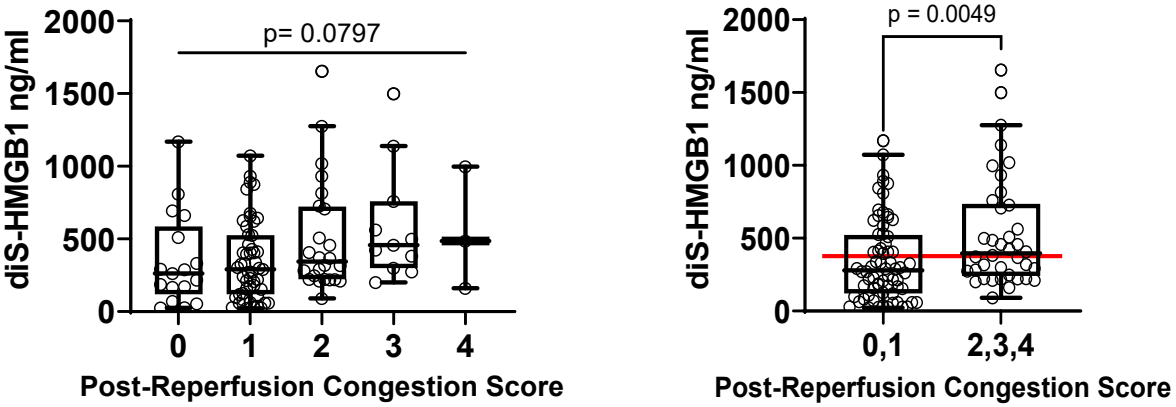

Figure 3-1D

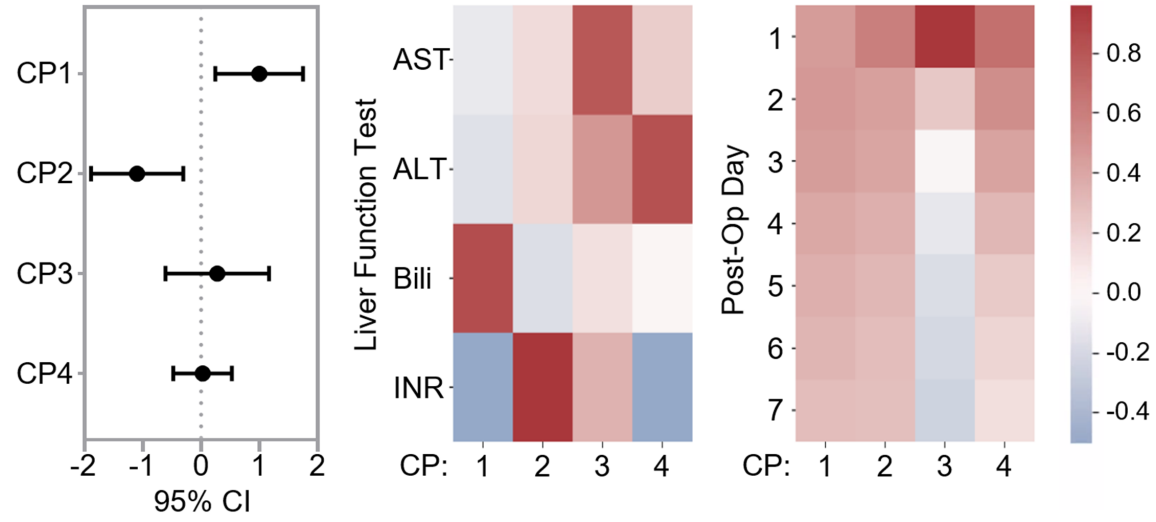

Figure 3-1E

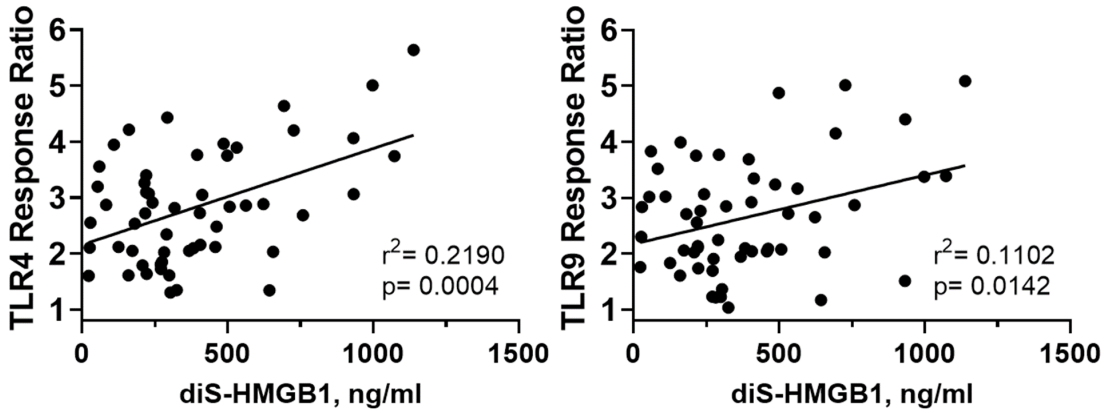

Figure 3-1F

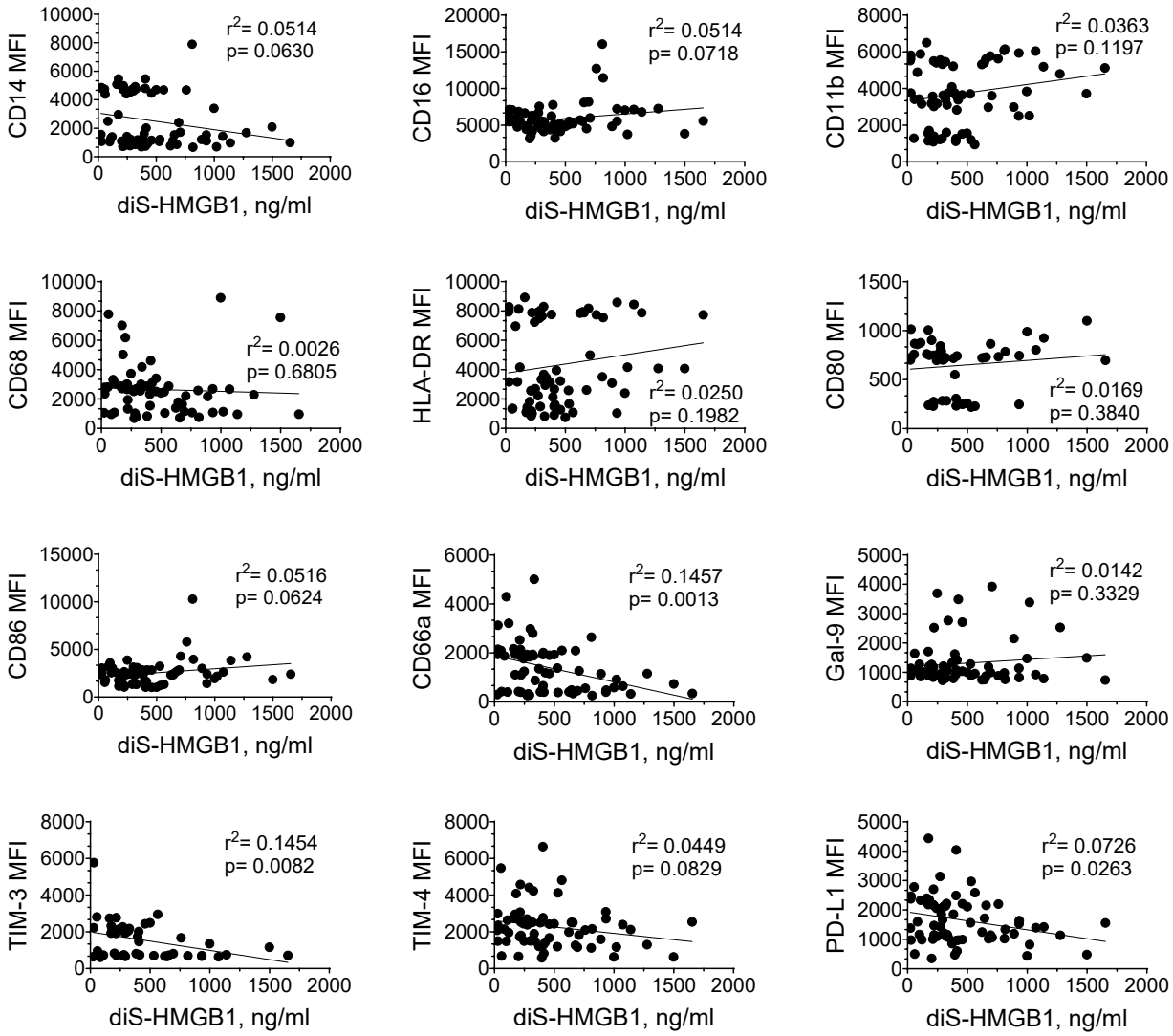

Figure 3-1. Disulfide-HMGB1 released during liver reperfusion correlates with a pro-inflammatory profile in OLT patients.

A. Patient sample collection and analysis.

B-F diS-HMGB1 concentration was assessed in LF patient samples regardless of IRI status and correlated with:

a. scoring (0-4) of 2-hour post-reperfusion biopsies and by grouping of “negative” (0, 1) vs “positive” (2, 3, 4) (n=106) for:

B. necrosis

C. sinusoidal congestion, with red line indicating overall population mean diS-HMGB1 concentration

D. LFT values for the first week post-transplant summarized by canonical polyadic (CP) decomposition (n=106)

E. LF activation of human TLR4- and TLR9-transfected HEK-Blue reporter cell lines (n=54)

F. surface marker expression of healthy volunteer monocytes after 3-day culture with LF samples (n=69)

i. Data are (B, C) Tukey plots: whiskers notate either 1.5 times the interquartile range or min and max values, whichever is closer to the median, boxes notate interquartile ranges, and lines indicate median values with all points shown; (D) left to right: regression coefficients and 95% confidence intervals of component regression against LF diS-HMGB1 concentration, component association heatmap with each of the four LFTs, and component association heatmap with LFT data from post-operative time-points; warmer colors denote positive associations, cooler colors denote negative associations; (E, F) dot plots and lines of best fit for individual patient TLR activation scores or surface markers MFIs and corresponding LF diS-HMGB1 concentration.

Figure 3-2A

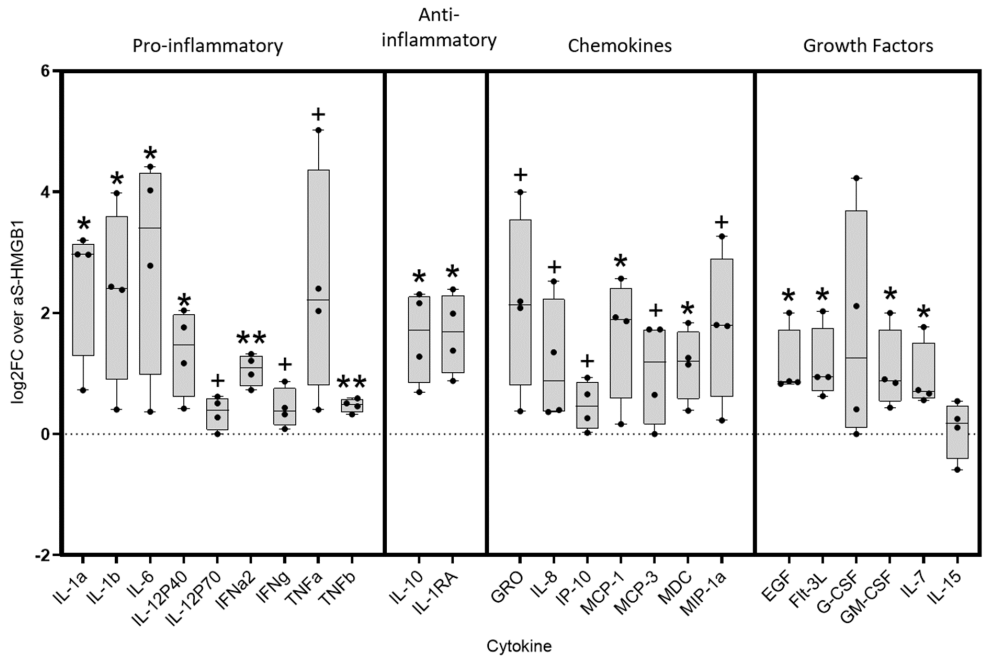

Figure 3-2B

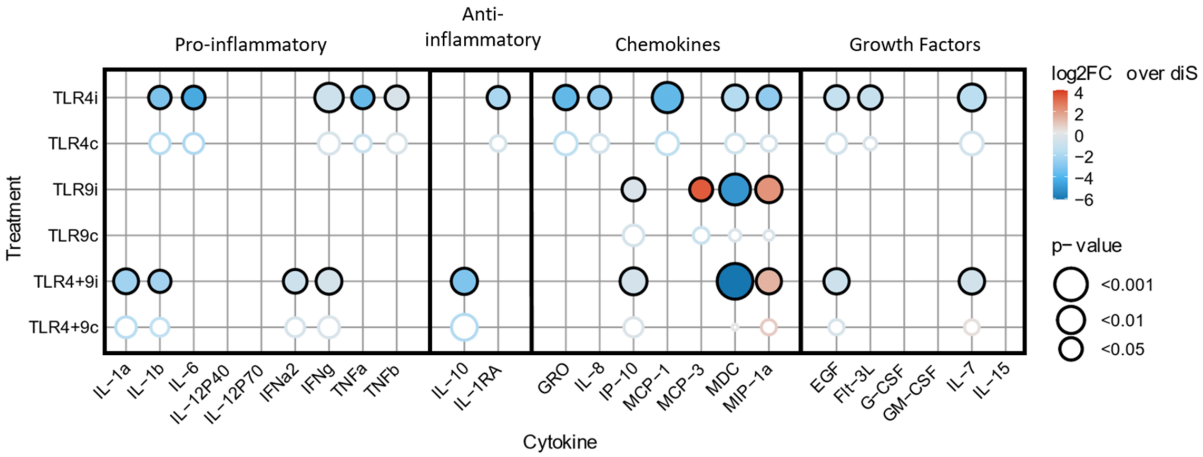

Figure 3-2. Disulfide-HMGB1 increases human monocyte pro-inflammatory phenotype through TLR4 and TLR9. Cytokine secretion from healthy volunteer monocytes stimulated with aS-HMGB1 or diS-HMGB1 and either TLR4 and/or TLR9 inhibitors or controls (TLR4i/TLR4c, TLR9i/TLR9c, TLR4+9i/TLR4+9c) after 24 hours.

A. Log2 fold-change of cytokines in diS-HMGB1 vs aS-HMGB1 supernatants (n=4). Data are Tukey plots: whiskers notate either 1.5 times the interquartile range or min and max

values, whichever is closer to the median, boxes notate interquartile ranges, and lines indicate median values with all points shown. One-sample t-tests, +$p<0.1$, *$p<0.05$, **$p<0.01$

B. Log2 fold-change of cytokines in diS-HMGB1+inhibitor or diS-HMGB1+control supernatants vs supernatants of diS-HMGB1 alone (n=4). Vertical axis: inhibitor/control treatments; Horizontal axis: cytokines. Point size represents the p-value of cytokine expression under inhibition compared to expression level under diS-HMGB1 treatment alone. Cooler colors denote a decrease under diS-HMGB1 alone, warmer colors denote an increase over diS-HMGB1 alone. Filled points indicate inhibitors, corresponding outlined points indicate respective controls. Only inhibitors with $p<0.05$ are shown. Paired t-tests.

Figure 3-3A

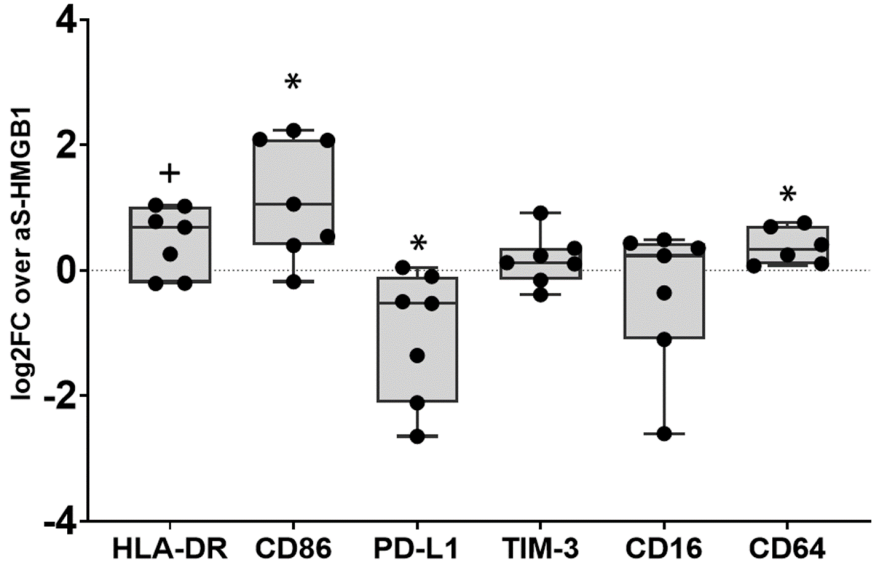

Figure 3-3B

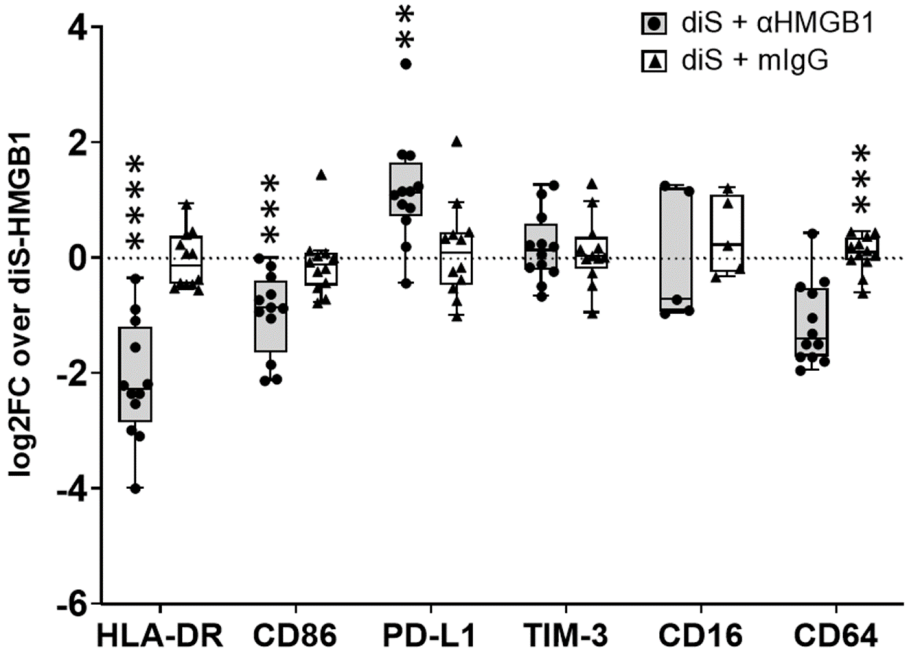

Figure 3-3C

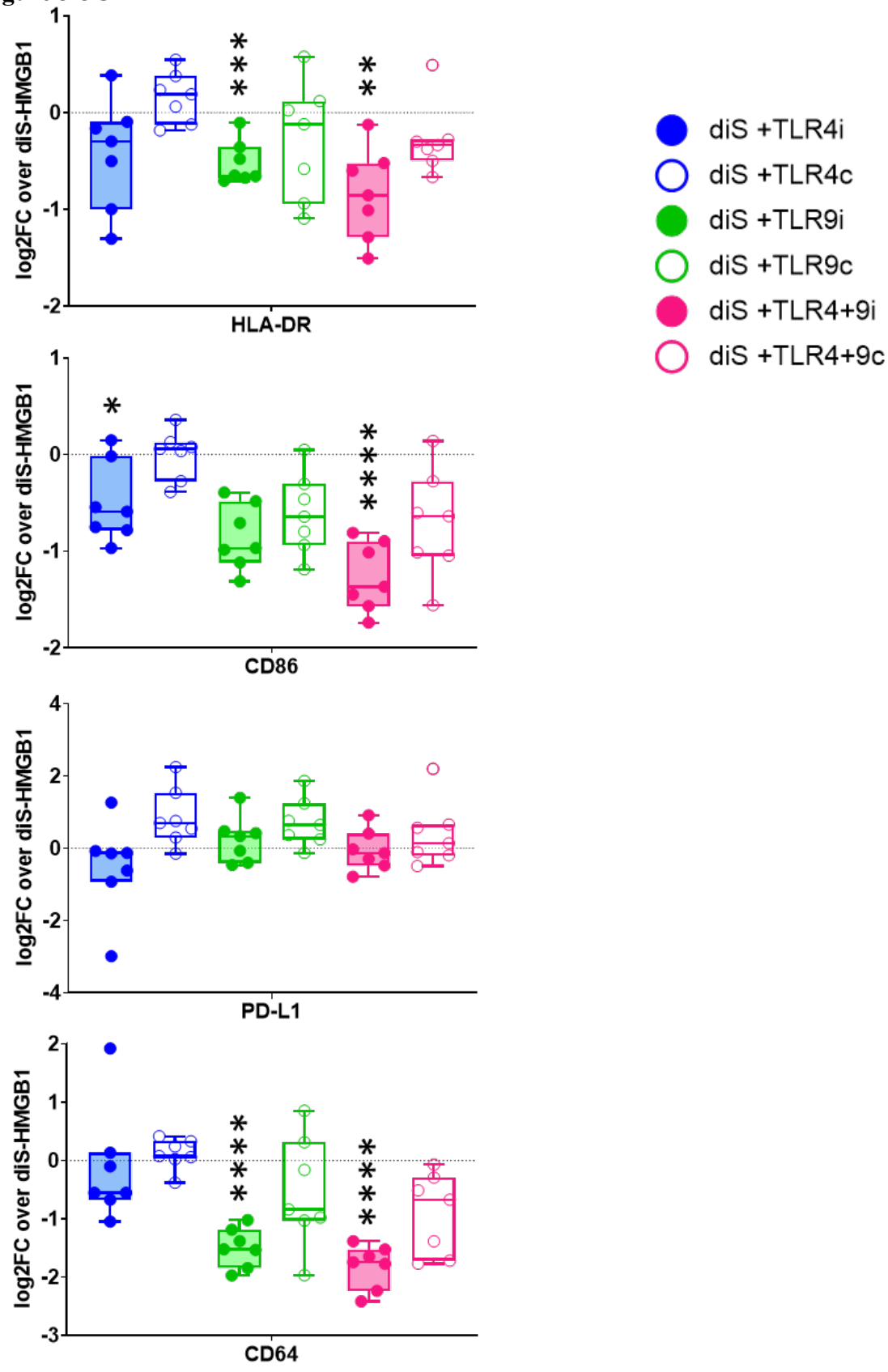
log2FC over diS-HMGB1
HLA-DR
CD86
PD-L1
CD64
diS +TLR4i
diS +TLR4c
diS +TLR9i
diS +TLR9c
diS +TLR4+9i
diS +TLR4+9c

Figure 3-3. Disulfide-HMGB1 increases human macrophages pro-inflammatory phenotype through TLR4 and TLR9. Day 5 surface marker expression on healthy volunteer monocytes stimulated with aS-HMGB1 or diS-HMGB1 and either HMGB1 neutralizing antibody and isotype control (αHMGB1, mIgG) or TLR4 and/or TLR9 inhibitors or controls (TLR4i/TLR4c, TLR9i/TLR9c, TLR4+9i/TLR4+9c).

A. Log2 fold-change on diS-HMGB1-stimulated vs aS-HMGB1-stimulated macrophages from the same donor (CD64 n=6, all others n=7).
B. Log2 fold-change on diS-HMGB1-stimulated macrophages during αHMGB1 treatment vs diS-HMGB1 stimulation alone (CD16 n=5, all others n=12).
C. Log2 fold-change on diS-HMGB1-stimulated macrophages during TLR inhibition vs diS-HMGB1 stimulation alone (n=7).

i. Data are Tukey plots: whiskers notate either 1.5 times the interquartile range or min and max values, whichever is closer to the median, boxes notate interquartile ranges, and lines indicate median values with all points shown. One-sample t-tests, +$p<0.06$, *$p<0.05$, **$p<0.01$, ***$p<0.001$, ****$p<0.0001$

Figure 3-4A

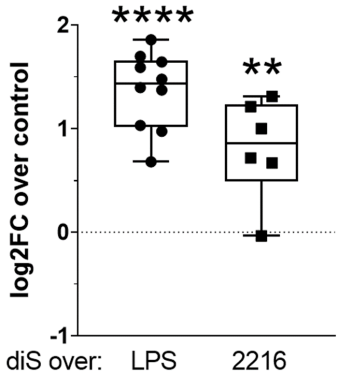

Figure 3-4B

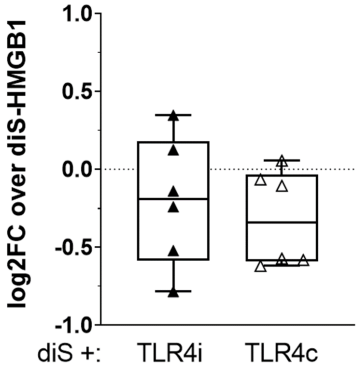

Figure 3-4C

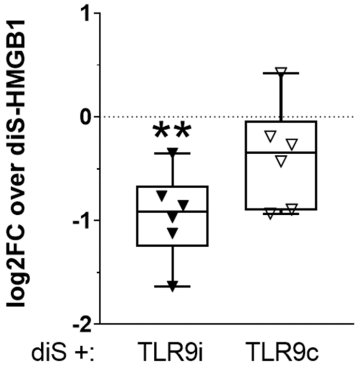

Figure 3-4D

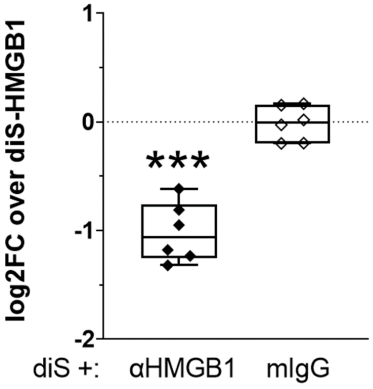

Figure 3-4E

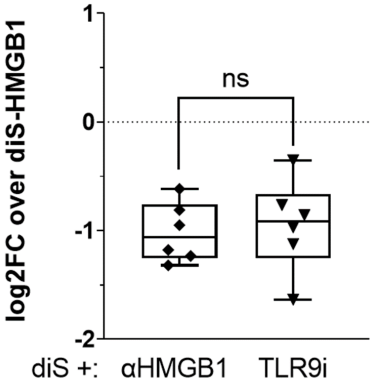

Figure 3-4. Disulfide-HMGB1 increases ROS production in human macrophages via TLR9. Day 5 ROS production by healthy volunteer monocytes stimulated with LPS (TLR4 ligand), ODN2216 (TLR9 agonist), or diS-HMGB1±HMGB1 neutralizing antibody and isotype control (αHMGB1, mIgG) or TLR4 and/or TLR9 inhibitors and respective controls (TLR4i/TLR4c, TLR9i/TLR9c).

A. diS-HMGB1-stimulated macrophages vs macrophages stimulated by LPS (n=10) or ODN2216 (n=6).

B-D diS-HMGB1-stimulated macrophages under (B) TLR4i, (C) TLR9i, or (D) αHMGB1 treatment (n=6/group) vs diS-HMGB1 alone.

E. Comparison of TLR9i and αHMGB1 treatments (n=6).

i. Data are Tukey plots: whiskers notate either 1.5 times the interquartile range or min and max values, whichever is closer to the median, boxes notate interquartile ranges, and lines indicate median values. All points are shown. (A-D) One-sample t-tests, (E) paired t-test. ns, not significant, **$p<0.01$, ***$p<0.001$, ****$p<0.0001$.

Figure 3-5A

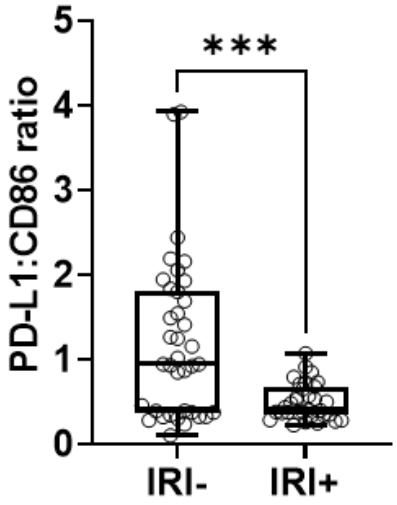

Figure 3-5B

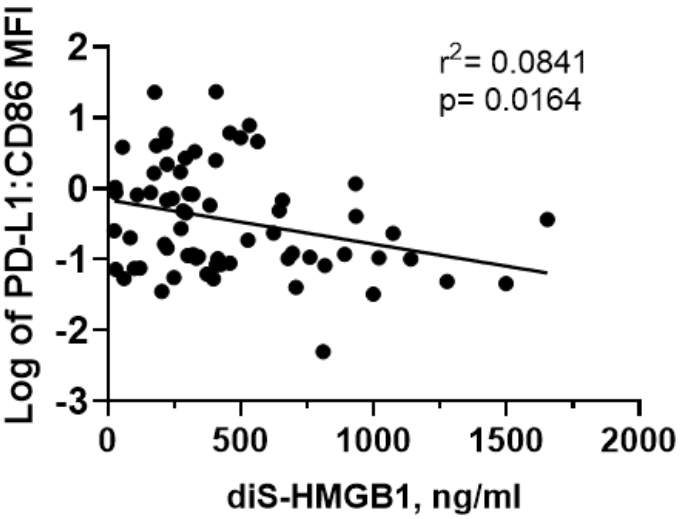

Figure 3-5C

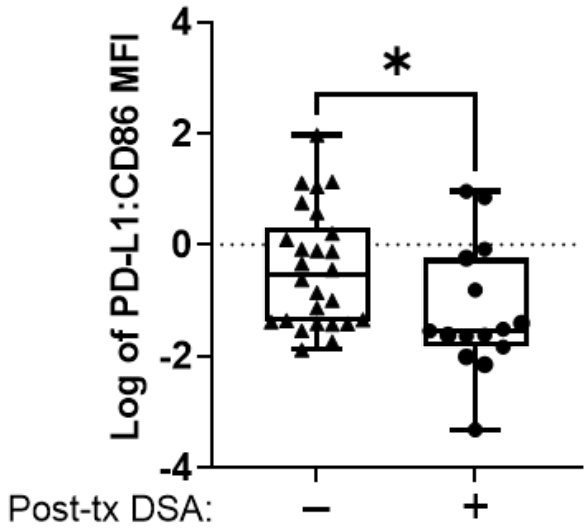

Figure 3-5D

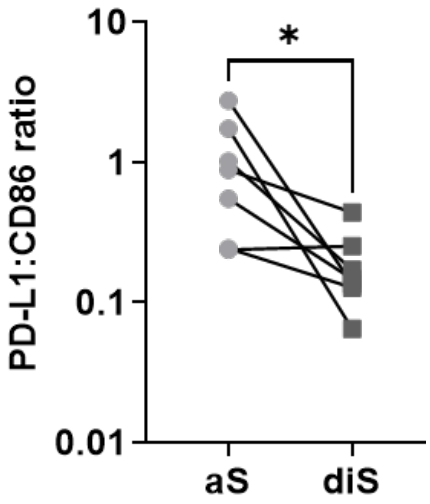

Figure 3-5E

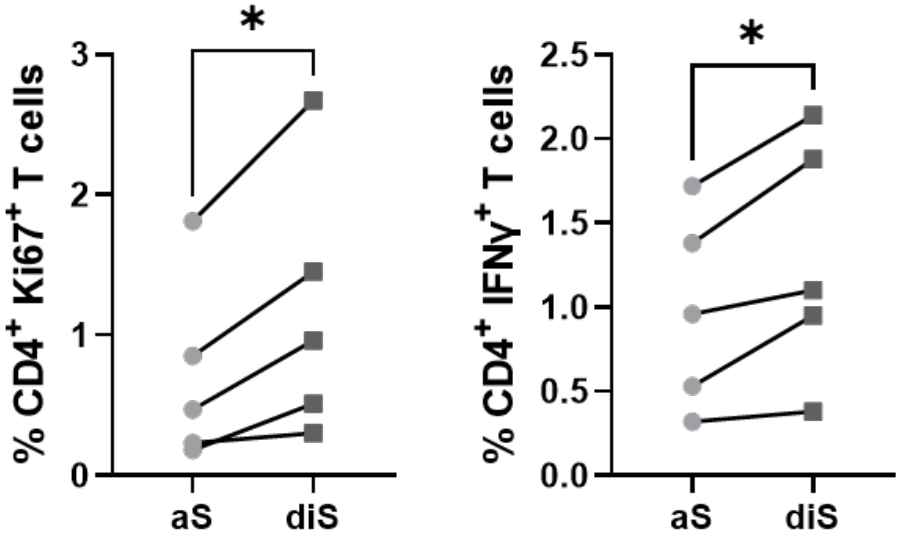

Figure 3-5. Disulfide-HMGB1 decreases macrophage PD-L1:CD86 ratio and increases T cell activation.

A. Ratio of MFIs for PD-L1 vs CD86 expression from monocytes cultured for three days with patient LF samples and separated by patient IRI status (IRI- n=37, IRI+ n=32). Unpaired Mann-Whitney.

B. Correlation of PD-L1:CD86 ratio from (A) with corresponding patient diS-HMGB1 concentration (n=69).

C. PD-L1:CD86 ratio from (A) separated by patient post-transplant donor-specific antibody (DSA) status (detectable or not; Post-tx DSA- n=26, Post-tx DSA+ n=15). Unpaired t-test.

D. Ratio of MFIs for PD-L1 vs CD86 expression from macrophages after 5 days of culture with aS-HMGB1 or diS-HMGB1 (n=7). Paired t-test.

E. Percent of CD4+ T cells positive for Ki67 or IFNγ after 24-hour culture with SARS-CoV-2 peptide as model antigen and autologous macrophages stimulated for 5 days with aS-HMGB1 or diS-HMGB1 (n=5). Paired t-test.

i. Data are (A, C) Tukey plots: whiskers notate either 1.5 times the interquartile range or min and max values, whichever is closer to the median, boxes notate interquartile ranges, and lines indicate median values, all points are shown. *$p<0.05$, ***$p<0.001$.

Figure 3-6A

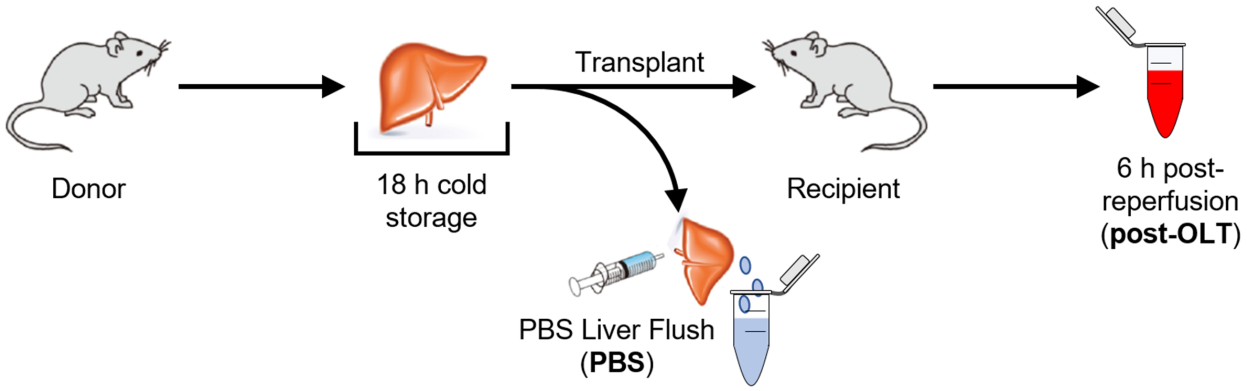

Figure 3-6B

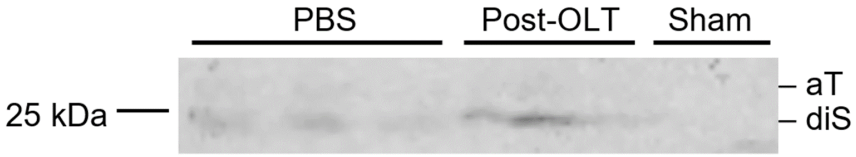

Figure 3-6C

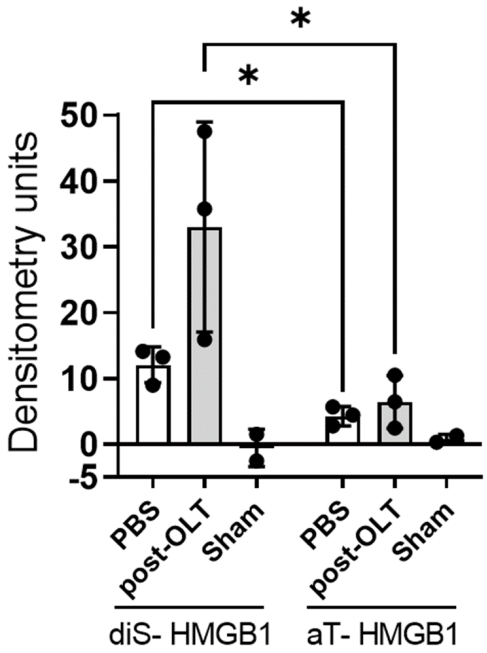

Figure 3-6D

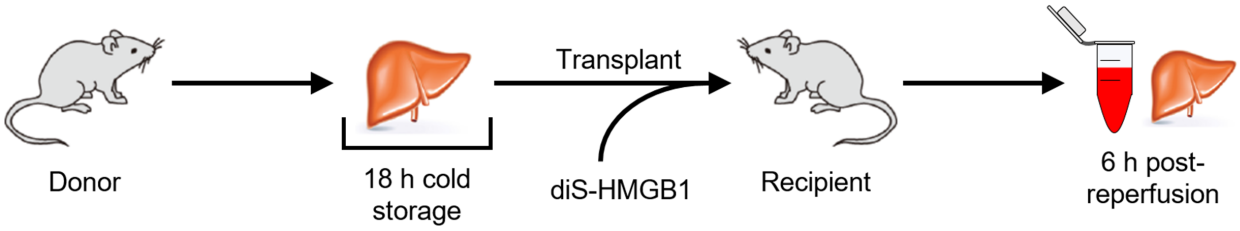

Figure 3-6E

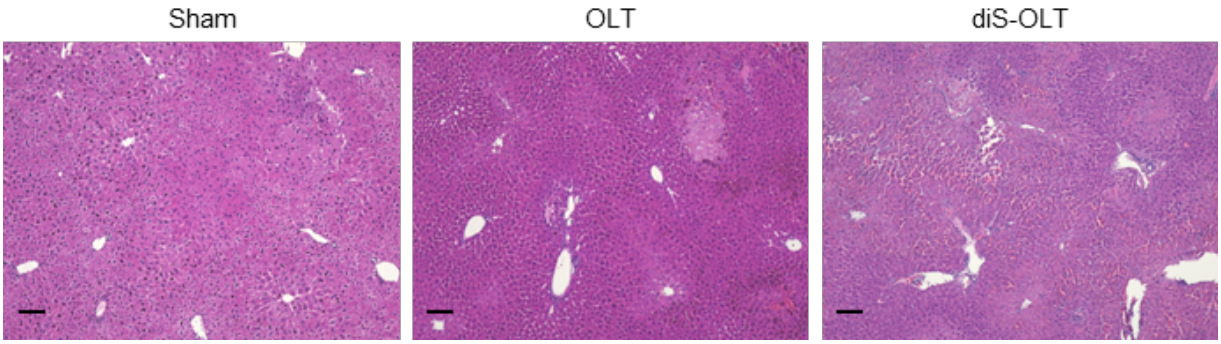

Figure 3-6F

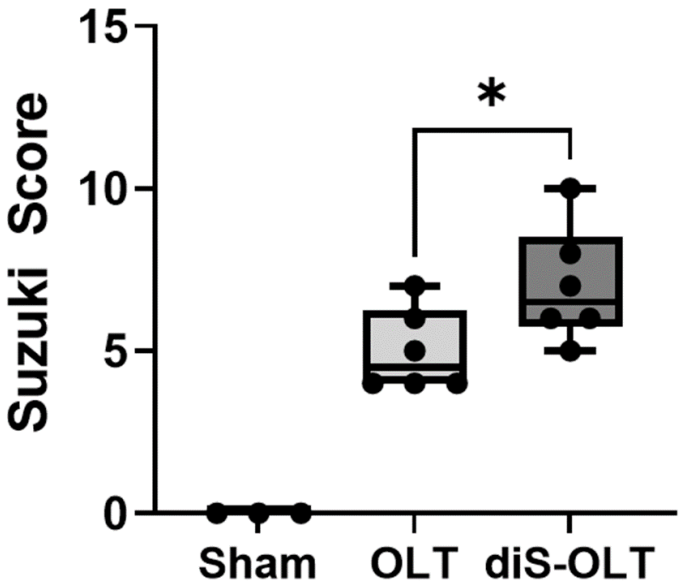

Figure 3-6G

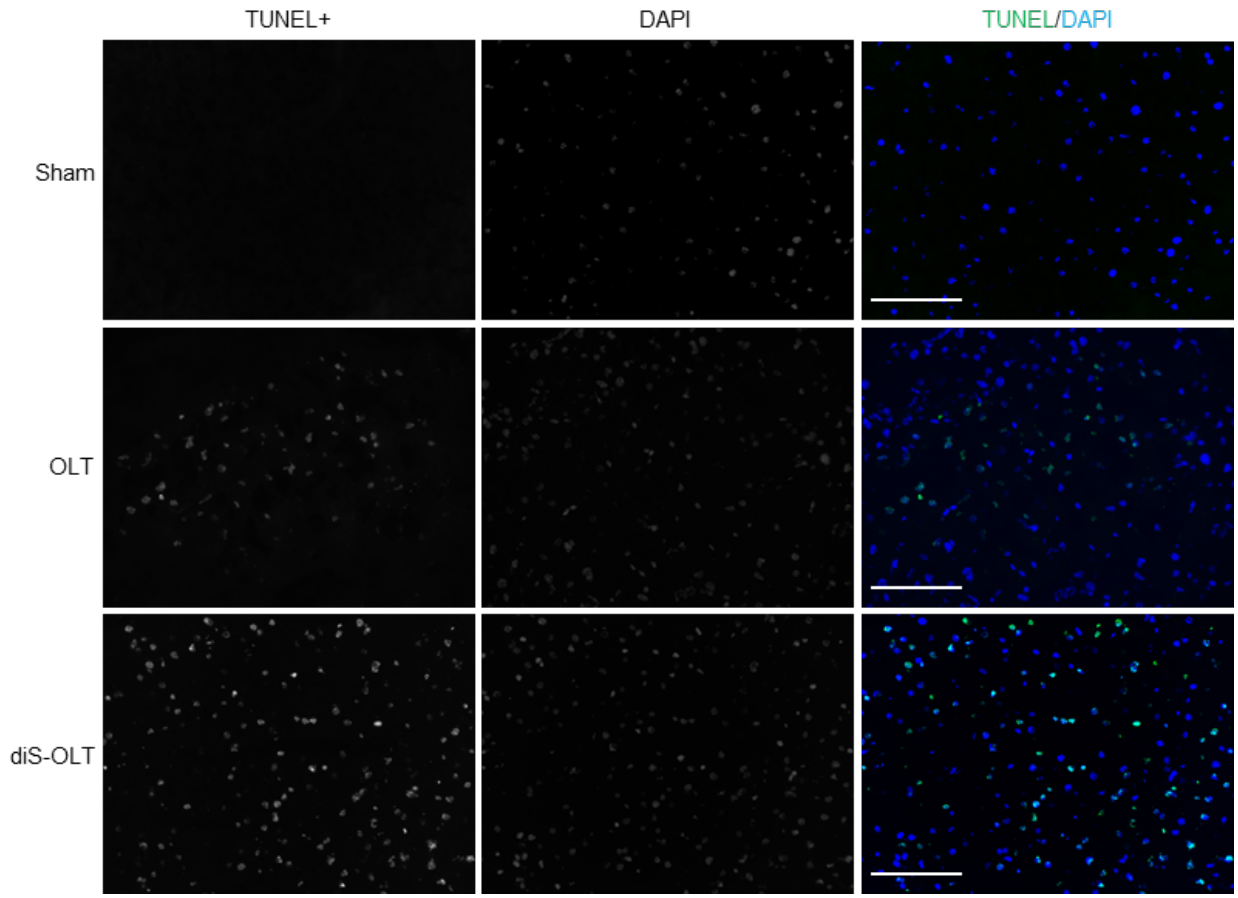

Figure 3-6H

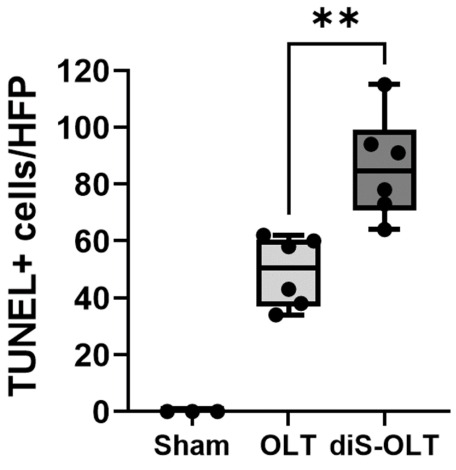

Figure 3-6I

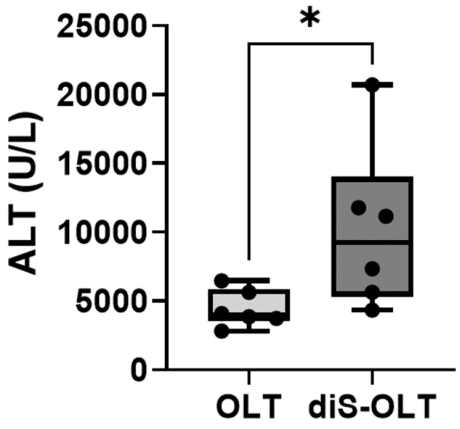

Figure 3-6. Disulfide-HMGB1 potentiates mouse OLT-IRI.

A. Experimental design for hepatic cold ischemia and OLT mouse model.
B. Non-reducing western blot of PBS (n=3), post-OLT (n=3), and Sham (n=2) serum samples.
C. Quantification of diS-HMGB1 and aT-HMGB1 levels in (B).
D. Experimental design for mice undergoing OLT with administration of exogenous diS-HMGB1 (diS-OLT). OLT control animals underwent the same procedure without diS-HMGB1 administration.
E. Representative H&E images of sham (n=3), OLT (n=6), and diS-OLT (n=6) livers 6 hours post-reperfusion, 100x, scale bar 100μm.
F. Suzuki's histological grading of liver IRI in (E).
G. Representative images of TUNEL staining for sham (n=3), OLT (n=6), and diS-OLT (n=6) liver grafts, 400x, scale bar 100μm; HPF, high-power field.
H. Quantification of TUNEL+ cells in (G).
I. Serum ALT levels in OLT and diS-OLT mice (n=6/group).

i. Data are (C) mean ± SD or (F, H, I) Tukey plots: whiskers notate either 1.5 times the interquartile range or min and max values, whichever is closer to the median, boxes notate interquartile ranges, and lines indicate median values with all points shown. *$p<0.05$, **$p<0.01$, paired t-test for Western blots, unpaired t-tests for mouse data.

Table 3-S1. Continuous Characteristics Correlated with diS-HMGB1 in LF Samples

Recipient	*r*	*P*
LFTs, opening		
AST	0.125	0.2
ALT	0.032	0.75
Bilirubin	0.126	0.2
INR	0.141	0.15
MELD at list	0.037	0.7
MELD at transplant	0.01	0.91
Donor	*r*	*P*
Cold ischemia, h	0.022	0.83
LFTs at procurement		
ALT	0.017	0.87
Bilirubin	0.01	0.94
Transplant, Recipient + Donor		*P*
Donor Risk Index	0.099	0.31

Supplementary Table 3-S1. Continuous Characteristics Correlated with diS-HMGB1 in LF Samples. Cohort characteristics that did not trend or reach significance when analyzed for correlation with diS-HMGB1 in patient LF samples using simple linear regression. *r* values represent the correlation coefficients of continuous factors with diS-HMGB1. Abbreviations: ALT, alanine transaminase; AST, aspartate aminotransferase; INR, international normalization ratio; LFTs, liver functions tests; MELD, model for end-stage liver disease.

Table 3-S2. Categorical Characteristics Correlated with diS-HMGB1 in LF Samples

Recipient	**diS-HMGB1, ng/ml [mean±SD]**	*P*
Gender		0.6
Female	393±345	
Male	427±325	
Race		0.23
Asian	296±301	
Black/African American	408±305	
White/Caucasian	352±229	
Hispanic/Latino	469±405	
Other	672±264	
Liver disease etiology		0.28
AIH	152±127	
ALF	320±481	
ETOH	482±328	
HBV	659±289	
HCV	446±409	
NAFLD/NASH	293±212	
PBC	276±315	
PSC	419±192	
Other/unknown	408±203	
Transplant liver type		0.37
Liver/Kidney	219±161	
Split right triseg	222	
Whole Liver	429±346	

Donor	**diS-HMGB1, ng/ml [mean±SD]**	*P*
Gender		0.57
Female	392±353	
Male	430±317	
Race		0.93
Asian	424±233	
Black/African American	348±351	
White/Caucasian	397±321	
Hispanic/Latino	452±363	
Other	415±525	
Status		0.37
DBD	418±33	
DCD	267±102	
Cause of death		0.53
Trauma	396±320	
CVS	410±304	
Anoxia	450±376	
Other	105±108	
DM		0.19
DM-	397±32	
DM+	532±135	
CAD		0.53
CAD-	409±33	
CAD+	517±221	

Transplant, Recipient + Donor	**diS-HMGB1, ng/ml [mean±SD]**	*P*
ABO		0.38
Identical	422±338	
Compatible	328±283	
Sharing		0.58
Local	386±324	
Regional	456±352	
National	370±181	

Supplementary Table 3-S2. Categorical Characteristics Correlated with diS-HMGB1 in LF Samples. Cohort characteristics that did not trend or reach significance when analyzed for correlation with diS-HMGB1 in patient LF samples using ANOVA models. Abbreviations: AIH,

autoimmune hepatitis; ALF, acute liver failure; CAD, coronary artery disease; CVS, cerebral vasospasm; DBD, donation after brain death; DCD, donation after cardiac death; DM, diabetes mellitus; EtOH, alcohol-associated; HBV, hepatitis B virus; HCC, hepatocellular carcinoma; HCV, hepatitis C virus; HTN, hypertension; NAFLD, non-alcoholic fatty liver disease; NASH, non-alcoholic steatohepatitis; PBC, primary biliary cirrhosis; PSC, primary sclerosing cholangitis

Supplementary Table 3-S3. Antibodies

Name	Supplier	Cat no.	Clone no.
mouse anti-human CD16 - BUV737	BD Bioscience	612786	3G8
mouse anti-human CD64 - AF488	Biolegend	305010	10.1
mouse anti-human CD86 - BV650	Biolegend	305430	IT2.2
mouse anti-human HLA-DR - BV711	Biolegend	307644	L243
mouse anti-human CD274 (PD-L1) - PE-CF549	BD Bioscience	563742	MIH1
mouse anti-human TIM-3 - BV510	Biolegend	345030	F38-2E2
mouse anti-human CD3 - AF700	Biolegend	344822	SK7
mouse anti-human CD4 - PerCP-Cy5.5	Biolegend	317428	OKT4
mouse anti-human CD8 - BUV737	BD Bioscience	741850	HIT8a
mouse anti-human Ki67 - BUV395	BD Bioscience	564071	B56
mouse anti-human IFNγ - PE	Biolegend	502509	4S.B3
rabbit polyclonal anti-HMGB1, used for western blot	Abcam	ab18256	polyclonal
Ultra-LEAF™ Purified mouse anti-HMGB1 Antibody, mIgG2b, used for neutralization	Biolegend	651414	3E8
mouse IgG2b isotype control	Biolegend	401216	MG2b-57
mouse anti-human CD14 - BUV496	BD Bioscience	750381	M5E2
mouse anti-human CD16 - BUV496	BD Bioscience	612944	3G8

Figure 3-S1A

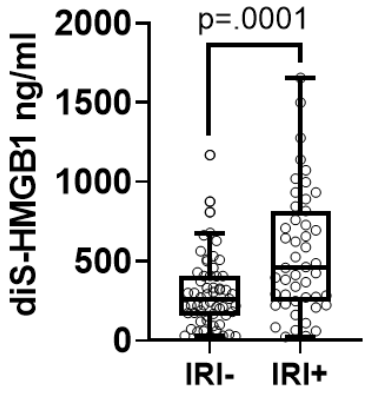

Figure 3-S1B

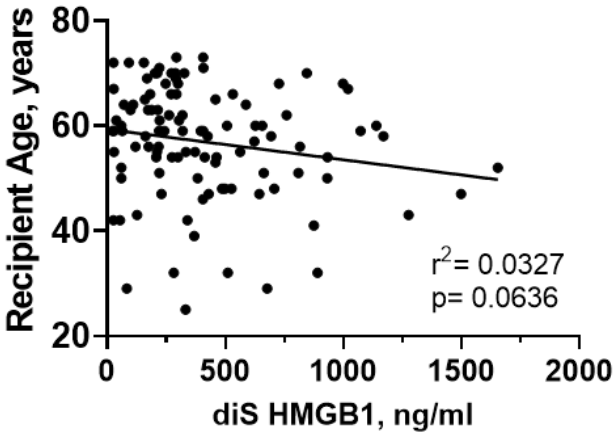

Figure 3-S1A

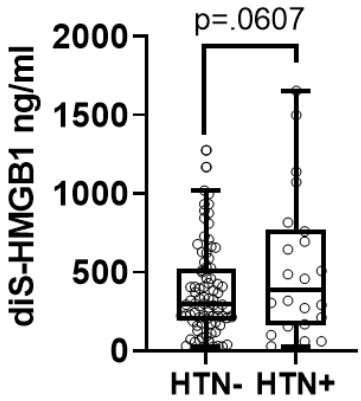

Figure 3-S1B

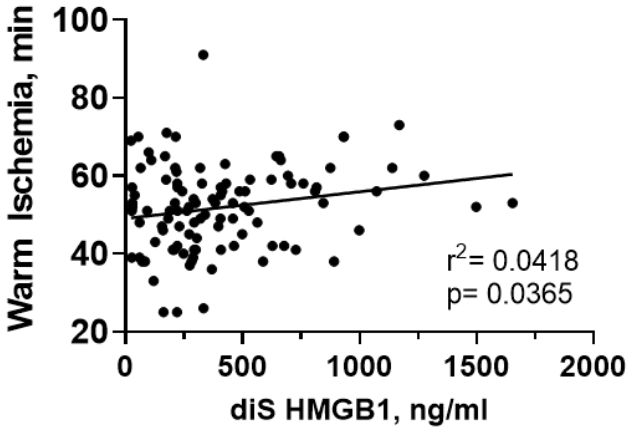

Supplementary Figure 3-S1. Cohort characteristics that trended or significantly associated with patient LF diS-HMGB1 concentration. diS-HMGB1 concentration in patient LF analyzed by:

A. IRI+ (n=47) vs IRI- patients (n=59)

B. Recipient age (n=106)

C. Donors with or without hypertension (HTN; HTN-, n=83; HTN+, n=22; not reported, n=1)

D. Warm ischemia time (n=106)

i. Data are (A, C) Mann-Whitney test and Tukey plots (whiskers notate either 1.5 times the interquartile range or min and max values, whichever is closer to the median, boxes notate interquartile ranges, and lines indicate median values with all points shown) or (B, D) Dot plots and lines of best fit for individual recipient age or warm ischemia time and corresponding LF diS-HMGB1 concentration.

Figure 3-S2

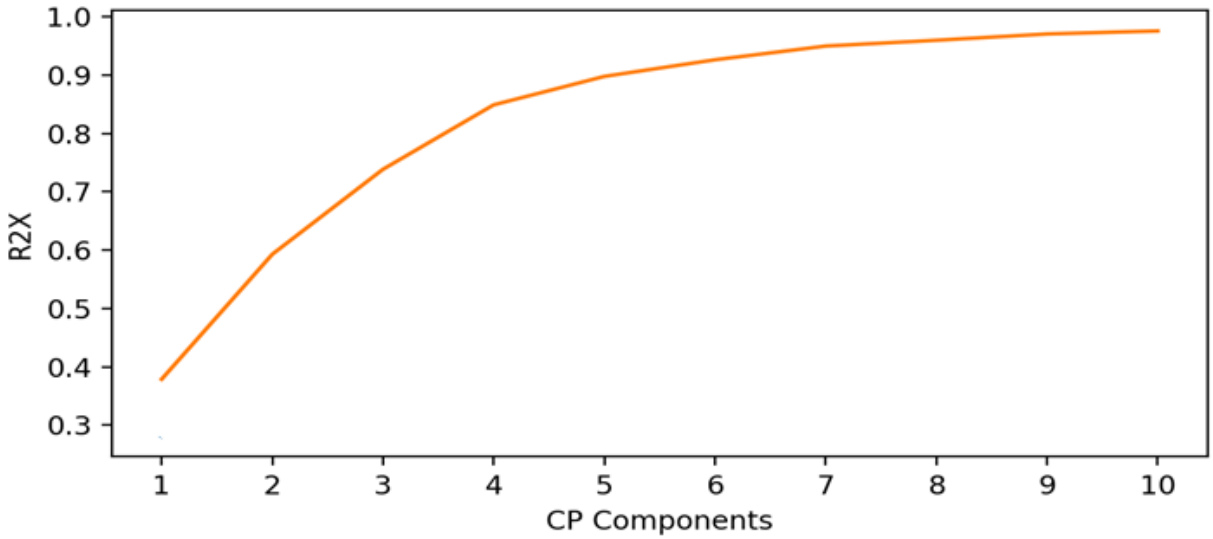

Supplementary Figure 3-S2. Percent of Variance explained by components in LFT tensor factorization. The canonical polyadic component (CP) factorization of liver function tests, time, and patients explains ~85% of the variance in the dataset (R2X) with four components. We used this four-component factorization for the study.

Figure 3-S3

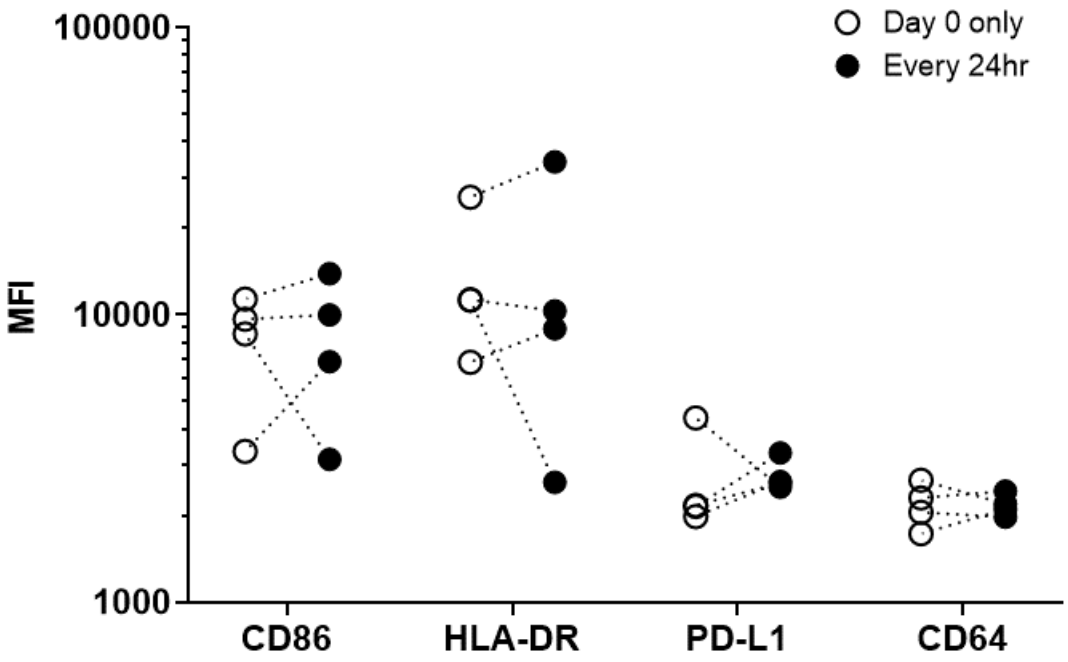

Supplementary Figure 3-S3. Disulfide-HMGB1 half-life is sufficient to differentiate macrophages with a single dose on Day 0. Healthy volunteer monocytes were stimulated on Day 0 or every day for 5 days. Expression of the four diS-HMGB1-induced surface markers was assessed on Day 5 by flow cytometry (n=4). There was no significant difference between the two dosing schedules, suggesting that one dose of diS-HMGB1 at the beginning of the culture is enough to reprogram macrophages. Paired t-test.

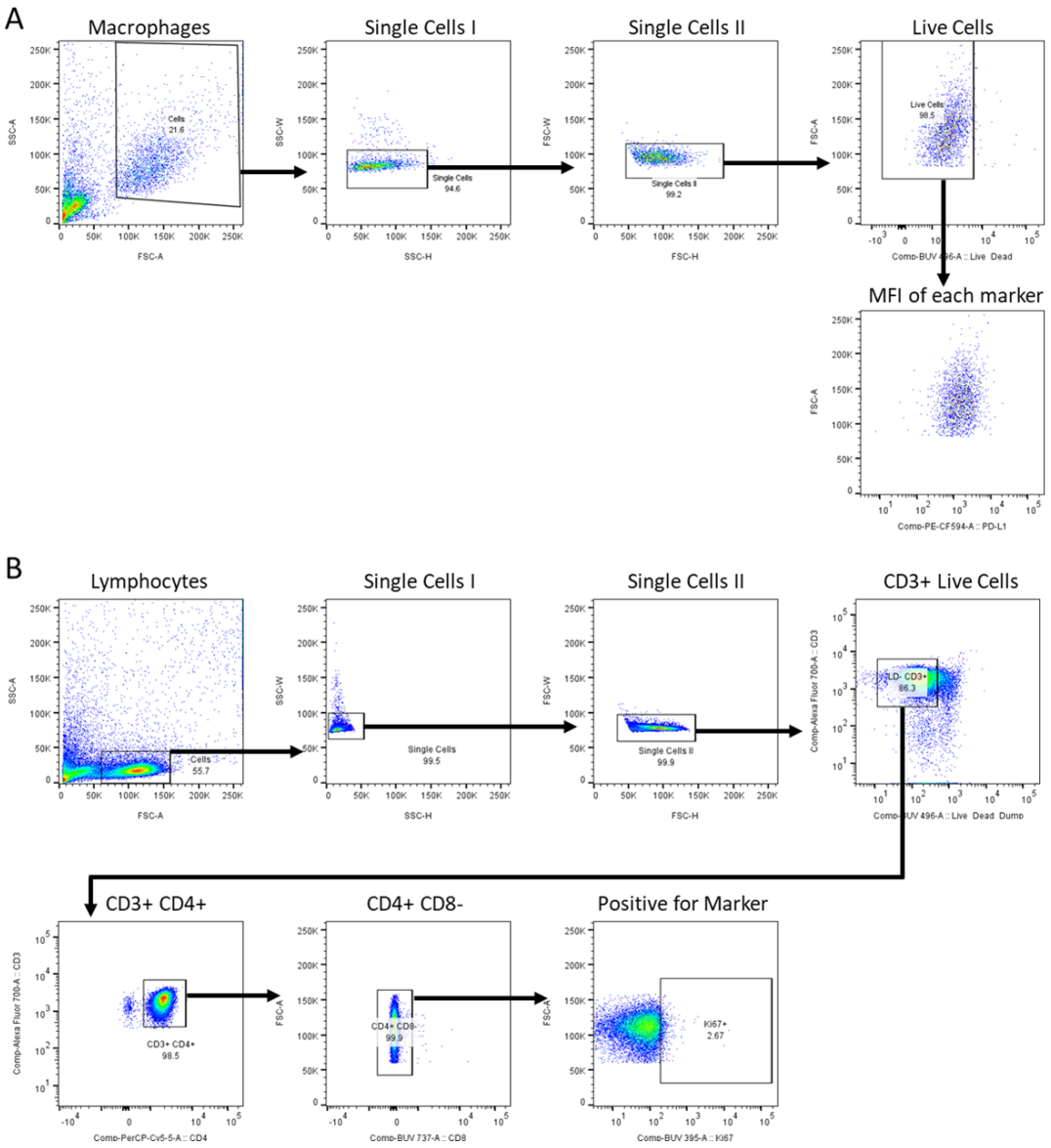

Supplementary Figure 3-S4. Gating strategy for flow cytometry analysis. Cells were selected based on size, singlets, and live/dead exclusion.

A. For macrophages, MFIs of markers were analyzed.

B. For CD4+ T cells, percent positive cells were analyzed for each marker.

3.8 REFERENCES

[1] Zhai Y, Petrowsky H, Hong JC, Busuttil RW, Kupiec-Weglinski JW. Ischaemia-reperfusion injury in liver transplantation--from bench to bedside. Nat Rev Gastroenterol Hepatol 2013;10:79-89.

[2] Kim WR, Lake JR, Smith JM, Schladt DP, Skeans MA, Noreen SM, et al. OPTN/SRTR 2017 Annual Data Report: Liver. 2019;19:184-283.

[3] Ali JM, Davies SE, Brais RJ, Randle LV, Klinck JR, Allison ME, et al. Analysis of ischemia/reperfusion injury in time-zero biopsies predicts liver allograft outcomes. Liver Transpl 2015;21:487-499.

[4] Sosa RA, Zarrinpar A, Rossetti M, Lassman CR, Naini BV, Datta N, et al. Early cytokine signatures of ischemia/reperfusion injury in human orthotopic liver transplantation. JCI Insight 2016;1:e89679.

[5] Chen GY, Nunez G. Sterile inflammation: sensing and reacting to damage. Nat Rev Immunol 2010;10:826-837.

[6] Kalogeris T, Baines CP, Krenz M, Korthuis RJ. Cell biology of ischemia/reperfusion injury. Int Rev Cell Mol Biol 2012;298:229-317.

[7] Giwa S, Lewis JK, Alvarez L, Langer R, Roth AE, Church GM, et al. The promise of organ and tissue preservation to transform medicine. Nat Biotechnol 2017;35:530-542.

[8] Yue S, Zhou H, Wang X, Busuttil RW, Kupiec-Weglinski JW, Zhai Y. Prolonged Ischemia Triggers Necrotic Depletion of Tissue-Resident Macrophages To Facilitate Inflammatory Immune Activation in Liver Ischemia Reperfusion Injury. J Immunol 2017;198:3588-3595.

[9] Lahiri A, Lahiri A, Das P, Vani J, Shaila MS, Chakravortty D. TLR 9 activation in dendritic cells enhances salmonella killing and antigen presentation via involvement of the reactive oxygen species. PLoS One 2010;5:e13772.

[10] Venereau E, Casalgrandi M, Schiraldi M, Antoine DJ, Cattaneo A, De Marchis F, et al. Mutually exclusive redox forms of HMGB1 promote cell recruitment or proinflammatory cytokine release. J Exp Med 2012;209:1519-1528.

[11] Yang H, Lundback P, Ottosson L, Erlandsson-Harris H, Venereau E, Bianchi ME, et al. Redox modification of cysteine residues regulates the cytokine activity of high mobility group box-1 (HMGB1). Mol Med 2012;18:250-259.

[12] Yang H, Hreggvidsdottir HS, Palmblad K, Wang H, Ochani M, Li J, et al. A critical cysteine is required for HMGB1 binding to Toll-like receptor 4 and activation of macrophage cytokine release. Proc Natl Acad Sci U S A 2010;107:11942-11947.

[13] Sosa RA, Terry AQ, Kaldas FM, Jin Y, Rossetti M, Ito T, et al. Disulfide-HMGB1 Drives Ischemia-Reperfusion Injury in Human Liver Transplantation. Hepatology 2020.

[14] Bertheloot D, Latz E. HMGB1, IL-1alpha, IL-33 and S100 proteins: dual-function alarmins. Cell Mol Immunol 2017;14:43-64.

[15] Tian Y, Charles EJ, Yan Z, Wu D, French BA, Kron IL, et al. The myocardial infarct-exacerbating effect of cell-free DNA is mediated by the high-mobility group box 1-receptor for advanced glycation end products-Toll-like receptor 9 pathway. J Thorac Cardiovasc Surg 2019;157:2256-2269 e2253.

[16] Bamboat ZM, Balachandran VP, Ocuin LM, Obaid H, Plitas G, DeMatteo RP. Toll-like receptor 9 inhibition confers protection from liver ischemia-reperfusion injury. Hepatology 2010;51:621-632.

[17] Tsung A, Sahai R, Tanaka H, Nakao A, Fink MP, Lotze MT, et al. The nuclear factor HMGB1 mediates hepatic injury after murine liver ischemia-reperfusion. J Exp Med 2005;201:1135-1143.

[18] Sosa RA, Rossetti M, Naini BV, Groysberg VM, Kaldas FM, Busuttil RW, et al. Pattern Recognition Receptor-reactivity Screening of Liver Transplant Patients: Potential for Personalized and Precise Organ Matching to Reduce Risks of Ischemia-reperfusion Injury. Ann Surg 2018.

[19] Ito T, Naini BV, Markovic D, Aziz A, Younan S, Lu M, et al. Ischemia-reperfusion injury and its relationship with early allograft dysfunction in liver transplant patients. American Journal of Transplantation 2020;21:614-625.

[20] Council NR. Guide for the Care and Use of Laboratory Animals. Guide for the Care and Use of Laboratory Animals. Washington (DC); 2011.

[21] Nakamura K, Kageyama S, Kaldas FM, Hirao H, Ito T, Kadono K, et al. Hepatic CEACAM1 expression indicates donor liver quality and prevents early transplantation injury. J Clin Invest 2020;130:2689-2704.

[22] Grifoni A, Weiskopf D, Ramirez SI, Mateus J, Dan JM, Moderbacher CR, et al. Targets of T Cell Responses to SARS-CoV-2 Coronavirus in Humans with COVID-19 Disease and Unexposed Individuals. Cell 2020;181:1489-1501 e1415.

[23] Blumberg JM, Gritsch HA, Reed EF, Cecka JM, Lipshutz GS, Danovitch GM, et al. Kidney paired donation in the presence of donor-specific antibodies. Kidney Int 2013;84:1009-1016.

[24] Kossaifi J PY, Anandkumar A, Pantic, M. TensorLy: Tensor Learning in Python. Journal of Machine Learning Research 2019;20:1-6.

[25] Kolda TG, Bader BW. Tensor Decompositions and Applications. SIAM Review 2009;51:455-500.

[26] Montgomery D. C. PEA, Vining G. G. Introduction to linear regression analysis: John Wiley & Sons; 2021.

[27] Seabold S PJ. Statsmodels: Econometric and statistical modeling with python. In: Millman SvdWaJ, editor.; 2010; 2010. p. 92-96.

[28] Paardekooper LM, Dingjan I, Linders PTA, Staal AHJ, Cristescu SM, Verberk W, et al. Human Monocyte-Derived Dendritic Cells Produce Millimolar Concentrations of ROS in Phagosomes Per Second. Front Immunol 2019;10:1216.

[29] de Andrade KQ, Moura FA, dos Santos JM, de Araujo OR, de Farias Santos JC, Goulart MO. Oxidative Stress and Inflammation in Hepatic Diseases: Therapeutic Possibilities of N-Acetylcysteine. Int J Mol Sci 2015;16:30269-30308.

[30] Shen T, Chen X, Chen Y, Xu Q, Lu F, Liu S. Increased PD-L1 expression and PD-L1/CD86 ratio on dendritic cells were associated with impaired dendritic cells function in HCV infection. J Med Virol 2010;82:1152-1159.

[31] Tian J, Avalos AM, Mao SY, Chen B, Senthil K, Wu H, et al. Toll-like receptor 9-dependent activation by DNA-containing immune complexes is mediated by HMGB1 and RAGE. Nat Immunol 2007;8:487-496.

[32] Muhammad S, Barakat W, Stoyanov S, Murikinati S, Yang H, Tracey KJ, et al. The HMGB1 receptor RAGE mediates ischemic brain damage. J Neurosci 2008;28:12023-12031.

[33] Wu H, Ma J, Wang P, Corpuz TM, Panchapakesan U, Wyburn KR, et al. HMGB1 contributes to kidney ischemia reperfusion injury. J Am Soc Nephrol 2010;21:1878-1890.

[34] Tsung A, Hoffman RA, Izuishi K, Critchlow ND, Nakao A, Chan MH, et al. Hepatic ischemia/reperfusion injury involves functional TLR4 signaling in nonparenchymal cells. J Immunol 2005;175:7661-7668.

[35] Yang H, Wang H, Andersson U. Targeting Inflammation Driven by HMGB1. Front Immunol 2020;11:484.

[36] Agopian VG, Harlander-Locke MP, Markovic D, Dumronggittigule W, Xia V, Kaldas FM, et al. Evaluation of Early Allograft Function Using the Liver Graft Assessment Following Transplantation Risk Score Model. JAMA Surgery 2018;153.

[37] Conde de la Rosa L, Schoemaker MH, Vrenken TE, Buist-Homan M, Havinga R, Jansen PL, et al. Superoxide anions and hydrogen peroxide induce hepatocyte death by different mechanisms: involvement of JNK and ERK MAP kinases. J Hepatol 2006;44:918-929.

[38] Ma X, Han S, Zhang W, Fan YJ, Liu MN, Liu AY, et al. Protection of cultured human hepatocytes from hydrogen peroxideinduced apoptosis by relaxin3. Mol Med Rep 2015;11:1228-1234.

[39] Dal-Secco D, Wang J, Zeng Z, Kolaczkowska E, Wong CH, Petri B, et al. A dynamic spectrum of monocytes arising from the in situ reprogramming of CCR2+ monocytes at a site of sterile injury. J Exp Med 2015;212:447-456.

[40] El-Zayat SR, Sibaii H, Mannaa FA. Toll-like receptors activation, signaling, and targeting: an overview. Bulletin of the National Research Centre 2019;43.

[41] Blackwell SE, Krieg AM. CpG-A-induced monocyte IFN-gamma-inducible protein-10 production is regulated by plasmacytoid dendritic cell-derived IFN-alpha. J Immunol 2003;170:4061-4068.

[42] Lee KW, Lee Y, Kim DS, Kwon HJ. Direct role of NF-kappaB activation in Toll-like receptor-triggered HLA-DRA expression. Eur J Immunol 2006;36:1254-1266.

[43] Zhan R, Han Q, Zhang C, Tian Z, Zhang J. Toll-Like receptor 2 (TLR2) and TLR9 play opposing roles in host innate immunity against Salmonella enterica serovar Typhimurium infection. Infect Immun 2015;83:1641-1649.

[44] West AP, Brodsky IE, Rahner C, Woo DK, Erdjument-Bromage H, Tempst P, et al. TLR signalling augments macrophage bactericidal activity through mitochondrial ROS. Nature 2011;472:476-480.

[45] Alegre ML, Chong A. Toll-like receptors (TLRs) in transplantation. Front Biosci (Elite Ed) 2009;1:36-43.

[46] McKay D, Shigeoka A, Rubinstein M, Surh C, Sprent J. Simultaneous deletion of MyD88 and Trif delays major histocompatibility and minor antigen mismatch allograft rejection. Eur J Immunol 2006;36:1994-2002.

[47] Bao W, Qin X, Guan N, Wang S, Zhu J, Sun X, et al. MyD88-silenced dendritic cells induce T-cell hyporesponsiveness and promote Th2 polarization in vivo. Cytotherapy 2015;17:1240-1250.

[48] Chen Y, Zhang W, Bao H, He W, Chen L. High Mobility Group Box 1 Contributes to the Acute Rejection of Liver Allografts by Activating Dendritic Cells. Front Immunol 2021;12:679398.

[49] Zou H, Yang Y, Gao M, Zhang B, Ming B, Sun Y, et al. HMGB1 is involved in chronic rejection of cardiac allograft via promoting inflammatory-like mDCs. Am J Transplant 2014;14:1765-1777.

[50] Farooq M, Batool M, Kim MS, Choi S. Toll-Like Receptors as a Therapeutic Target in the Era of Immunotherapies. Front Cell Dev Biol 2021;9:756315.

Chapter 4:

Discussion and Future Directions

4.1 INTRODUCTION

Ischemia-reperfusion injury (IRI) is an immune-mediated risk factor for poorer graft and patient survival during and following orthotopic liver transplantation (OLT) [1]. Studies in murine liver transplantation models provide evidence that HMGB1, a damage-associated molecular pattern (DAMP) is an early mediator of IRI, as administration of an HMGB1 neutralizing antibody ameliorates hepatocyte necrosis, pro-inflammatory cytokine expression, and NF-κB signaling compared to controls and TLR4-defective mutant mice show similar decreases in IRI readouts [2]. A follow-up study pinpointed the role of TLR4 signaling in non-parenchymal cells as crucial to the manifestation of IRI [3]. A separate group revealed that TLR9 is also implicated in manifestation of IRI in mice in an HMGB1-dependent manner, although simultaneous TLR9 inhibition and HMGB1 neutralization proved to be synergistic in ameliorating IRI [4]. Finally, HMGB1 can promote inflammatory dendritic cells (DCs), leading to chronic allograft rejection in mice [5]. The source of the HMGB1 released during OLT-IRI remains a question, especially since both monocytes/macrophages and hepatocytes can secrete HMGB1, with the former being through a non-classical vesicle-mediate mechanism and the latter being through a TLR4- and ROS-dependent mechanism [6-8]. A number of caveats also exist for these studies, including the use of warm ischemia mouse models – the clamping and unclamping of 70% of the liver instead of cold storage of a donor liver transplanted into a recipient – and that they were performed prior to the discovery that the oxidative state of HMGB1 determined its function [9-11]. We postulated that the disulfide form of HMGB1 (diS-HMGB1) is the specific oxidative form responsible for driving IRI during OLT, that diS-HMGB1 induces a pro-inflammatory response during IRI, and that this inflammation contributes to the development of long-term adaptive alloimmune responses.

4.2 KEY FINDINGS

The present work aimed to elucidate if diS-HMGB1 increases the occurrence of IRI and, if so, the mechanistic underpinnings by which it contributes to a post-transplant pro-inflammatory immune response mediated by recipient monocytes and macrophages. There are three key findings. First, we show that diS-HMGB1 is a driver of IRI in mouse models and human OLT patients. We believe these studies are the first to pinpoint the disulfide oxidative form of HMGB1 in occurrence of liver IRI. Second, we demonstrate what secreted factors, surface markers, and oxidative functions are induced by diS-HMGB1 to constitute a pro-inflammatory phenotype in monocytes and macrophages of the innate immune system. These pro-inflammatory macrophages ultimately have the capacity to activate a more durable, adaptive alloimmune response against the donor graft through their interactions with CD4+ T cells. Finally, we report how both TLR4 and TLR9 contribute to the manifestation of this phenotype. The insight gained from these studies provides new information about how diS-HMGB1 functions to activate the immune system and offers potential therapeutic targets for decreasing IRI and/or early detection methods to identify OLT patients at-risk of poor graft health post-transplant.

4.3 THE FUNCTION OF DISULFIDE-HMGB1 DURING OLT-IRI

IRI is an intrinsic risk of solid organ transplantation. Our murine and human studies provide mechanistic insight into the involvement of diS-HMGB1 in the occurrence of IRI during OLT.

4.3.1 Graft injury during IRI

We show increased levels of diS-HMGB1 in the LF samples of IRI+ patients compared to IRI- patients (**Fig. 2-2B**) and that this increase correlates with degree of IRI severity (**Fig. 2-2C**). We

also show increases from pre- to post-transplant of acetylated (**Fig. 2-5B**) HMGB1 and HMGB1 located in LAMP1$^+$ vesicles (**Fig. 2-4D, E**) in the cytoplasm of macrophages in intraoperative liver biopsies. When treated with diS-HMGB1-containing LF from IRI+ patients or with purified diS-HMGB1, healthy volunteer monocytes displayed the same increase in hyperacetylated, lysosomal HMGB1 (**Fig. 2-6A, B; Fig. 2-S6**). In Chapter 3, we show that diS-HMGB1 concentration in LF positively correlates with the degree of necrosis and sinusoidal congestion in 2-hour post-reperfusion biopsies in human OLT recipients (**Fig. 3-1B, C**), the same biopsies containing macrophages with hyperacetylated, lysosomal HMGB1 from Chapter 2. Necrosis and congestion are components of the Suzuki scoring system used to assess IRI severity in mouse models of liver IRI [12]. We show that administration of exogenous diS-HMGB1 increases hepatocellular injury, death, and liver function in a mouse model of OLT following extended cold storage of the donor organ (**Fig. 3-6F, H, I**), matching our human data. This data supports a role for diS-HMGB1 in the induction of parenchymal damage during OLT-IRI.

4.3.2 Immune activation during IRI

The release of DAMPS, either diS-HMGB1 from activated macrophages or from necrotic hepatocytes, can trigger TLR signaling within minutes of detection [13, 14]. Both TLR4 and TLR9 are implicated in liver IRI in mouse models [3, 4]. diS-HMGB1 concentration in LF samples positively correlated with LF activation of both TLR4 and TLR9 reporter cell lines (**Fig. 3-1E**). IRI+ patient LF also induced higher levels of TNFα secretion from healthy volunteer monocytes in a TLR4-dependent manner within 8 hours of culture (**Fig. 2-2D**). This suggests that TLR signaling is triggered in recipients immediately following the reperfusion maneuver. A mechanistic study of bone marrow-derived murine macrophages even revealed that TLR4 and the

receptor for advanced glycation end products (RAGE), the surface receptor responsible for endocytosis of HMGB1 for detection by TLR9, reciprocally regulate surface localization of one another [15, 16]. Activation of TLR4 and TLR9 generates pro-inflammatory cytokine release and production of chemokines that influence immune cell infiltration into the graft, providing mechanisms by which both TLRs increase IRI in liver transplantation [2-4, 8].

4.3.3 Model of diS-HMGB1 function during IRI

Together, this data supports a role for diS-HMGB1 as a driver of IRI in both humans and a clinically-relevant mouse model of OLT-IRI [17]. We envision diS-HMGB1 functioning through a mechanism whereby during and immediately following IRI (≤6 hours post-reperfusion), diS-HMGB1 is translocated into the cytoplasm of liver resident macrophages and released at the time of reperfusion triggering hepatocyte damage, poor graft function, cytokine and chemokine release, immune activation, and a positive feedback loop of diS-HMGB1 detection and secretion by resident donor and infiltrating recipient myeloid cells. This culminates in causing a degree of injury and immune activation severe enough to influence the long-term health of the donor allograft and recipient.

4.4 THE FUNCTION OF DISULFIDE-HMGB1 FOLLOWING OLT-IRI

Once diS-HMGB1 is released into the recipient at the time of reperfusion, it can impact the immune response. Our extensive profiling of clinical and *in vitro* immune activation and the mechanisms behind it offer new insight into diS-HMGB1 biology following OLT.

4.4.1 Graft function and immune response following IRI in OLT patients

Analysis of clinical and functional patient characteristics revealed a broader view of how diS-HMGB1 can influence graft health through the first week post-transplant. Four liver function tests (LFTs) are used to assess liver health: aspartate transaminase (AST), alanine transaminase (ALT), bilirubin, and the international normalization ratio (INR) for pro-thrombin time [18]. Using high dimensionality reduction, we found that diS-HMGB1 positively correlated with bilirubin levels and negatively correlated with INR levels, and that the two modules containing these correlations showed no relationship with time across the first seven days post-OLT (**Fig. 3-1D**). This data supports previous studies linking IRI to poorer outcomes including early allograft dysfunction (EAD) and recipient survival within 5 years post-transplant [1]. Therefore, the initial insult of diS-HMGB1 during reperfusion hinders the ability of the allograft to achieve normal function post-transplant. This is direct evidence supporting the hypothesis that increased diS-HMGB1 released at the time of transplant has a negative impact on post-transplant graft health and recovery.

The positive correlation between diS-HMGB1 and the tensor factorization module associated with high bilirubin supports the detrimental post-transplant effects of diS-HMGB1 as increased bilirubin indicates poor liver function (**Fig. 3-1D**). Interestingly, although patient INR levels are higher than the healthy range (0.8-1.1) [19], diS-HMGB1 negatively correlated with INR values in both modules (**Fig. 3-1D**). There are two possible explanations for this unanticipated data. Dr. Doug Farmer, chief of liver transplantation at UCLA, suggested an alternative explanation for this inverse correlation in personal communications after presentation of this data. Dr. Farmer explained that INR is manageable by clinicians while bilirubin, ALT, and AST levels are not [20]. If OLT recipient INR values are not satisfactorily recovering post-transplant, the clinical team can

administer treatment to manage these values. Therefore, the relationship between diS-HMGB1 and INR can be influenced by outside factors, such as clinical interventions, that were not accounted for in our analysis. However, if patients are not recovering well, it is tempting to hypothesize that they suffered increased IRI and therefore require more management by the clinical team. The second explanation for this is that the liver is responsible for synthesizing clotting factors and a higher INR indicates a longer prothrombin time, normally implying liver dysfunction. However, inflammation induces a shift from anti-coagulation to coagulation [21]. Given this connection, it is reasonable to see an inverse relationship between the pro-inflammatory diS-HMGB1 and decreased prothrombin time post-transplant. These LFTs again provide direct evidence that increased diS-HMGB1 released at the time of reperfusion leads to poor graft function following OLT.

We also show that the amount of diS-HMGB1 in patient LF samples negatively correlates with anti-inflammatory surface markers and trends positively with pro-inflammatory markers on healthy volunteer monocytes after three days of culture with LF (**Fig. 3-1F**). Monocytes differentiate into macrophages and DCs capable of stimulating a more persistent, adaptive immune response via T cells [22, 23]. This is accomplished through antigen presentation by HLA molecules such as HLA-DR and the balance of costimulatory molecules such as CD86 and inhibitory molecules such as PD-L1. Multiple groups support the idea of a PD-L1:CD86 ratio on antigen presenting cells as a measurement of T cell activation potential, with a lower ratio signaling increased T cell activation [24-26]. IRI+ patient LF induces a lower PD-L1:CD86 ratio on healthy volunteer monocytes and higher diS-HMGB1 (**Fig. 3-5A**), regardless of patient IRI status, correlates with a lower PD-L1:CD86 ratio (**Fig. 3-5B**). CD4+ T cells are responsible for

influencing B cell production of antibodies [23]. When examining long-term outcomes post-transplant, we found a lower LF-induced PD-L1:CD86 ratio to correlate with increased presence of antibodies specific for donor HLA antigen (donor-specific antibodies, DSA) in patient peripheral blood ≥1 month post-OLT (**Fig. 3-5C**). These DSA can go on to initiate antibody-mediated rejection (AMR) that is detrimental to the graft [1, 27]. Although LF samples contain a milieu of released proteins, the correlation of this overall pro-inflammatory monocyte/early macrophage phenotype, a lower PD-L1:CD86 ratio specifically with diS-HMGB1 levels and the correlation of the PD-L1:CD86 ratio with DSA post-transplant supports our hypothesis that diS-HMGB1 is not only a main driver of IRI, but increases the likelihood of increased alloimmune activation following OLT.

4.4.2 Monocyte Cytokine Expression

Using a purified form of diS-HMGB1 to stimulate healthy volunteer primary monocytes allowed us to elucidate the specific effects of diS-HMGB1 on macrophage phenotypes and function and the mechanisms by which these cells become activated to influence the adaptive immune response. Previous studies attribute IL-6, TNFα, and IL-10 secretion to diS-HMGB1 [17, 28]. Our study confirms those molecules and expands the panel to reveal over 20 cytokines and chemokines that increased compared to the aS-HMGB1 control (**Fig. 3-2A**). Pro-inflammatory IFNα and TNFβ displayed the most significant increases. IFNα is a potent inducer of HLA class II (including HLA-DR) [29] while TNFβ is important for establishing secondary and tertiary lymphoid organs such as lymph nodes and Peyer's patches and is a risk factor for acute myocardial infarction, another setting of ischemic injury [30, 31]. All seven of the chemokines examined showed increases above the control with the increases of both MCP-1 and MDC being significant (**Fig. 3-2A**). MCP-1 is

elevated in mouse models of IRI [4] and is responsible for extravasation of monocytes and macrophages into tissue during inflammation [32]. MDC/CCL22 is produced by macrophages and DCs and promotes chemotaxis of DCs, T cells, and natural killer cells [33]. The functions of these molecules and the fact that their expression is augmented by diS-HMGB1 demonstrates how diS-HMGB1 can induce a local pro-inflammatory environment and contribute to the recruitment of multiple immune cell types into the allograft to perpetuate the post-transplant immune response. One recent study examined the effect of diS-HMGB1 on murine bone marrow-derived macrophages and showed it also augments pro-inflammatory cytokine production at the transcriptional level [34]. Although their model stimulated differentiated macrophages with diS-HMGB1 instead of fresh monocytes, our models confirm one another with similar results from RNA and protein datasets. Given this link, the epigenetic landscape of diS-HMGB1-stimulated macrophages is an exciting direction for future studies. **Section 4.5.1** provides an expanded discussion on this future topic.

4.4.3 Macrophage surface marker expression and subsequent innate-adaptive crosstalk

diS-HMGB1 increased antigen presentation and co-stimulation machinery (HLA-DR, CD86) and decrease in T cell inhibitory molecule PD-L1 on the surface of monocyte-derived macrophages (MDMs) after 5 days of culture (**Fig. 3-3A, B**). This matched the correlation of diS-HMGB1 concentration with these markers when healthy volunteer monocytes were cultured with OLT patient LF (**Fig. 3-1F**). While HLA-DR molecules are specifically responsible for presenting peptides, CD86 and PD-L1 are involved in reciprocally controlling the state of T cell activation. Studies exploring control of Hepatitis C viremia in human patients show that a lower ratio of PD-L1 to CD86 on both monocytes and dendritic cells correlates with lower viral loads and thus a

more robust T cell-mediated immune response [24, 25]. A productive T cell response is important during viremia, but this magnitude of response can be detrimental to donor allografts following transplantation. These *in vitro* experiments supported our patient-based findings as diS-HMGB1-stimulated macrophages had lower PD-L1:CD86 ratios (**Fig. 3-5D**) and induced increased CD4+ T cell proliferation and IFNγ production (**Fig. 3-5E**) compared to their aS-HMGB1-stimulated counterparts. This data provides a specific mechanism by which diS-HMGB1 can influence the CD4+ T cell-mediated post-transplant alloimmune response via activation of infiltrating recipient monocytes at the time of allograft reperfusion. Clinical trials in multiple autoimmune diseases and kidney transplantation use tolerogenic monocyte-derived dendritic cells to subdue unwanted immune function, with Zahorchak et. Al. suggesting a high PD-L1:CD86 ratio be considered as an important release criterion for these GMP products [26, 35, 36]. Therefore, preventing diS-HMGB1 from inducing a low PD-L1:CD86 ratio in OLT patients could contribute to lower immune activation and better post-LT outcomes.

diS-HMGB1-stimulated macrophages also display increased Fc gamma receptor I (FcγRI, CD64) (**Fig. 3-3A, B**), the high-affinity Fc receptor that binds IgG1, IgG3, and IgG4 [37]. Phagocytosis of antibody-opsonized particles is a main mechanism by which macrophages interact with antibodies, although macrophage antibody-dependent cell-mediated cytotoxicity is also reported [27]. CD64 was the primary mediator of increased mucosal-associated invariant T cell activation by monocytic antigen-presenting cells (APCs) in a model of *E. coli* phagocytosis and peptide presentation [38]. CD64 also serves as a marker for monocytes and macrophages recruited into lymph nodes to induce a Th1 response in a murine model of colitis [39] and is increased on circulating monocytes in systemic lupus erythematosus patients [40]. With increased CD64

expression, diS-HMGB1-stimulated macrophages are primed for not only increased antigen presentation via HLA-DR, CD86, PD-L1, but are also primed for increased uptake of antigens bound to antibodies, including alloantigens bound to DSA, via CD64.

4.4.4 Macrophage ROS production

IRI induces oxidative stress on the donor organ which contributes to cellular damage and release of DAMPs [41, 42]. Neutrophils, macrophages, and dendritic cells all produce ROS at differing rates and for differing periods of time (minutes to hours) to clear bacterial pathogens [43]. Previous studies document the impact of ROS generation on the release of HMGB1 from macrophages but do not interrogate the impact of HMGB1 on ROS generation [44]. Our results suggest that diS-HMGB1 increases ROS production even at Day 5 in macrophages when compared to canonical macrophage stimuli (**Fig. 3-4A**). This prolonged ability to produce ROS has multiple potential contributions to the post-transplant health of the donor allograft. First, there is the potential of ROS production and HMGB1 secretion to perpetuate each other in a positive feedback loop to induce a longer period of inflammation post-OLT. Second, an oxidatively-stressed microenvironment contributes to the pathogenesis of multiple liver diseases through hepatocyte death and hepatic stellate cell activation [41, 45, 46]. Increased levels of diS-HMGB1-induced ROS can therefore contribute to post-transplant tissue damage and subsequent poorer graft function, as seen with the positive correlation of diS-HMGB1 concentration with hepatocyte necrosis and sinusoidal congestion in post-reperfusion biopsies (**Fig. 3-1B, C**) and sustained poorer liver function tests in the first week post-transplant (**Fig. 3-1D**). Finally, NOX2, an enzyme responsible for ROS production, is directly linked to MHC class II antigen processing abilities in macrophages [47]. Along with elevated HLA-DR and CD86 in our macrophage phenotyping data, it is tempting to

hypothesize that increased diS-HMGB1-induced ROS production contributes to both increased donor hepatocyte death and increased processing of phagocytosed allogeneic antigens, providing a mechanism for linking diS-HMGB1 released at the time of transplant to post-transplant development or enhancement of alloimmunity.

4.4.5 TLR involvement in the diS-HMGB1-induced macrophage phenotype

In vitro inhibitor studies revealed 4 main categories of diS-HMGB1-receptor interaction: molecules that were 1) induced by TLR4 signaling, 2) induced by TLR9 signaling, 3) relied on concurrent/synergistic signaling through both TLRs, or 4) activated by diS-HMGB1 but not through TLR4 or TLR9. Both receptors belong to the TLR family, a group of receptors that each have unique ligands and but use similar adaptor molecules to induce intracellular signaling cascades. TLR4 signals through MyD88 and TRIF adaptor molecules to induce pro-inflammatory cytokine secretion such as IL-1β, IL-6, and TNFα, while TLR9 only signals through MyD88 and can induce a Type I interferon response [48].

Our data reveals that diS-HMGB1 stimulates a broad range of secreted factors, including IL-1β, IL-6, and TNFα, through TLR4 independent of TLR9 and that TLR9 influences chemokine production independent of TLR4. IL-1α, IFNα, and IL-10 were found to be redundantly controlled by both TLRs while MDC/CCL22 was found to be synergistically controlled by both TLRs (**Fig. 3-2B**). Surface markers show a similar pattern where TLR4 alone controls CD86 expression and TLR9 alone controls HLA-DR and CD64 expression yet all three are synergistically decreased when both TLRs are inhibited (**Fig. 3-3C**). PD-L1 was decreased by diS-HMGB1 but not through TLR4 or TLR9, suggesting another receptor is responsible for controlling this molecule. In the

context of innate-adaptive interactions, and antigen presentation specifically, TLR4 and TLR9 both are needed in order to stimulate CD4+ T cell activation. ROS production was the only component of the diS-HMGB1 phenotype that was solely controlled through TLR9 signaling (**Fig. 3-4C, E**). There are conflicting reports about the role of TLR4 and TLR9 in ROS production with sources attributing ROS production to either receptor in different human and cell-based experimental systems [49-51]. Given the evidence that ROS can be produced from either TLR and neither report explored the impact of diS-HMGB1, our human data sheds new light on how TLR9 is specifically involved in the diS-HMGB1-mediated ROS pathway. Overall, this data exemplifies the concept that, although each receptor had its own functions, when they are activated together they induce the most pro-inflammatory diS-HMGB1-induced MDM phenotype.

4.4.6 Model of diS-HMGB1 function following IRI

We propose the following model for how the release of diS-HMGB1 during transplant can impact the long-term immune landscape in OLT recipients:

1. Within the first 24 hours, diS-HMGB1 induces expression of cytokines that create a local pro-inflammatory environment and chemokines that recruit immune cells into this inflammatory setting.
2. By Day 5, higher levels of ROS production in diS-HMGB1-stimulated MDMs contributes to the perpetuation of an inflamed microenvironment, an increase in donor hepatocyte damage/death that provides a source of alloantigens, and an increase in presentation of phagocytosed proteins, including donor hepatocytes. This ROS-induced inflammation can also contribute to poorer recovery of graft function post-transplant.

3. Alloantigens created by the oxidative stress induced by ROS are phagocytosed and presented to CD4+ T cells by increased HLA-DR while a pro-inflammatory CD4+ T cell response is induced a low PD-L1:CD86 ratio. This leads to the activation of an adaptive alloimmune response in the recipient.
4. Activated CD4+ T cells then influence B cell maturation/class switching and antibody secretion, leading to production of DSA. When DSA bind HLA molecules on donor hepatocytes, potentially those succumbed to ROS-induced damage, they facilitate uptake of these HLA antigens via increased CD64 on MDMs.
5. The cycle of ROS-induced hepatocyte necrosis, CD64-mediated alloantigen uptake, alloantigen presentation, and adaptive immune activation continues, leading to a decline in graft health and, ultimately, rejection.

Together, this work demonstrates the relationship between diS-HMGB1 released at the time of transplant, the pro-inflammatory post-transplant clinical and functional characteristics in human OLT patients, and the mechanisms by which diS-HMGB1 impacts macrophage differentiation, via TLR4 and TLR9, to promote a durable and detrimental alloimmune response following OLT.

4.5 THE FUTURE OF DISULFIDE-HMGB1 RESEARCH

The present body of work reveals opportunities for further investigation into diS-HMGB1, TLR4, and TLR9 biology and mechanistic underpinnings. These opportunities are discussed below.

4.5.1 Disulfide-HMGB1 and macrophage polarization

The current studies focused on TLR4 and TLR9 due to previous data linking these receptors to IRI in OLT patients and mouse models [3, 16, 52]. As mentioned in Chapter 3, the receptor repertoire of diS-HMGB1 extends beyond TLR4 and TLR9 [53]. In our studies, IL-12p40, IL-12p70, GM-CSF, and IL-3 secretion is increased by diS-HMGB1 but remains unchanged under TLR4 and/or TLR9 inhibition (**Fig. 3-2**). Likewise, PD-L1 surface expression is decreased by diS-HMGB1 but remains unchanged under TLR4 and/or TLR9 inhibition (**Fig. 3-3**). diS-HMGB1-stimulated MDMs also have a decreased PD-L1:CD86 ratio and a subsequent increase in $CD4^+$ T cell activation (**Fig. 3-5D, E**). We were able to attribute control of CD86 expression to TLR4 and TLR9 (**Fig. 3-3C**). Uncovering the receptor responsible for diS-HMGB1's impact on PD-L1 expression could offer an alternative potential target for modulating the PD-L1:CD86 ratio on diS-HMGB1-stimulated MDMs and decreasing the ability of this cell population to trigger T cell activation. Together with the cytokines, future work can explore the impact of other HMGB1 receptors, such as TLR2 or CXCR4, individually and/or in concert with the TLR4 and TLR9 pathways uncovered in this study, on monocyte cytokine secretion and MDM phenotypes [53].

A topic briefly explored in Chapter 2 is the mechanism by which diS-HMGB1 is secreted from monocytes and macrophages during IRI, and suggests a positive feedback loop between detection and secretion of diS-HMGB1 by these myeloid cells. In these experiments, RNA transcripts of the histone deacetylase HDAC5 and the histone acetyltransferase GTF3C4 correlated with increased acetylated HMGB1 in $LAMP1^+$ vesicles, and thus diS-HMGB1 poised for secretion, in IRI+ patients (**Fig. 2-5C**). Kwak et al show how peroxiredoxins I and II function to translocate HMGB1 from the nucleus into the cytoplasm by forming the disulfide bond between C23 and C45 of the

HMGB1 protein and that this process is required for nucleocytoplasmic translocation [54]. HMGB1 translocation is decreased, but not abrogated, when the group disrupted acetylation or phosphorylation of the nuclear localization sequence in transfected HEK and mouse embryonic fibroblast cell lines, confirming these other post-translational modifications are involved in diS-HMGB1 translocation and secretion [54]. HDAC1 and HDAC4 contribute to HMGB1 translocation in hepatocytes during liver IRI and HDACs 4 and 5 contribute to HMGB1 release in rat cerebral IRI [55]. It remains to be elucidated if and how HDAC5 and GTF3C4 contribute to this translocation process in human monocytes/MDMs and if exposure to diS-HMGB1 alters expression or function of these proteins. Answering these questions would uncover more details about HMGB1 redox and translocation biology, potentially providing new targets for therapeutic interventions aimed at decreasing the release of diS-HMGB1.

Histone modifications like those introduced by HDAC5 and GTF3C4 can also have longer-term implications on the immune response. Cells of the innate immune system were previously thought to not have a memory component as cells of the adaptive immune system do. However, the concept of trained immunity, an altered response from innate immune cells after an initial exposure to a stimulus, has expanded in recent years [56]. There are also ongoing conversations concerned with defining specific differences between trained immunity, priming, differentiation, and tolerance [57]. The work presented in Chapter 3 (**Fig 3-3, 3-4, 3-5**) shows that 5 days after initial exposure to diS-HMGB1, MDMs have an altered phenotype, including the ability to produce ROS and to activate $CD4^+$ T cells. These longer-term alterations suggest that diS-HMGB1 induces epigenetic changes that sustain a pro-inflammatory macrophage phenotype. Future work examining how diS-HMGB1-stimulated MDMs respond to secondary stimulation with physiologically relevant

stimuli such as LPS, modeling bacteria translocated to the liver from the gut, or viral antigens, modeling viral hepatitis or CMV infections that are more common in the post-transplant population due to immunosuppression regimens [58], would shed more light on diS-HMGB1 mechanisms and the importance of decreasing its immune activation potential in sterile inflammation settings such as transplant, myocardial infarction, and ischemic stroke [16, 59-61].

There is also an interesting angle of diS-HMGB1-mediated epigenetic research that I would like to thank Dr. Alex Hoffmann of UCLA for commenting on during a presentation of this research. HMGB1 is a ubiquitous, histone-like DNA binding protein and is translocated from the nucleus to the cytoplasm for secretion by monocytes and macrophages. How the kinetics of nuclear HMGB1 depletion and replacement functions, and the impacts of this location shift on short- and long-term DNA accessibility is currently unknown. The Hoffmann lab previously published kinetic characteristics of the transcription factor NF-κB during stimulation with different TLR ligands [62]. Discovering how diS-HMGB1 stimulation not only modulates overall epigenetic mechanisms, but also modulates nuclear epigenetic mechanisms specific to DNA-HMGB1 interactions would add more understanding to the overarching functions of HMGB1, its oxidative forms, and its post-translational modifications.

4.5.2 Disulfide-HMGB1 and *in vitro* models of OLT-IRI

The *in vitro* models used in these studies focused on the impact of diS-HMGB1 on the recipient monocyte- and MDM-mediated immune response following OLT-IRI. However, other immune cell types are present in the recipient during and following this activation. $CD4^+$ T cells are an important orchestrator of the immune response following OLT. $CD4^+$ T cells contribute to liver

IRI in an antigen-independent manner by activating myeloid cells via CD40-CD40L interactions [63, 64]. CD4+ T cells also contribute to the post-transplant alloimmune response [65]. Although not thought of as a traditional pathway, $CD4^+$ T cells are documented to express multiple TLRs, including TLR4 and TLR9 [66-68]. MDMs differentiated by diS-HMGB1 have an increased capacity to present antigen and activate CD4+ T cells (**Fig. 3-5E**). It is tempting to hypothesize that diS-HMGB1 released at the time of transplant can be sensed not only by infiltrating recipient monocytes but by recipient T cells as well. Future studies examining the impact of purified diS-HMGB1 on 1) antigen-independent $CD4^+$ T cell activation, 2) CD40-CD40L-dependent monocyte activation by diS-HMGB1-stimulated $CD4^+$ T cells, and/or 3) concurrent activation of monocytes and $CD4^+$ T cells would allow for a broader understanding of diS-HMGB1-driven immune activation following OLT. We also show how a lower, T cell-activating, LF-induced PD-L1:CD86 ratio on macrophages correlates with increased incidence of post-OLT DSA in our human patients (**Fig. 3-5C**). B cells are responsible for production and secretion of anti-HLA antibodies that comprise the humoral alloimmune response and $CD4^+$ T cells are involved in the B cell maturation process [69]. Once the above T cell-based mechanisms are uncovered, it will also be important to determine the impact of these T cells on B cell class-switching and antibody production.

One mechanism proposed in Chapter 3 for how diS-HMGB1 impacts post-OLT graft health and the perpetuation of inflammation is through the release of pro-inflammatory cytokines (**Fig. 3-2A**) and ROS (**Fig. 3-4A,D**) that can induce infiltration of immune cells and/or cause damage to liver parenchymal cells, respectively [41, 70]. Parenchymal damage is specifically supported by our findings in mice and human OLT patients that higher concentrations of diS-HMGB1 correlate with increased hepatocyte necrosis (**Fig. 3-1B; 3-6E-H**). We further hypothesize that peptides from

cleared necrotic parenchymal cells are presented by HLA-DR molecules on macrophages to induce an adaptive alloimmune response. The current studies did not focus on macrophage interactions with these cell populations. Therefore, there are multiple avenues for future research to examine the direct effect of diS-HMGB1 on graft health. The first is determining how diS-HMGB1-induced monocyte cytokine secretion impacts graft infiltration by recipient immune populations. Second, it will be crucial to uncover the mechanisms responsible for how diS-HMGB1 and diS-HMGB1-induced ROS directly impacts hepatocyte necrosis and apoptosis. Additionally, uncovering the likelihood of hepatocyte peptide presentation by diS-HMGB1-stimulated macrophages remains a link between hepatocyte death and alloimmunity yet to be confirmed. Finally, the use of *in vitro* three-dimensional liver organoids in combination with diS-HMGB1 treatment provides an opportunity to study diS-HMGB1-mediated mechanisms in the context of the larger liver microenvironment [71]. Answering these research questions will push the field of diS-HMGB1-mediated liver transplant pathobiology forward.

4.5.3 Disulfide-HMGB1 and *in vivo* models of OLT-IRI

Our *in vitro* data focused on the underlying mechanisms behind post-transplant immune activation by diS-HMGB1 (**Fig. 2-6**; **Fig. 3-2 through 3-5**). We used an *in vivo* model of syngeneic OLT-IRI with cold storage of the donor graft to confirm that diS-HMGB1 increased IR injury and decreased graft function (**Fig. 3-6**). However, mechanistic questions remain about the post-transplant function of diS-HMGB1 *in vivo*, including:

- Does diS-HMGB1 affect development of post-transplant liver pathology (e.g. fibrosis)?
- Do diS-HMGB1-stimulated infiltrating recipient monocytes stay in the liver?
- Do these monocytes/MDMs traffic to lymph nodes and/or the spleen?

- Are these cells capable of inducing an alloimmune response *in vivo*?
- Do TLR4 and TLR9 function as expected from our human-based *in vitro* cultures?

An unfortunate technical detail about the cold ischemia model in our study is that recipient mice do not live more than ~5 days post-transplant (personal communication with mouse surgery team). The questions addressing longer-term outcomes (development of pathology, development of alloimmunity, etc.) therefore require use of a warm ischemia model where 70% of a mouse liver is clamped for 90 minutes and released but an entire liver is not transplanted [72]. This model is successfully used in studies examining the repopulation of Kupffer cells with infiltrating monocytes, allowing data to be collected even 14 days post-ischemic injury [73]. Further, allogeneic skin grafts are an established model for studying alloimmunity *in vivo* [74]. Utilizing a skin graft model to study diS-HMGB1, by itself or combined with warm ischemia of the liver, would allow future research to directly address the link between diS-HMGB1 and development and/or augmentation of alloimmunity in liver transplant recipients. Together, these studies would shed more light on diS-HMGB1-mediated mechanisms *in vivo* and allow for more robust translation of this biology to the clinic.

4.6 THE FUTURE OF DISULFIDE-HMGB1 AND OLT-IRI IN THE CLINIC

The present body of work also reveals opportunities for using diS-HMGB1, TLR4, and TLR9 in the clinic to improve donor allograft and transplant recipient health. These opportunities are discussed below.

4.6.1 Disulfide-HMGB1 as a marker of early allograft dysfunction

Early allograft dysfunction (EAD) is the presentation of poor graft function within the first week post-OLT. In 2010, Olthoff et al defined EAD by the presence of 1 or more of 3 static data points within the first week post-transplant: peak ALT or AST and day 7 bilirubin and/or INR values above specific thresholds [75]. More recently, the liver transplant team at UCLA created an updated system for determining EAD called the Liver Graft Assessment Following Transplantation (L-GrAFT) risk score. The L-GrAFT system uses an expanded panel of LFT values and incorporates their *change* over the first 7-10 days post-transplant to assess the risk of a patient experiencing EAD [18]. A disadvantage to these scoring systems is the need to wait 7-10 days after transplant to determine if a recipient is at risk for EAD.

Analysis of LFTs in our OLT patient cohort revealed that diS-HMGB1 concentration at the time of reperfusion associates with LFT levels that do not resolve in the first seven days post-transplant (**Fig. 3-1D**). This opens the opportunity for diS-HMGB1 to be used as an earlier marker of EAD, especially in combination with L-GrAFT system that is concerned with LFT rates-of-change. The process we developed for determining diS-HMGB1 concentration in recipient LF samples takes 4-5 days – a shorter window than either of the above EAD assessment strategies. Further, there is potential for that timeline to be decreased by one day with a newer ELISA kit for total HMGB1 detection and another day by optimizing the gel-to-membrane transfer strategy of the Western blot with faster technologies [76, 77]. Future efforts can explore the use of diS-HMGB1 as an EAD marker and validation of clinical sample processing workflows towards this end.

4.6.2 Disulfide-HMGB1, TLR4, and TLR9 as targets for therapeutics aimed at decreasing occurrence of IRI during OLT

We believe our data present a strong case that neutralizing diS-HMGB1 and/or inhibiting TLR4 and TLR9 during the transplant process can decrease occurrence of IRI and improve post-transplant immune activation and overall health of OLT recipients. There are no treatments currently approved to target these molecules in the United States [78]. However, there are multiple HMGB1-targeting treatments and TLR4/TLR9 antagonists either approved internationally or in clinical trials in the US, while metformin is already approved in the clinic for treating type 2 diabetes in the US and inhibits the extracellular functions of HMGB1 in mice [78, 79]. TAK-242, the TLR4 inhibitor used in Chapter 3, failed to alleviate sepsis in a clinical trial but proved to have a good safety profile in patients [80]. These proven-to-be-safe and/or currently-approved treatment options seem to have low barriers of entry for initiating clinical trials for the prevention of IRI. We envision these treatment options to be administered to recipients before entering the surgical theater for transplantation. Pre-transplant treatment would allow the therapeutics to be present in the portal vein blood used for allograft reperfusion to neutralize or inhibit diS-HMGB1/TLR4/TLR9 at the same moment these molecules are released or activated, respectively. We show that by 24 hours post-OLT, total HMGB1 levels have returned to baseline in peripheral blood of OLT patients (**Fig. 2-1A**). Therefore, continuation of neutralizing or inhibiting treatments would potentially not be required long-term post-transplant. Future studies can explore the viability of this plan to decrease IRI in and increase recovery of OLT recipients.

4.6.3 Disulfide-HMGB1 in combination with normothermic machine perfusion

In 2022, there were 10,625 patients on the waitlist for a liver but only 9,528 transplants performed, leaving almost 1,100 patients without the lifesaving treatment of a new liver [81]. Current efforts are in place to expand the pool of available donor livers and overcome this deficit by transplanting grafts from extended criteria donors (ECD) that might not be ideal. Normothermic perfusion (NMP) is a technology developed to increase the health of these marginal allografts. NMP allows recovered grafts to be perfused with oxygenated, nutrient-rich blood and kept at body temperature (37°C) during the transport process from donor to recipient to decrease occurrence of IRI and other transplant-related damage [82]. NMP is successful at increasing the health of these ECD grafts in the clinic [83]. NMP also provides clinicians with the advantage to assess liver function prior to transplant by sampling the circulating blood in the machine and the potential to introduce treatments aimed at improving the health of marginal grafts [82]. We envision two potential avenues for incorporating diS-HMGB1 and its receptors TLR4 and TLR9 into the NMP process.

First, higher diS-HMGB1 concentrations associate with patients scored as IRI+ (**Fig. 2-2B, Table 3-2**) with OLT patients being 2.4-times more likely to experience IRI for every 333ng/ml of diS-HMGB1 released at the time of reperfusion. diS-HMGB1 is also already present during the ischemic stage of IRI in human patients and in mice (**Fig. 2-4B; Fig. 3-6B**). These data support the use of "circulating" diS-HMGB1 concentration during NMP as a potential biomarker for damage and post-transplant graft health. More studies are required to determine if there is a specific diS-HMGB1 threshold concentration useful for determining if an NMP-connected liver will be amenable to transplant. A limitation still to be overcome for this type of strategy to be valuable is the development of a method to rapidly detect diS-HMGB1. There is currently no quick or

straightforward way to determine the concentration of diS-HMGB1 in a given sample. The methods used in our studies requires a 28-hour ELISA for total HMGB1 concentration and a 3-day Western blot with densitometry analysis for a ratio of aT-HMGB1 to diS-HMGB1 to calculate the final diS-HMGB1 concentration. The only other technology available today to determine this concentration is mass spectrometry [9]. The disulfide bond in diS-HMGB1 causes a conformational change in the protein [84]. It is therefore reasonable to postulate an antibody could be developed towards specific diS-HMGB1 epitopes. Development of this reagent would advance diS-HMGB1 studies in the research lab and allow for quicker detection in the clinic, both for NMP diagnostic and as an early indicator of EAD (discussed in **Section 4.6.1**).

Second, incorporating treatments to neutralized diS-HMGB1 and/or inhibit TLR4/TLR9 activation during NMP could help achieve to goal of decreasing the occurrence of IRI and the subsequent poorer outcomes post-OLT as discussed in **Section 4.6.2**. One benefit of administering treatment during NMP instead of systemically to the recipient is the pharmacokinetics of the treatment options. Accumulation of treatment in organs other than the liver will not be a factor during NMP given that the liver is the only organ attached to the blood supply. This will increase the likelihood of a treatment reaching its target and limiting any adverse effects a treatment might have *in vivo*. This might also allow for lower doses of treatments to be used, further limiting adverse effects once the graft is placed into the recipient.

4.7 CONCLUSION

In conclusion, this work shows that diS-HMGB1 1) is present during and a driver of IRI at the time of OLT, 2) can drive monocytes to differentiate into macrophages with the capacity to activate

an adaptive immune response, and 3) functions through the two main receptors TLR4 and TLR9 to manifest these changes. These results contribute knowledge to HMGB1 biology and transplant immunology, and offer intra- and/or post-transplant avenues for decreasing occurrence of IRI during OLT to improve the lives of liver transplant recipients.

4.8 REFERENCES

[1] Ali JM, Davies SE, Brais RJ, Randle LV, Klinck JR, Allison ME, et al. Analysis of ischemia/reperfusion injury in time-zero biopsies predicts liver allograft outcomes. Liver Transpl 2015;21:487-499.

[2] Tsung A, Sahai R, Tanaka H, Nakao A, Fink MP, Lotze MT, et al. The nuclear factor HMGB1 mediates hepatic injury after murine liver ischemia-reperfusion. J Exp Med 2005;201:1135-1143.

[3] Tsung A, Hoffman RA, Izuishi K, Critchlow ND, Nakao A, Chan MH, et al. Hepatic ischemia/reperfusion injury involves functional TLR4 signaling in nonparenchymal cells. J Immunol 2005;175:7661-7668.

[4] Bamboat ZM, Balachandran VP, Ocuin LM, Obaid H, Plitas G, DeMatteo RP. Toll-like receptor 9 inhibition confers protection from liver ischemia-reperfusion injury. Hepatology 2010;51:621-632.

[5] Zou H, Yang Y, Gao M, Zhang B, Ming B, Sun Y, et al. HMGB1 is involved in chronic rejection of cardiac allograft via promoting inflammatory-like mDCs. Am J Transplant 2014;14:1765-1777.

[6] Bonaldi T, Talamo F, Scaffidi P, Ferrera D, Porto A, Bachi A, et al. Monocytic cells hyperacetylate chromatin protein HMGB1 to redirect it towards secretion. EMBO J 2003;22:5551-5560.

[7] Gardella S, Andrei C, Ferrera D, Lotti LV, Torrisi MR, Bianchi ME, et al. The nuclear protein HMGB1 is secreted by monocytes via a non-classical, vesicle-mediated secretory pathway. EMBO reports 2002;3:995.

[8] Tsung A, Klune JR, Zhang X, Jeyabalan G, Cao Z, Peng X, et al. HMGB1 release induced by liver ischemia involves Toll-like receptor 4 dependent reactive oxygen species production and calcium-mediated signaling. J Exp Med 2007;204:2913-2923.

[9] Venereau E, Casalgrandi M, Schiraldi M, Antoine DJ, Cattaneo A, De Marchis F, et al. Mutually exclusive redox forms of HMGB1 promote cell recruitment or proinflammatory cytokine release. J Exp Med 2012;209:1519-1528.

[10] Tang D, Billiar TR, Lotze MT. A Janus tale of two active high mobility group box 1 (HMGB1) redox states. Mol Med 2012;18:1360-1362.

[11] Yang H, Lundback P, Ottosson L, Erlandsson-Harris H, Venereau E, Bianchi ME, et al. Redox modification of cysteine residues regulates the cytokine activity of high mobility group box-1 (HMGB1). Mol Med 2012;18:250-259.

[12] Suzuki S T-PL, Rodriguez FJ, Cejalvo D. Neutrophil Infiltration as an Important Factor in Liver Ischemia and Reperfusion Injury. Modulating Effects of FK506 and Cyclosporine. Transplantation 1993;55:1265-1272.

[13] Gong T, Liu L, Jiang W, Zhou R. DAMP-sensing receptors in sterile inflammation and inflammatory diseases. Nat Rev Immunol 2020;20:95-112.

[14] Sheu JR, Chen ZC, Hsu MJ, Wang SH, Jung KW, Wu WF, et al. CME-1, a novel polysaccharide, suppresses iNOS expression in lipopolysaccharide-stimulated macrophages through ceramide-initiated protein phosphatase 2A activation. J Cell Mol Med 2018;22:999-1013.

[15] Zhong H, Li X, Zhou S, Jiang P, Liu X, Ouyang M, et al. Interplay between RAGE and TLR4 Regulates HMGB1-Induced Inflammation by Promoting Cell Surface Expression of RAGE and TLR4. J Immunol 2020;205:767-775.

[16] Tian Y, Charles EJ, Yan Z, Wu D, French BA, Kron IL, et al. The myocardial infarct-exacerbating effect of cell-free DNA is mediated by the high-mobility group box 1-receptor for advanced glycation end products-Toll-like receptor 9 pathway. J Thorac Cardiovasc Surg 2019;157:2256-2269 e2253.

[17] Sosa RA, Terry AQ, Kaldas FM, Jin Y, Rossetti M, Ito T, et al. Disulfide-HMGB1 Drives Ischemia-Reperfusion Injury in Human Liver Transplantation. Hepatology 2020.

[18] Agopian VG, Harlander-Locke MP, Markovic D, Dumronggittigule W, Xia V, Kaldas FM, et al. Evaluation of Early Allograft Function Using the Liver Graft Assessment Following Transplantation Risk Score Model. JAMA Surgery 2018;153.

[19] UCSF_Health. Medical Tests - Prothrombin time (PT). 2019 [cited; Available from: https://www.ucsfhealth.org/medical-tests/prothrombin-time-(pt)

[20] Clevenger B, Mallett SV. Transfusion and coagulation management in liver transplantation. World J Gastroenterol 2014;20:6146-6158.

[21] Esmon CT. The impact of the inflammatory response on coagulation. Thromb Res 2004;114:321-327.

[22] Yankovskaya AA, Shevela EY, Sakhno LV, Tikhonova MA, Dome AS, Ostanin AA, et al. Allostimulatory activity as a criterion of the functional phenotype of human macrophages. Hum Immunol 2019;80:890-896.

[23] Siu JHY, Surendrakumar V, Richards JA, Pettigrew GJ. T cell Allorecognition Pathways in Solid Organ Transplantation. Front Immunol 2018;9:2548.

[24] Shen T, Chen X, Chen Y, Xu Q, Lu F, Liu S. Increased PD-L1 expression and PD-L1/CD86 ratio on dendritic cells were associated with impaired dendritic cells function in HCV infection. J Med Virol 2010;82:1152-1159.

[25] Zheng J, Liang H, Xu C, Xu Q, Zhang T, Shen T, et al. An unbalanced PD-L1/CD86 ratio in CD14(++)CD16(+) monocytes is correlated with HCV viremia during chronic HCV infection. Cell Mol Immunol 2014;11:294-304.

[26] Zahorchak AF, Macedo C, Hamm DE, Butterfield LH, Metes DM, Thomson AW. High PD-L1/CD86 MFI ratio and IL-10 secretion characterize human regulatory dendritic cells generated for clinical testing in organ transplantation. Cell Immunol 2018;323:9-18.

[27] Valenzuela NM, Hickey MJ, Reed EF. Antibody Subclass Repertoire and Graft Outcome Following Solid Organ Transplantation. Front Immunol 2016;7:433.

[28] Salo H, Qu H, Mitsiou D, Aucott H, Han J, Zhang XM, et al. Disulfide and Fully Reduced HMGB1 Induce Different Macrophage Polarization and Migration Patterns. Biomolecules 2021;11.

[29] Keskinen P RT, Matikainen S, Lehtonen A, Julkunen I. Regulation of HLA class I and II expression by interferons and influenza A virus in human peripheral blood mononuclear cells. Immunology 1997;91:421-429.

[30] Ruddle NH. Lymphotoxin and TNF: how it all began-a tribute to the travelers. Cytokine Growth Factor Rev 2014;25:83-89.

[31] Tirdea C, Hostiuc S, Moldovan H, Scafa-Udriste A. Identification of Risk Genes Associated with Myocardial Infarction-Big Data Analysis and Literature Review. Int J Mol Sci 2022;23.

[32] Deshmane SL, Kremlev S, Amini S, Sawaya BE. Monocyte chemoattractant protein-1 (MCP-1): an overview. J Interferon Cytokine Res 2009;29:313-326.

[33] Vulcano M, Albanesi C, Stoppacciaro A, Bagnati R, D'Amico G, Struyf S, et al. Dendritic cells as a major source of macrophage-derived chemokine/CCL22 in vitro and in vivo. Eur J Immunol 2001;31:812-822.

[34] Qu H, Heinback R, Salo H, Ewing E, Espinosa A, Aulin C, et al. Transcriptomic Profiling Reveals That HMGB1 Induces Macrophage Polarization Different from Classical M1. Biomolecules 2022;12.

[35] Sawitzki B, Harden PN, Reinke P, Moreau A, Hutchinson JA, Game DS, et al. Regulatory cell therapy in kidney transplantation (The ONE Study): a harmonised design and analysis of seven non-randomised, single-arm, phase 1/2A trials. The Lancet 2020;395:1627-1639.

[36] Bouchet-Delbos L, Even A, Varey E, Saiagh S, Bercegeay S, Braudeau C, et al. Preclinical Assessment of Autologous Tolerogenic Dendritic Cells From End-stage Renal Disease Patients. Transplantation 2021;105:832-841.

[37] Bruhns P, Iannascoli B, England P, Mancardi DA, Fernandez N, Jorieux S, et al. Specificity and affinity of human Fcgamma receptors and their polymorphic variants for human IgG subclasses. Blood 2009;113:3716-3725.

[38] Boulouis C, Gorin JB, Dias J, Bergman P, Leeansyah E, Sandberg JK. Opsonization-Enhanced Antigen Presentation by MR1 Activates Rapid Polyfunctional MAIT Cell Responses Acting as an Effector Arm of Humoral Antibacterial Immunity. J Immunol 2020;205:67-77.

[39] Tamoutounour S, Henri S, Lelouard H, de Bovis B, de Haar C, van der Woude CJ, et al. CD64 distinguishes macrophages from dendritic cells in the gut and reveals the Th1-inducing role of mesenteric lymph node macrophages during colitis. Eur J Immunol 2012;42:3150-3166.

[40] Li Y, Lee PY, Sobel ES, Narain S, Satoh M, Segal MS, et al. Increased expression of FcgammaRI/CD64 on circulating monocytes parallels ongoing inflammation and nephritis in lupus. Arthritis Res Ther 2009;11:R6.

[41] de Andrade KQ, Moura FA, dos Santos JM, de Araujo OR, de Farias Santos JC, Goulart MO. Oxidative Stress and Inflammation in Hepatic Diseases: Therapeutic Possibilities of N-Acetylcysteine. Int J Mol Sci 2015;16:30269-30308.

[42] Zhai Y, Petrowsky H, Hong JC, Busuttil RW, Kupiec-Weglinski JW. Ischaemia-reperfusion injury in liver transplantation--from bench to bedside. Nat Rev Gastroenterol Hepatol 2013;10:79-89.

[43] Paardekooper LM, Dingjan I, Linders PTA, Staal AHJ, Cristescu SM, Verberk W, et al. Human Monocyte-Derived Dendritic Cells Produce Millimolar Concentrations of ROS in Phagosomes Per Second. Front Immunol 2019;10:1216.

[44] Yu Y, Tang D, Kang R. Oxidative stress-mediated HMGB1 biology. Front Physiol 2015;6:93.

[45] Conde de la Rosa L, Schoemaker MH, Vrenken TE, Buist-Homan M, Havinga R, Jansen PL, et al. Superoxide anions and hydrogen peroxide induce hepatocyte death by different mechanisms: involvement of JNK and ERK MAP kinases. J Hepatol 2006;44:918-929.

[46] Ma X, Han S, Zhang W, Fan YJ, Liu MN, Liu AY, et al. Protection of cultured human hepatocytes from hydrogen peroxideinduced apoptosis by relaxin3. Mol Med Rep 2015;11:1228-1234.

[47] Allan ER, Tailor P, Balce DR, Pirzadeh P, McKenna NT, Renaux B, et al. NADPH oxidase modifies patterns of MHC class II-restricted epitopic repertoires through redox control of antigen processing. J Immunol 2014;192:4989-5001.

[48] El-Zayat SR, Sibaii H, Mannaa FA. Toll-like receptors activation, signaling, and targeting: an overview. Bulletin of the National Research Centre 2019;43.

[49] Lahiri A, Lahiri A, Das P, Vani J, Shaila MS, Chakravortty D. TLR 9 activation in dendritic cells enhances salmonella killing and antigen presentation via involvement of the reactive oxygen species. PLoS One 2010;5:e13772.

[50] West AP, Brodsky IE, Rahner C, Woo DK, Erdjument-Bromage H, Tempst P, et al. TLR signalling augments macrophage bactericidal activity through mitochondrial ROS. Nature 2011;472:476-480.

[51] Adachi Y, Kindzelskii AL, Petty AR, Huang JB, Maeda N, Yotsumoto S, et al. IFN-gamma primes RAW264 macrophages and human monocytes for enhanced oxidant production in response to CpG DNA via metabolic signaling: roles of TLR9 and myeloperoxidase trafficking. J Immunol 2006;176:5033-5040.

[52] Sosa RA, Rossetti M, Naini BV, Groysberg VM, Kaldas FM, Busuttil RW, et al. Pattern Recognition Receptor-reactivity Screening of Liver Transplant Patients: Potential for Personalized and Precise Organ Matching to Reduce Risks of Ischemia-reperfusion Injury. Ann Surg 2018.

[53] Bertheloot D, Latz E. HMGB1, IL-1alpha, IL-33 and S100 proteins: dual-function alarmins. Cell Mol Immunol 2017;14:43-64.

[54] Kwak MS, Kim HS, Lkhamsuren K, Kim YH, Han MG, Shin JM, et al. Peroxiredoxin-mediated disulfide bond formation is required for nucleocytoplasmic translocation and secretion of HMGB1 in response to inflammatory stimuli. Redox Biol 2019;24:101203.

[55] Evankovich J, Cho SW, Zhang R, Cardinal J, Dhupar R, Zhang L, et al. High mobility group box 1 release from hepatocytes during ischemia and reperfusion injury is mediated by decreased histone deacetylase activity. J Biol Chem 2010;285:39888-39897.

[56] Netea MG, Dominguez-Andres J, Barreiro LB, Chavakis T, Divangahi M, Fuchs E, et al. Defining trained immunity and its role in health and disease. Nat Rev Immunol 2020;20:375-388.

[57] Divangahi M, Aaby P, Khader SA, Barreiro LB, Bekkering S, Chavakis T, et al. Trained immunity, tolerance, priming and differentiation: distinct immunological processes. Nat Immunol 2021;22:2-6.

[58] Azevedo LS, Pierrotti LC, Abdala E, Costa SF, Strabelli TM, Campos SV, et al. Cytomegalovirus infection in transplant recipients. Clinics (Sao Paulo) 2015;70:515-523.

[59] Tian J, Avalos AM, Mao SY, Chen B, Senthil K, Wu H, et al. Toll-like receptor 9-dependent activation by DNA-containing immune complexes is mediated by HMGB1 and RAGE. Nat Immunol 2007;8:487-496.

[60] Muhammad S, Barakat W, Stoyanov S, Murikinati S, Yang H, Tracey KJ, et al. The HMGB1 receptor RAGE mediates ischemic brain damage. J Neurosci 2008;28:12023-12031.

[61] Wu H, Ma J, Wang P, Corpuz TM, Panchapakesan U, Wyburn KR, et al. HMGB1 contributes to kidney ischemia reperfusion injury. J Am Soc Nephrol 2010;21:1878-1890.

[62] Adelaja A, Taylor B, Sheu KM, Liu Y, Luecke S, Hoffmann A. Six distinct NFkappaB signaling codons convey discrete information to distinguish stimuli and enable appropriate macrophage responses. Immunity 2021;54:916-930 e917.

[63] Shen X-DK, Bibo; Zhai, Yuan; Amersi, Farin; Gao, Feng; Anselmo, Dean M.; Busuttil, Ronald W.; Kupiec-Weglinski, Jerzy W. CD154-CD40 T-cell costimulation pathway is required in the mechanism of hepatic ischemia/reperfusion injury, and its blockade facilitates and depends on heme oxygenase-1 mediated cytoprotection. Transplantation 2002;74:315-319.

[64] Shen X, Wang Y, Gao F, Ren F, Busuttil RW, Kupiec-Weglinski JW, et al. CD4 T cells promote tissue inflammation via CD40 signaling without de novo activation in a murine model of liver ischemia/reperfusion injury. Hepatology 2009;50:1537-1546.

[65] DeWolf S, Sykes M. Alloimmune T cells in transplantation. J Clin Invest 2017;127:2473-2481.

[66] Zarember KA, Godowski PJ. Tissue expression of human Toll-like receptors and differential regulation of Toll-like receptor mRNAs in leukocytes in response to microbes, their products, and cytokines. J Immunol 2002;168:554-561.

[67] Komai-Koma M, Jones L, Ogg GS, Xu D, Liew FY. TLR2 is expressed on activated T cells as a costimulatory receptor. Proc Natl Acad Sci U S A 2004;101:3029-3034.

[68] Gelman AE, Zhang J, Choi Y, Turka LA. Toll-like receptor ligands directly promote activated CD4+ T cell survival. J Immunol 2004;172:6065-6073.

[69] Louis K, Macedo C, Lefaucheur C, Metes D. Adaptive immune cell responses as therapeutic targets in antibody-mediated organ rejection. Trends Mol Med 2022;28:237-250.

[70] Koyama Y, Brenner DA. Liver inflammation and fibrosis. J Clin Invest 2017;127:55-64.

[71] Harrison SP, Baumgarten SF, Verma R, Lunov O, Dejneka A, Sullivan GJ. Liver Organoids: Recent Developments, Limitations and Potential. Front Med (Lausanne) 2021;8:574047.

[72] Kadono K, Kageyama S, Nakamura K, Hirao H, Ito T, Kojima H, et al. Myeloid Ikaros-SIRT1 signaling axis regulates hepatic inflammation and pyroptosis in ischemia-stressed mouse and human liver. J Hepatol 2021.

[73] Zhang H, Ni M, Wang H, Zhang J, Jin D, Busuttil RW, et al. Gsk3beta regulates the resolution of liver ischemia/reperfusion injury via MerTK. JCI Insight 2023;8.

[74] Cheng CH, Lee CF, Fryer M, Furtmuller GJ, Oh B, Powell JD, et al. Murine Full-thickness Skin Transplantation. J Vis Exp 2017.

[75] Olthoff KM, Kulik L, Samstein B, Kaminski M, Abecassis M, Emond J, et al. Validation of a current definition of early allograft dysfunction in liver transplant recipients and analysis of risk factors. Liver Transpl 2010;16:943-949.

[76] Tecan IaII, Inc. HMGB1 Express ELISA Product Information Page.

[77] Barkovits K, Pfeiffer K, Eggers B, Marcus K. Protein Quantification Using the "Rapid Western Blot" Approach.

[78] Yang H, Wang H, Andersson U. Targeting Inflammation Driven by HMGB1. Front Immunol 2020;11:484.

[79] Farooq M, Batool M, Kim MS, Choi S. Toll-Like Receptors as a Therapeutic Target in the Era of Immunotherapies. Front Cell Dev Biol 2021;9:756315.

[80] Rice TW, Wheeler AP, Bernard GR, Vincent JL, Angus DC, Aikawa N, et al. A randomized, double-blind, placebo-controlled trial of TAK-242 for the treatment of severe sepsis. Crit Care Med 2010;38:1685-1694.

[81] Health Resources and Services Administration UG. 2022 Transplant and Waiting List Numbers. 2023.

[82] Ceresa CDL, Nasralla D, Coussios CC, Friend PJ. The case for normothermic machine perfusion in liver transplantation. Liver Transpl 2018;24:269-275.

[83] Mergental H, Laing RW, Kirkham AJ, Perera M, Boteon YL, Attard J, et al. Transplantation of discarded livers following viability testing with normothermic machine perfusion. Nat Commun 2020;11:2939.

[84] Fassi EMA, Sgrignani J, D'Agostino G, Cecchinato V, Garofalo M, Grazioso G, et al. Oxidation State Dependent Conformational Changes of HMGB1 Regulate the Formation of the CXCL12/HMGB1 Heterocomplex. Comput Struct Biotechnol J 2019;17:886-894.